Dissertation

Transcriptional Regulation of Cox-2 Expression in human Osteosarcoma Cells

submitted by

Mag.ª rer.nat. Kerstin KITZ

for the Academic Degree of

Doctor of Philosophy (Ph.D.)

at the

Medical University of Graz

University Clinic of Pediatrics and Adolescent Medicine

under supervision of

Ass.-Prof. Priv.-Doz. Mag. Dr.rer.nat. Werner Windischhofer

2011

ACKNOWLEDGMENTS

I'm grateful to my supervisor, Prof. Werner Windischhofer, for the careful guidance during the last years. Werner, I appreciate your deep knowledge in the field, your positive attitude and continuous support. You challenged me with interesting tasks and were always open to new suggestions. It was great to have the opportunity to present my work at excellent international conferences.

I'd like to thank all members of the laboratory tract for providing a friendly atmosphere. Special thanks go to Evelyn and Karin for the greatest technical support one can image. Thank you also to Bettina for the help with the fluorescence microscopy.

I'm thankful to the Thesis Committee Members, Prof. Hans-Jörg Leis and Prof. Ernst Malle for their feedback and suggestions.

I'm particularly grateful to Ernst – it was a fruitful collaboration. Thanks for the fine-tuning of the manuscript and for the critical reading of the thesis. I always felt warmly welcome in your group - thanks for any experimental help and funny off-work activities!

I'm indebted to the PhD faculty, the Medical University of Graz and to the head of the Pediatrics, Prof. Müller, for the financial support of my work.

I'd like to thank all friends for the emotional support, inspiring scientific- and non-scientific discussions, and the uncountable leisure time activities that were essential to free my mind and soak up new energy!

Finally, I'm grateful to my family for the continuous support during the last years. Thank you for believing in me!

ABSTRACT

Prostaglandins (PGs) are important modulators in bone biology and may contribute to tumor formation and progression also in human osteosarcoma. The inducible cyclooxygenase-2 (Cox-2) is a candidate inflammatory marker in human osteosarcoma and a rate-limiting enzyme in PG biosynthesis. 15-deoxy-$\Delta^{12,14}$-PGJ_2 (15d-PGJ_2), a metabolite of PGD_2 and PPARγ ligand, exerts a panel of different biological activities via receptor-dependent and receptor-independent mechanisms. The present study aimed at investigating the intracellular redox status and signalling cascades leading to Cox-2 induction in human MG-63 osteosarcoma cells. 15d-PGJ_2 induced an accumulation of reactive oxygen species (ROS) that in turn led to upregulation of Cox-2 via different routes in a PPARγ- and PGD_2-receptor-independent manner. First, phosphorylation of p38 MAPK directly enhanced Cox-2 expression by promoting mRNA stability. Second, 15d-PGJ_2 induced activation of EGF receptors and downstream activation of Cox-2 via phosphorylation of p42/44 MAPK. Functional activity of Cox-2 expression was tested by measurements of PGE_2 and $PGF_{2\alpha}$. Glutathione precursor molecules reversed enhanced ROS levels and Cox-2 expression. The synthetic compound 9,10-dihydro-15d-PGJ_2 lacking the α,β-unsaturated carbonyl group in the cyclopentenone ring did not exhibit cellular responses observed with 15d-PGJ_2. Thus, it is concluded that the electrophilic carbon atom of 15d-PGJ_2 is responsible for alterations in the intracellular redox status and Cox-2 expression.

The electrophilic character of 15d-PGJ_2 was also related to the induction of apoptotic markers such as caspase-3 activation and PARP cleavage. Apoptosis was regulated independently of MAPK activation, PPARγ, and PGD_2 receptors. Both, death receptor- and mitochondria-dependent pathways might be involved in 15d-PGJ_2-induced programmed cell death, as procaspase-8 cleavage was upregulated and expression levels of the pro-apoptotic Bcl-2 family member Puma were increased. Furthermore, 15d-PGJ_2 mediated the elevation of the intracellular GSH content and expression of heme oxygenase-1 (HO-1), both events that might act in a cytoprotective manner preventing cytotoxic effects of 15d-PGJ_2. HO-1 expression might be regulated by Nrf-2 or Egr-1, as these candidate transcription factors underwent nuclear translocation upon 15d-PGJ_2 treatment.

ZUSAMMENFASSUNG

Prostaglandine (PGs) spielen eine wichtige regulatorische Rolle im Knochenstoffwechsel und sind möglicherweise auch bei Entstehung und Progression von Knochenkrebs beteiligt. Die induzierbare Cyclooxygenase-2 (Cox-2) ist ein limitierender Faktor in der PG-Biosynthese und ist im Zusammenhang mit Knochenkrebs als ein kritischer Entzündungsmarker beschrieben. 15-deoxy-$\Delta^{12,14}$-PGJ_2 (15d-PGJ_2), ein PGD_2-Metabolit und PPARγ-Ligand, aktiviert eine Fülle biologischer Abläufe über Rezeptor-abhängige oder Rezeptor-unabhängige Mechanismen. Das Ziel der vorliegenden Studie war den intrazellulären Redoxstatus und die damit verbundene Aktivierung von Signaltransduktionswegen, welche zu einer Induktion der Cox-2 Expression in humanen MG-63 Knochenkrebszellen führen, zu untersuchen. 15d-PGJ_2 bewirkte eine Akkumulation von reaktiven Sauerstoffspezies (ROS), welche in weiterer Folge zu erhöhter Cox-2 Expression führte. Die Regulation der Cox-2 Expression erfolgte über verschiedene Wege, welche unabhänging von PPARγ oder PGD_2 Rezeptoren aktiviert wurden. (i) Durch den p38 MAPK Signaltransduktionsweg wurde die Cox-2 Expression durch vermehrte mRNA Stabilität reguliert. (ii) Weiters induzierte 15d-PGJ_2 die Aktivierung von EGF Rezeptoren, was in weiterer Folge zu p42/44 MAPK Phosphorylierung und erhöhter Cox-2 Expression führte. Die Aktivität der exprimierten Cox-2 wurde mittels Messungen der durch das Enzym gebildeten PGs, PGE_2 und $PGF_{2\alpha}$, bestätigt. Die Erhöhung von ROS und die induzierte Cox-2 Expression wurden durch die Zugabe von Glutathionvorstufen vermindert. Mit dem synthetischen Molekül 9,10-dihydro-15d-PGJ_2, welchem die α,β-ungesättige Kohlenstoffgruppe im Cyclopentenon-Ring fehlt, konnten all diese mit 15d-PGJ_2 beschriebenen Reaktionen, nicht beobachtet werden. Daraus folgt der Schluss, dass das elektrophile Kohlenstoffatom von 15d-PGJ_2 für die Veränderungen im intrazellulären Redoxstatus und die erhöhte Cox-2 Expression verantwortlich ist.

Die elektrophilen Eigenschaften von 15d-PGJ_2 konnten auch mit der Induktion von Apoptosemarkern wie Caspase-3-Aktivierung und PARP-Spaltung in Zusammenhang gebracht werden. Die Apoptose wurde unabhänging von MAPK Aktivierung, PPARγ und PGD_2 Rezeptoren reguliert. Sowohl Todesrezeptoren- als auch Mitochondrien-vermittelte Mechanismen scheinen bei der Regulation des

kontrollierten Zelltods eine Rolle zu spielen, da die Behandlung von MG-63 Zellen mit 15d-PGJ_2 sowohl zu Caspase-8-Spaltung als auch zu einer erhöhten Expression von Puma, einem pro-apoptotischen Mitglied der Bcl-2 Familie, führte. Weiters vermittelte 15d-PGJ_2 eine Erhöhung des intrazellularen Glutathionstatus und gesteigerte Expression der Hämoxygenase-1 (HO-1). Diese Ereignisse haben möglicherweise protektive Auswirkungen auf zellulärer Ebene, indem sie zytotoxischen Effekten von 15d-PGJ_2 entgegenwirken. Die HO-1 Expression könnte von Nrf-2 oder Egr-1 reguliert werden, da diese Transkriptionsfaktoren in 15d-PGJ_2-stimulierten Zellen in den Kern translozierten.

CONTENTS

ABBREVIATIONS

15d-PGJ_2	15-deoxy-$^{\Delta 12,14}$-prostaglandin J_2
AA	arachidonic acid
ActD	actinomycin D
AIF	apoptosis inducing factor
Akt/PKB	protein kinase B
Apaf-1	apoptosis activating factor 1
AP-1	activator protein-1
ARE/EpRE	antioxidant/electrophile response element
Ask-1	apoptosis signal-regulating kinase-1
Bcl-2	B-cell leukemia 2 protein
Bcl-x_L	B-cell leukemia x_L protein
BH domain	Bcl-2 homology domain
BK	bradykinin
BSO	L-buthionine-sulfoximine
CBP	CREB binding protein
CDK	cyclin dependent kinase
C/EBP	CCAAT/enhancer binding protein
CO	carbon monoxide
Cox	cyclooxygenase
CREB	cAMP response element binding protein
CRTH2	chemoattractant receptor-homologous molecule expressed on Th2
Cul3	cullin 3
CXCR	chemokine (C-X-C motif) receptor
DCF-DA	dichlorofluorescein-diacetate
DD	death domain
DIABLO	direct IAP binding protein with low PI
DISC	death-inducing signalling complex
DK-PGD_2	dihydro-keto-PGD_2
DP	prostaglandin D_2 receptor
DR	death receptor
EGF(R)	epidermal growth factor (receptor)
Egr-1	early response gene 1
ER	endoplasmic reticulum
ET-1	endothelin-1
FADD	Fas-associated death domain

FCS	fetal calf serum
FLIP	FADD-like IL-1β-converting enzyme-like inhibitory protein
GCL	glutamyl cysteine ligase
GC/MS	gas chromatography/mass spectrometry
GPCR	G-protein-coupled receptor
GSH	glutathione
GSSG	glutathione disulfide
GTPase	guanosin triphosphatase
HO-1	heme oxygenase 1
HRP	horseradish peroxidase
HSF-1	heat shock factor 1
Hsp	heat shock protein
HtrA2	heat activated tyrosine kinase A2
IAP	caspase inhibitory proteins
IκBα	inhibitor of NF-κB alpha
IKK	inhibitor of NF-κB kinase
IL-1	interleukin-1
JNK	c-Jun N-terminal kinase
Keap1	Kelch-like ECH-associated protein 1
LPA	lysophosphatidic acid
LPS	lipopolysaccharide
MAPK	mitogen-activated protein kinase
MAPKAPK-2	MAPK-activated protein kinase 2
MDM2	murine double minute 2
MDR	multidrug resistance protein
MEM	minimal essential medium
miRNA	micro RNA
MMP	matrix metalloproteinase
MPG	N-2-mercaptopropionyl-glycine
mRNA	messenger ribonucleic acid
MTT	3-(4,5-dimethylthiozol-2-yl)-2,5-dipheyltetrazolium bromide
NAC	N-acetyl-L-cysteine
NFAT	nuclear factor of activated T-cells
NF-κB	nuclear factor kappa B
Nrf-2	nuclear erythroid factor 2-related factor 2
NSAID	non-steroidal anti-inflammatory drug
PARP	poly (ADP-ribose) polymerase
PDGFR	platelet-derived growth factor receptor

PEA-3	polyomavirus enhancer A binding protein
PG	prostaglandin
PI3K	phosphatidyl-inositol-3-kinase
(p)JNK1/2	(phosphorylated) c-Jun N-terminal kinase
PKC	protein kinase C
PLA_2	phospholipase A_2
(p)p38 MAPK	(phosphorylated) p38 mitogen-activated protein kinase
(p)p42/44 MAPK	(phosphorylated) p42/44 mitogen-activated protein kinase
PPARγ	peroxisome proliferator activated receptor gamma
PPRE	peroxisome proliferator response element
qPCR	quantitative polymerase chain reaction
RA	retinoic acid
RAR	retinoic acid receptor
RB	retinoblastoma
RECK	reversion-inducing-cysteine-rich protein with kazal motifs
ROS	reactive oxygen species
RTK	receptor tyrosine kinase
RT-PCR	reverse transcriptase polymerase chain reaction
RXR	retinoid X receptor
siRNA	silencer ribonucleic acid
SP-1	specificity protein-1
tBid	truncated Bid
TBP	TATA-binding protein
TIA-1	T-cell intracellular antigen 1
TNF-α	tumor necrosis factor alpha
TNFR	tumor necrosis factor receptor
TRADD	tumor necrosis factor receptor-associated death domain
TRAIL	tumor necrosis factor-related apoptosis-inducing ligand
Trx	thioredoxin
UTR	untranslated region
VEGF	vascular endothelial growth factor
XIAP	x-linked inhibitor of apoptosis
Z-VAD-FMK	benzyloxycarbonyl-Val-Ala-Asp (OMe) fluoromethylketone

1 INTRODUCTION

1.1 Human osteosarcoma

1.1.1 Pathophysiology and Epidemiology

Osteosarcoma is defined as a malignant tumor of connective tissue that originates from cells of the mesenchymal lineage. The tumor is characterized by the presence of extracellular osteoid (unmineralized organic component of bone) which is directly deposited by the carcinogenic cells [Lamoureux et al., 2007]. Osteosarcomas are divided into osteoblastic, chondroblastic, and fibroblastic types, depending on the dominant histologic element [Sandberg and Bridge, 2003]. Typical affected sites are femur, tibia and humerus. The majority of osteosarcomas are *de novo* primary tumors, but an important minority occurs in the setting of a previous malignancy [Bramwell, 2000].

The peak incidence of osteosarcoma in humans occurs in the second decade, with an additional smaller peak after the age of 50. Almost all osteosarcomas are of high grade and have a poor prognosis [Sandberg and Bridge, 2003], related to the highly metastatic potential. Metastasis occur early in osteosarcoma development and mostly affect the lung, followed by bone [Vanel et al., 1984].

Although human osteosarcoma is a rare tumor type, it represents the most common non-hematologic malignant tumor of bone. The tumor incidence is about 0.2 – 0.3 per 100,000 per year in Middle Europe. Risk factors that may contribute to osteosarcoma are: (i) rapid bone growth especially at the metaphyseal area adjacent to the growth plate of long bones, (ii) environmental factors such as ionizing radiation, and (iii) genetic predisposition due to familial cancer syndromes or the dysregulation of genes involved in osteosarcoma pathogenesis [Tan et al., 2009].

1.1.2 Genetic alterations

Genetic alterations promoting osteosarcoma development include hereditary cancer syndromes as well as sporadic chromosomal abnormalities such as point mutations, loss of heterozygosity, and structural rearrangements. These genetic

alterations frequently lead to dysregulation of p53 and retinoblastoma (RB) pathways.

Patients with germline mutations of p53 (Li-Fraumeni syndrome) or RB gene have an increased risk of developing osteosarcomas. Furthermore, an increased osteosarcoma incidence has been associated with genetic disorders, such as Paget's disease (bone disorder characterized by abnormal bone formation), Rothmund-Thomson syndrome, Bloom syndrome, and Werner syndrome. The latter syndromes display mutations in recombinase Q helicase genes [Abed and Grimer, 2010; Kansara and Thomas, 2007; Tang et al., 2008].

The majority of osteosarcomas do not occur from genetic disorder but sporadic mutations resulting in inactivation of tumor suppressor genes and/or overexpression of oncogenes. Cytogenetic abnormalities have been found in about 70% of osteosarcomas, with multiple clones of different degrees of ploidy ranging from haploidy to near-hexaploidy [Gorlick et al., 2003; Sandberg and Bridge, 2003]. The complex imbalanced karyotypes frequently provoke inhibition of p53 and/or RB pathways leading to a dysfunction of cell cycle control. Genetic alterations that influence the regulation of these pathways are, for instance, inhibitor of cyclin-dependent kinase 4a deletion [Wei et al., 1999], murine double minute 2 (MDM2) overexpression [Ladanyi et al., 1993; Leach et al., 1993] or cyclin dependent kinase 4 (CDK4) overexpression [Ragazzini et al., 1999]. Furthermore, a variety of molecular markers rather unrelated to RB and p53 pathways are overexpressed or activated in a proportion of osteosarcomas. These oncogenes include for instance MYC, FOS, MET, SAS, GLI, MAPK7, GAS3, and c-JUN [Abed and Grimer, 2010; Kansara and Thomas, 2007; Ta et al., 2009; Tan et al., 2009; Tang et al., 2008; Wachtel and Schafer, 2010] which are often linked to the severeness of disease and/or poor response to therapy [Kansara and Thomas, 2007; Sandberg and Bridge, 2003]. Moreover, the Fas/Fas ligand (FasL) apoptotic pathway has been associated with decreased chemosensitivity and increased pulmonary metastasis of tumors including human osteosarcoma [Koshkina et al., 2007]. Drug resistance pathways are likely to play a role in osteosarcoma tumor recurrence. Elevated expression of the ATP-dependent efflux pump, p-glycoprotein, which is encoded by multidrug resistance protein 1 (MDR1), is suggested to be associated with poorer metastasis-free survival and poorer overall survival. A similar prognosis is documented in case of a decreased expression of the reduced folate carrier which regulates the intracellular drug influx [Gorlick et al., 2003].

1.1.3 Therapy

Due to the early development of subclinical metastases, treatment of human osteosarcoma by surgery alone is often not sufficient as almost 90% of patients develop recurrence. As this tumor type is extremely resistant to radiation therapy, the standard osteosarcoma therapy includes combinations of chemotherapy (neoadjuvant/adjuvant) and surgery [Ta et al., 2009]. Limb salvage is currently the standard surgery method in bone sarcoma. The excised malignant bone material is usually replaced by a prosthetic compound but also successful bone reconstruction by an autograft or allograft was achieved [Abed and Grimer, 2010].

The backbone of osteosarcoma chemotherapy includes doxorubicin, cisplatin, ifosfamide, and high-dose methotrexate. Additionally, other agents such as carboplatin, etoposide, and cyclophosphamide have been employed [Goldsby et al., 2008; Strander, 2007]. The use of adjuvant chemotherapy turned out to be very successful in osteosarcoma treatment from the 1970s up to now, as it has increased the 5-year survival rate from 20% to approximately 65%. However, for patients with metastasis at the date of diagnosis, the survival rate remains poor [Kansara and Thomas, 2007; Lamoureux et al., 2007]. Beside the anti-carcinogenic effects, the chemotherapeutics are connected to severe side effects like neutropenia, leucopenia, cardiotoxicity, ototoxicity, and nephrotoxicity [Bramwell, 2000; Tan et al., 2009]. Neoadjuvant therapy may also favor second malignancies such as leukemia [Shen et al., 2009].

As the advantages of the common therapy outweigh the disadvantages, it will most probably not be completely displaced by a new strategy. However, there are some new drugs that have shown benefits in the therapy of other cancers and might also be considered for treatment of osteosarcoma. These include the cytostatic drug gemcitabine, the monoclonal antibody trastuzumab that targets ERBB2, heat shock protein (Hsp)-90 inhibitor 17-AAG, mTOR inhibitor AP23573, and MMP inhibitors [Gorlick et al., 2003; Lamoureux et al., 2007]. Moreover, bisphosphonates have shown benefits in treatment of bone metastasis [Langer and Hirsh, 2010].

1.1.4 Preclinical Osteosarcoma Studies

As the common osteosarcoma drugs exhibit severe side effects, a combination with new targets that sensitize the tumor cells to chemotherapy or

reduce the toxicity should be considered. That implies preclinical osteosarcoma biology studies to find new molecular targets for drug development. Novel agents might act as biological-response modifiers, anti-angiogenesis factors or growth receptor modulators that may be applied in immune-based therapy, gene therapy or hormone therapy [Gorlick et al., 2003; Lamoureux et al., 2007; Tan et al., 2009].

To date relatively little is known about the various interactions that occur between host and tumor cells that govern growth and progression of osteosarcoma *in vivo*. Different model systems are used to elucidate the underlying mechanisms. Mouse (K7M2, K12), rat (UMR 160-01) and human (U2OS, SaOS, MG-63, HOS, 143B) osteosarcoma cell lines are employed to study basic research and to get first attempts to clinical research. Furthermore, mice and rats are used for the screening of potential therapeutics whereas canine models are also well established for the development of surgery methods [Gorlick et al., 2003; Mueller et al., 2007].

To mimic the pathology of this tumor, animals are injected with osteosarcoma cell lines or genetically modified mice are used to investigate the tumorigenic potential of overexpression, knock-out or mutation of candidate genes that might be involved in osteosarcoma regulation [Ek et al., 2006]. Thus, a variety of potential oncogenes have been identified in preclinical studies as well as in microarray analysis of osteosarcoma samples. The following targets are considered to be promising for new therapy approaches: vascular endothelial growth factor (VEGF), pigment epithelium-derived factor, RECK, urokinase plasminogen activator and its receptor, p-glycoprotein, chemokine receptor CXCR4, Ezrin, parathyroid hormone-related peptide and its receptor, and insulin-like growth factor 1 [Kansara and Thomas, 2007; Ta et al., 2009; Tan et al., 2009; Tang et al., 2008; Wachtel and Schafer, 2010]. As a pronounced expression of cyclooxygenase 2 (Cox-2) was detected in a high proportion of patient samples [Dickens et al., 2003; Urakawa et al., 2009], specific Cox-2 inhibitors have been suggested as potential therapeutics for treatment of human osteosarcoma. However, if high Cox-2 levels may serve as a prognostic factor is still under debate.

1.2 Cyclooxygenases and Prostanoid Metabolism

1.2.1 Biology of Cyclooxygenases

Cyclooxygenases (Coxs) are specific enzymes catalyzing the rate-limiting step in prostanoid synthesis. Prostanoids are a subclass of eicosanoids consisting of PGs and thromboxanes. There are two Cox isoforms, Cox-1 and Cox-2, which have a high homology in the primary structure (about 60%) as well as catalytic similarities. Cox-1 and Cox-2 are homodimers of about 70 kDa subunits; dimerization is required for the enzymatic activity. Both enzymes catalyze a cyclooxygenase and a peroxidase reaction at separate but neighbouring active sites. These membrane-bound enzymes are located on the luminal surfaces of the endoplasmic reticulum (ER) and on the inner and outer membrane of the nuclear envelope [Blackwell et al., 2010; Blobaum and Marnett, 2007; Morita, 2002; Smith and Song, 2002]. However, the two Cox isoforms differ substantially in their regulation, expression profiles, and physiological properties. Cox-1 is constitutively expressed in many tissues and exerts homeostatic functions. Cox-2 is the inducible isoform in most cells and tissues whose expression is stimulated by growth factors, cytokines, and tumor promoters [Morita, 2002; Surh and Kundu, 2005]. However, Cox-2-derived prostanoid synthesis may also regulate homeostatic processes as Cox-2 knock-out mice exhibit deficiencies in kidney development, in the cardiovascular system and in female fertility [Rouzer and Marnett, 2009].

Cox isoenzymes are also involved in a wide range of pathologies that include for Cox-1 thrombosis, and for Cox-2 inflammation, pain and fever, various cancers, and neurological disorders like Alzheimer's and Parkinson's diseases [Garavito et al., 2002]. Big success was achieved with the development of non-steroidal anti-inflammatory drugs (NSAIDs) such as aspirin for treatment of fever and pain. Some of the initial NSAIDs which target both Cox isoforms provoked gastric toxicity due to inhibition of Cox-1. This problem was reduced by the development of selective Cox-2 inhibitors like celecoxib (Celebrex®), rofecoxib (Vioxx®), and valdecoxib (Bextra®). However, clinical studies demonstrated that selective Cox-2 inhibitors significantly increased the risk of cardiovascular toxicity confirming a homeostatic function for Cox-2-derived PGs in the heart. As a consequence of this side effect, the NSAIDs

rofecoxib and valdecoxib were removed from the market [Blobaum and Marnett, 2007; Rouzer and Marnett, 2009].

1.2.2 Prostanoid Synthesis

Cells produce prostanoids through the enzymatic metabolism of arachidonic acid (AA), a polyunsaturated fatty acid primarily esterified to cell membrane phospholipids at the *sn*-2 position (Scheme 1). The first step in prostanoid synthesis is the hydrolysis of membrane phospholipids to produce free AA in a reaction catalyzed by phospholipase A_2 (PLA_2). AA is oxygenated in the cyclooxygenase active site of Cox enzymes to produce an unstable intermediate, prostaglandin (PG) G_2, which is rapidly converted to PGH_2 by the peroxidase activity of Cox enzymes. PGH_2 serves as a substrate for tissue-specific PG synthase enzymes, which are responsible for the production of the five principal bioactive prostanoids generated *in vivo*: PGD_2, PGE_2, $PGF_{2\alpha}$, PGI_2 (also known as prostacyclin), and thromboxane A_2 (TXA_2) [Telliez et al., 2006; Wang and Dubois, 2010].

After biosynthesis, prostanoids are rapidly exported from cells and act in an autocrine or paracrine manner via specific cell surface and/or nuclear receptors. Cell surface receptors belong to the family of G-protein-coupled rhodopsin-type receptors (GPCRs), and are designated DP and CRTH2 (alias GPR44) for the PGD_2 receptors, EP1-4 for the PGE_2 receptors, FP for the $PGF_{2\alpha}$ receptor, IP for the PGI_2 receptor and TP for the TXA_2 receptor. Moreover, PGI_2 and metabolites of PGD_2 such as 15-deoxy-$\Delta^{12,14}$-PGJ_2 (15d-PGJ_2) can transactivate members of the peroxisome proliferator activated receptor (PPAR) family of nuclear hormone receptors (PPARδ and γ, respectively) [Telliez et al., 2006; Wang and Dubois, 2010].

Prostanoid production can be regulated via alterations in Cox-2 enzymatic activity or Cox-2 expression levels. For example, nitric oxide, which exhibits high affinity to the iron heme centre in the catalytic domain of Cox-2, increases its enzyme activity [Tsatsanis et al., 2006]. The regulation of Cox-2 expression at the (post)transcriptional is summarized below.

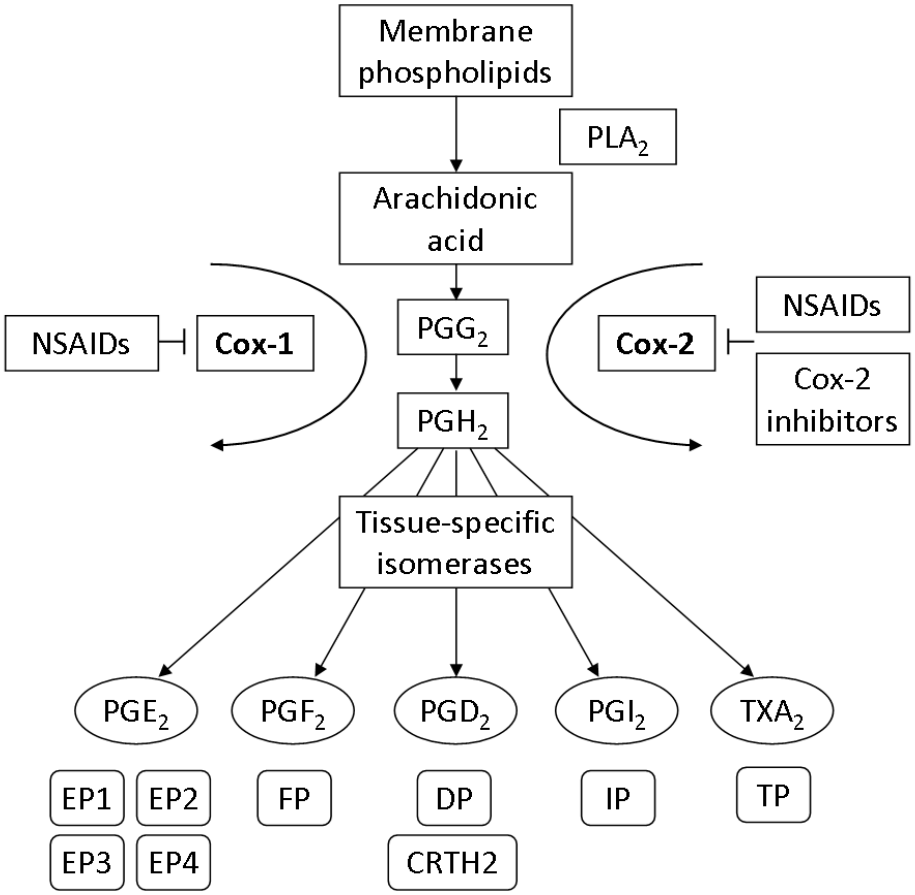

Scheme 1: Flow diagram of prostanoid synthesis.

PLA_2 generates free AA from membrane phospholipids. Cox-1 and Cox-2 convert AA to PGG_2 via a cyclooxygenase reaction followed by conversion to PGH_2 via a peroxidase reaction in separated active sites. PGH_2 is further metabolized into other PG isoforms and TXA_2 by tissue-specific isomerases. Non-steroidal anti-inflammatory drugs (NSAIDs) inhibit both Cox-1 and Cox-2, whereas specific Cox-2 inhibitors inhibit Cox-2 only. Prostanoids are rapidly exported from cells and activate specific cell surface receptors in an autocrine or paracrine manner. Cell surface receptors belong to the family of GPCRs, and are designated DP and CRTH2 for the PGD_2 receptor, EP1-4 for the PGE_2 receptors, FP for the $PGF_{2\alpha}$ receptor, IP for the PGI_2 receptor, and TP for the TXA_2 receptor. This scheme was adapted from [Liao et al., 2007].

1.2.3 Regulation of Cox-2 Expression

A growing body of evidence indicates that expression of Cox-2 is differently regulated in different cell types. Cox-2 belongs to the group of early response genes which are usually transiently expressed during stress periods. Additionally to the

transcriptional regulation of these genes, the protein expression levels are often determined by changes in mRNA stability. A simplified overview of signalling pathways that are involved in Cox-2 expression are shown in Scheme 2.

1.2.3.1 Transcriptional Regulation of Cox-2 Expression

A variety of extracellular and intracellular stimuli can rapidly induce Cox-2, including different growth factors and pro-inflammatory agents such as tumor necrosis factor (TNF)-α, interleukin (IL)-1β, lipopolysaccharide (LPS), endothelin (ET)-1 and lysophosphatidic acid (LPA) [Telliez et al., 2006]. Thus, various signalling transduction pathways are switched on which converge on transcription factors such as nuclear factor-κB (NF-κB), activator protein-1 (AP-1), CCAAT/enhancer binding protein (C/EBP), and cAMP response element binding protein (CREB). Putative binding sites for polyomavirus enhancer A binding protein (PEA)-3, nuclear factor of activated T-cells (NFAT), AP-2, and specificity protein (SP)-1 have also been identified in the 5' flanking region of the Cox-2 coding sequence [Chun and Surh, 2004; Telliez et al., 2006]. Moreover, the transcriptional machinery at the Cox-2 promoter requires the general transcription co-activator p300/CBP for the recruitment of the RNA polymerase complex [Tsatsanis et al., 2006].

Among the multiple signal transduction routes inducing Cox-2 expression, the Ras pathway is one of the main regulators. Ras stimulates activation of phosphatidyl-inositol-3-kinase (PI3K), p38 mitogen-activated protein kinase (MAPK), p42/44 MAPK, and c-Jun N-terminal kinase (JNK) pathways. Other important factors involved in the regulation of Cox-2 expression are protein kinase C (PKC), Akt/protein kinase B (PKB), Rho GTPases, cyclic GMP, and Wnt [Surh and Kundu, 2005; Telliez et al., 2006].

Cox-2 expression may also be negatively regulated by factors like glucocorticoids, IL-4, IL-13, and the anti-inflammatory cytokine IL-10 [Surh and Kundu, 2005]. Furthermore, tumor suppressor genes such as p53 [Subbaramaiah et al., 1999] and nuclear receptors such as PPARγ [Subbaramaiah et al., 2001] negatively regulate Cox-2 induction by competing for general transcription factors like TATA-binding protein (TBP) and CBP/p300, respectively.

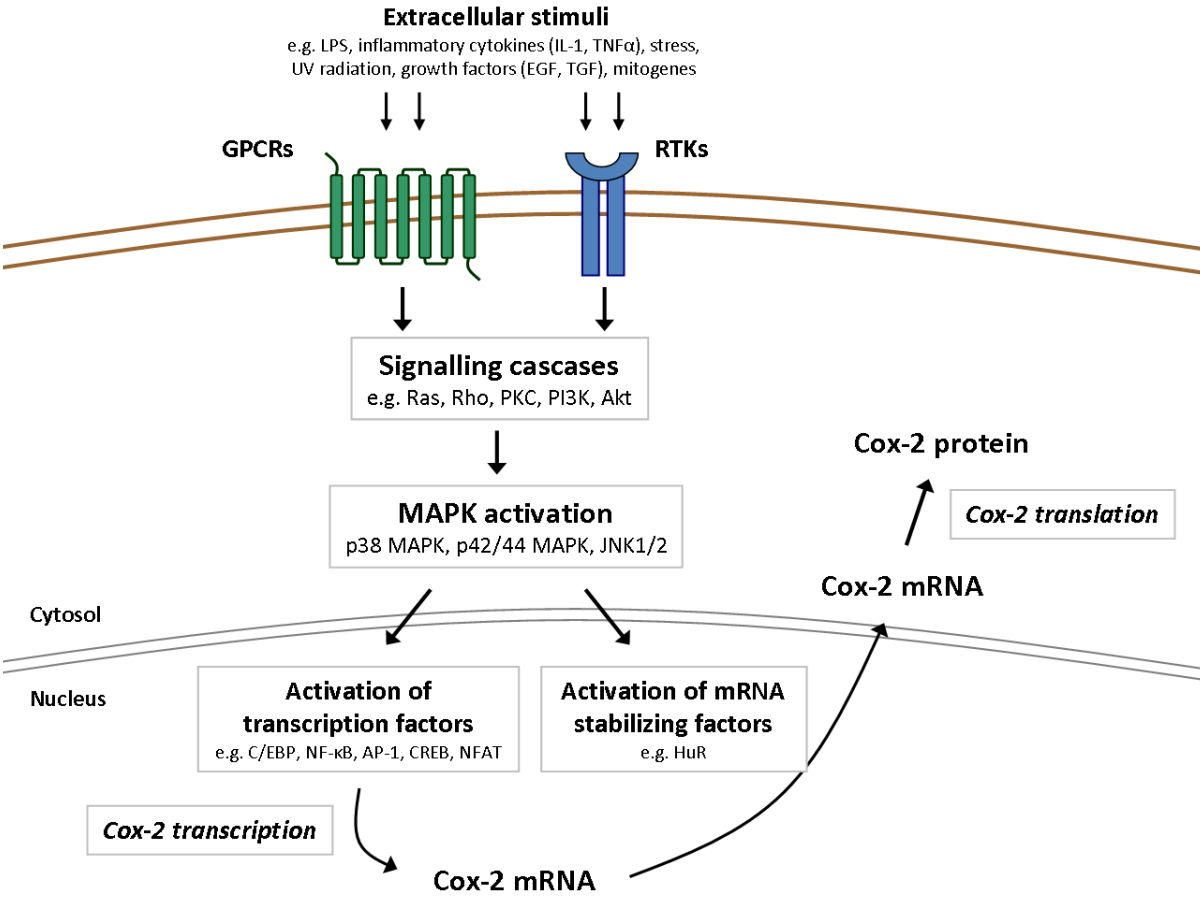

Scheme 2: Signalling pathways involved in the regulation of Cox-2 expression.
Cox-2 expression is upregulated by a variety of extracellular stimuli including LPS, cytokines, stress factors, and growth factors. Through activation of GPCRs and receptor tyrosine kinases (RTKs) different signalling cascades are activated that converge on MAPK phosphorylation. Signal transduction pathways are either involved in the activation of transcription factors involved in Cox-2 transcription or in the activation of mRNA stabilizing factors enhancing Cox-2 mRNA half-life time.

1.2.3.2 Post-transcriptional Regulation of Cox-2 Expression

Important regulators of mRNA half-life time are AU-rich elements in the 3' untranslated region (UTR). These *cis*-acting short sequences are recognized by RNA-binding proteins that mediate either stabilization or degradation of the message. AREs are present in the 3' UTR of Cox-2 mRNA [Harper and Tyson-Capper, 2008]. The RNA-binding protein HuR was determined as a key regulator of increased Cox-2 mRNA stability in several studies [Cok et al., 2003; Sengupta et al., 2003; Subbaramaiah et al., 2003] whereas T-cell intracellular antigen 1 (TIA-1) and TIA-1-

related protein [Dixon et al., 2003; Piecyk et al., 2000] act as Cox-2 translational silencers. Furthermore, decreased binding of heterogeneous nuclear ribonuclear protein K (hnRNPK) had a stabilizing effect on Cox-2 mRNA in human monocytes [Shanmugam et al., 2008]. Major signalling pathways regulating elevated Cox-2 mRNA stability involve activation of p38 MAPK/PKC [Cao et al., 2007; Subbaramaiah et al., 2003], PI3K [Cao et al., 2007], and c-Src [Xu et al., 2007]. Recently, micro RNAs (miRNA) have been identified as post-transcriptional regulators of Cox-2 expression, as miRNA-101a, miRNA-199a [Chakrabarty et al., 2007], and miRNA-16 [Shanmugam et al., 2008] bind to AU-rich elements and favor Cox-2 mRNA degradation.

1.2.4 Cox-2 and PGs in Carcinogenesis

Elevated Cox-2 expression has been implicated in tumorigenesis and metastasis. High Cox-2 expression was detected in many malignant and premalignant organs such as colon, pancreas, liver, lung, breast, bladder, skin, stomach, head, neck, and oesophagus [Telliez et al., 2006]. The relevance of high Cox-2 expression in tumorigenesis was investigated in several animal models. Transgenic mice overexpressing Cox-2 in mammary glands [Liu et al., 2001], skin [Muller-Decker et al., 2002] or pancreas [Colby et al., 2008] developed malignancies of these organs. Disruption of the COX-2 gene suppressed the development of intestinal tumors [Chulada et al., 2000], breast cancer [Howe et al., 2005] or skin papillomas [Tiano et al., 2002]. Moreover, blockade of Cox-2 activity by either NSAIDs or selective Cox-2 inhibitors protected against certain types of cancer [Di Cello et al., 2008; Narko et al., 2005; Oshima et al., 2001].

The contribution of Cox-2 to tumorigenesis is closely linked to PG overproduction. The most abundant eicosanoid produced by many human solid tumors is PGE_2, a potent modulator of tumor cell proliferation, angiogenesis, invasion and immunosuppression [Telliez et al., 2006; Wang and Dubois, 2006]. As PGs are related to tumor development, NSAIDs might be useful cancer preventive agents. Studies have demonstrated that prolonged regular intake (> 2 years) of NSAIDs can decrease the relative risk of developing certain types of cancer such as esophageal, stomach, breast and bladder. Most consistently, a decrease for colon cancer has been observed with reductions of up to 50% [Liao et al., 2007].

Several studies report on a link between Cox-2 and epidermal growth factor receptor (EGFR) pathways in human cancers. The observation that forced expression of Cox-2 stimulates cellular proliferation through induction of the EGFR indicated the possibility of a crosstalk between these two pathways [Wang and Dubois, 2006]. It was shown that PGE_2 can activate the EGFR via the shedding of active EGFR ligands from the plasma membrane or directly by induction of the Src pathway [Ghosh et al., 2010]. EGFR transactivation may result in the stimulation of cell migration through increased PI3K-Akt signalling [Wang and Dubois, 2006] and AP-1-mediated induction of Cox-2 expression and thus PGE_2 expression, resulting in a loop of cross-stimulation [Ghosh et al., 2010]. In this context, preclinical studies support the notion that combined treatment of NSAIDs plus EGFR tyrosine kinase inhibitors is more effective than either single agent alone in several models [Wang and Dubois, 2006].

1.2.4.1 Cyclooxygenases and PGs in Bone and Osteosarcoma

The role of Coxs and PGs in bone homeostasis and bone tumorigenesis in not clearly defined. Generally, Cox-1 is expressed in normal bone tissues, while Cox-2 expression is elevated under various conditions, which makes it difficult to define simple roles of PGs and their receptors in bone metabolism. PGs seem to be involved in bone resorption [Gamradt et al., 2005; Ohshiba et al., 2003] as well as bone formation [Xie et al., 2008; Zhang et al., 2002] processes.

Regarding human osteosarcoma, high levels of Cox-2 expression have been observed in tumor tissue samples by immunohistochemical studies and microarray gene analysis [Dickens et al., 2002; Masi et al., 2007]. However, two studies did not reveal a statistical correlation with prognosis such as histologic classification, stage or location [Dickens et al., 2002; Dickens et al., 2003]. In contrast, Urakawa and coworkers [Urakawa et al., 2009] reported that Cox-2 levels were associated with the occurrence of lung metastasis and could also affect metastasis-free survival. Preclinical studies revealed that selective Cox-2 inhibitors exhibit beneficial effects leading to growth inhibition and induction of apoptosis in various osteosarcoma cell lines [Liu et al., 2008; Masi et al., 2007; Naruse et al., 2006].

Although PGE_2 is considered the major PG in bone metabolism, recent evidence suggests that significant levels of PGD_2 contribute to cellular migration and

matrix calcification of bone tissue [Gallant et al., 2005]. The influence of PGD_2 in the development of human osteosarcoma has not been studied in detail.

Generally, the role of PGD_2 in carcinogenesis seems to be ambiguous. Disruption of PGD_2 synthase in mice accelerates intestinal tumor growth whereas overexpression of PGD_2 synthase shows the opposite outcome, suggesting that PGD_2 has anti-tumor effects [Park et al., 2007]. However, the knock-out of DP has no effect on colon cancer formation and does not support this hypothesis [Mutoh et al., 2002]. The reduced tumor growth might be explained by a shift in the conversion of PGH_2 away from PGE_2 when PGD_2 synthase is overexpressed. Alternatively, the phenotype differences could be related to the activity of the PGD_2-derived product 15d-PGJ_2 which exhibits anti-inflammatory and pro-apoptotic effects in several cell culture studies [Wang and Dubois, 2010].

1.3 Cyclopentenone Prostaglandins

Cyclopentenone PGs are metabolites of the A and J series; PGA_2, PGA_1, and PGJ_2 are formed by dehydration within the cyclopentane ring of PGE_2, PGE_1, and PGD_2. PGJ_2 is metabolized further to yield Δ^{12}-PGJ_2 and 15d-PGJ_2 (Scheme 3). These group of PGs contain a cyclopentenone ring structure, which is characterized by the presence of a chemically reactive α,β-unsaturated carbonyl. This polar carbonyl group contains an electrophilic centre which makes these PGs susceptible to undergoing Michael addition reactions with nucleophiles [Na and Surh, 2003].

Various compounds within the cyclopentenone PG family possess potent anti-inflammatory, anti-neoplastic, and anti-viral activity. Most actions of the cyclopentenone PGs do not appear to be mediated by binding to GPCRs. Rather, the bioactivity of these compounds results from their interaction with other cellular target proteins, including signalling molecules and transcription factors such as PPARγ, NF-κB, and AP-1 [Straus and Glass, 2001].

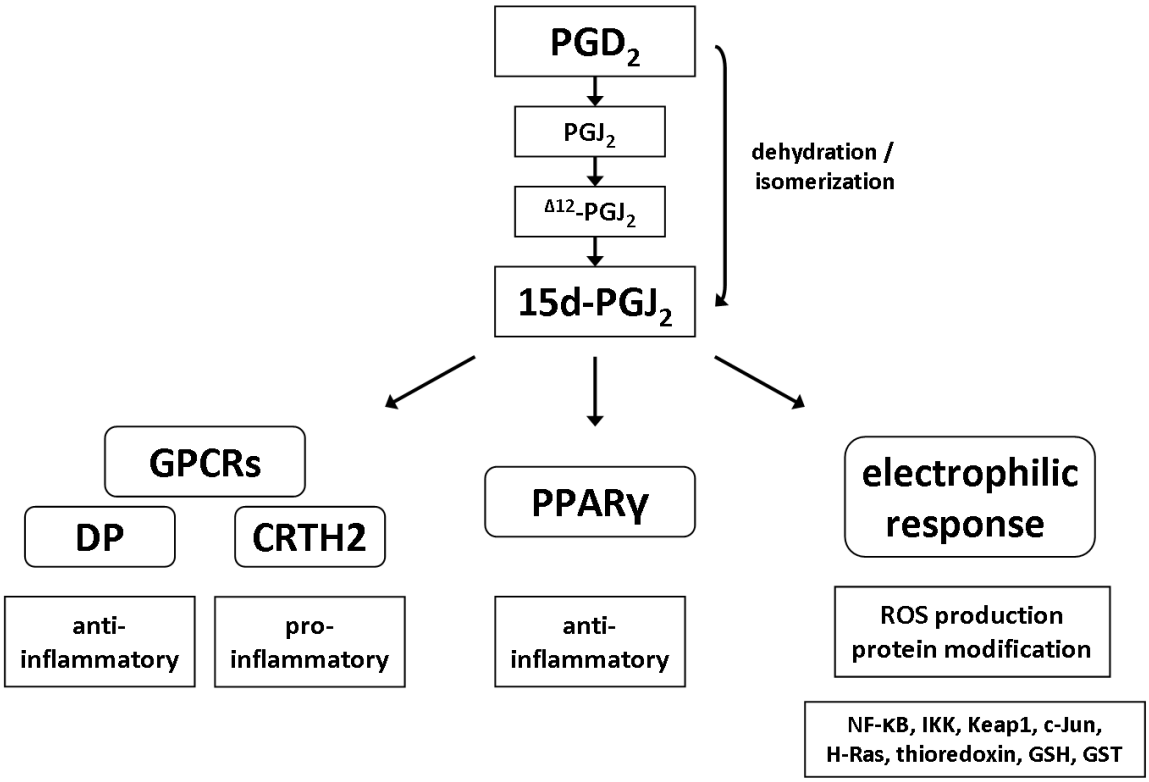

Scheme 3: 15d-PGJ_2 formation and its cellular responses.

PGJ_2 is formed by dehydration within the cyclopentane ring of PGD_2. PGJ_2 is further metabolized to yield Δ^{12}-PGJ_2 and 15d-PGJ_2. 15d-PGJ_2 exerts a number of cellular responses including (i) activation of PGD_2 receptor subtypes DP and CRTH2, (ii) activation of the nuclear receptor PPARγ, and (iii) redox alterations due to increased ROS production and/or modifications of redox-sensitive proteins. The impact of 15d-PGJ_2 on oxidative stress induction has been widely related to the electrophilic character of the cyclopentenone PG, mediated by an α,β-unsaturated carbon group.

1.3.1 The Cyclopentenone 15d-PGJ_2

The PGD_2 metabolite 15d-PGJ_2 regulates a variety of cellular responses like cell growth and differentiation, apoptosis, anti-inflammatory processes, protein turnover, cytoskeletal dysfunction, and redox alterations by various mechanisms [Uchida and Shibata, 2008]. 15d-PGJ_2 has been identified as a ligand for PGD_2 receptor subtypes, DP and CRTH2, as well as for the nuclear receptor PPARγ [Scher and Pillinger, 2005]. Anti-inflammatory effects of 15d-PGJ_2 are associated with interruption of NF-κB and subsequent blockade of inflammatory gene expression. Furthermore, 15d-PGJ_2 induces the expression of phase II detoxification or stress-

responding enzymes, which may confer cellular resistance or adaptation to oxidative stress. Part of biological functions of 15d-PGJ_2 are related to the presence of a reactive α,β-unsaturated carbonyl moiety in the cyclopentenone ring (at position C9). Via this polar group 15d-PGJ_2 directly modifies target molecules provoking functional alterations [Na and Surh, 2003], e. g. NF-κB subunit p65 [Straus et al., 2000], c-jun [Perez-Sala et al., 2003], and H-ras [Oliva et al., 2003] (Scheme 3).

1.3.1.1 15d-PGJ_2 and PGD_2 Receptor Subtypes

PGD_2 exerts its effects by binding and activating two distinct GPCRs – DP and CRTH2. DP is member of the prostanoid GPCR subfamily and is expressed by a variety of cell types [Hata and Breyer, 2004]. This receptor is coupled to $G_{\alpha s}$ and ligand binding activates adenylyl cyclase and raises intracellular cAMP levels and PKA activity [Boie et al., 1995]. In contrast, CRTH2 is far exclusively expressed in Th2 cells, T cytotoxic cells, eosinophils, and basophils and may play a role in allergic inflammation, through induction of chemotactic migration and/or the activation of these immune cells [Hata and Breyer, 2004; Scher and Pillinger, 2005]. CRTH2 is a member of the formyl peptide receptor superfamily and is coupled to $G_{\alpha i}$ which inactivates adenylyl cyclase activity and intracellular cAMP levels [Sawyer et al., 2002]. Furthermore, PGD_2 [Sawyer et al., 2002] and 15d-PGJ_2 [Monneret et al., 2002] induced CRTH2-dependent intracellular calcium mobilization; PGD_2-mediated calcium flux was sensitive to pertussis toxin and could be accelerated by overexpression of $G_{\alpha 15}$ [Sawyer et al., 2002].

PGD_2 analogues and metabolites exert different affinities to these receptors types. 15d-PGJ_2 has been identified as a weak DP agonist being around 300 times less potent than PGD_2 [Sawyer et al., 2002]. In contrast, 15d-PGJ_2 activates CRTH2 in the low nanomolar range, comparable with PGD_2 concentrations needed for CRTH2 stimulation [Monneret et al., 2002; Sawyer et al., 2002]. Thus, one mechanism for 15d-PGJ_2 action may involve activation of PGD_2 receptors. CRTH2-dependent activation of eosinophils in response to 15d-PGJ_2 contributes to allergic inflammation processes [Almishri et al., 2005; Monneret et al., 2002] whereas 15d-PGJ_2-dependent DP activation resulted in anti-inflammatory responses; 15d-PGJ_2, synthesized during inflammatory processes, regulates leukocyte influx and

monocyte-derived macrophage efflux from inflammation sites to draining lymph nodes leading to resolution [Rajakariar et al., 2007].

1.3.1.2 15d-PGJ_2 and PPARγ

PPARs are nuclear transcription factors that regulate biochemical events for maintaining lipid homeostasis such as adipocyte differentiation, and regulation of lipoprotein and lipid metabolism [Kim and Surh, 2006]. PPARs form heterodimers with retinoid X receptors (RXRs) and activate gene expression by binding to PPAR response elements (PPRE) located in enhancer or promoter regions of target genes. The PPARs exhibit different patterns of tissue-specific expression and distinct binding specificities for a wide range of ligands. The PPAR family includes three subtypes, PPARα, β/δ, and γ. PPARγ is the molecular target for thiazolidinedione antidiabetic drugs such as troglitazone and rosiglitazone [Straus and Glass, 2007]. In 1995, 15d-PGJ_2 was identified as a high affinity ligand for PPARγ [Forman et al., 1995; Kliewer et al., 1995]. 15d-PGJ_2 upregulates the expression, transcriptional activity, and DNA binding activity of PPARγ, and many of the cellular events mediated by 15d-PGJ_2 have been shown to be PPARγ-dependent [Kim and Surh, 2006]. For example, 15d-PGJ_2 induces apoptosis of T cells [Harris et al., 2002] and endothelial cells [Bishop-Bailey and Hla, 1999] by a PPARγ-dependent mechanism. Recent findings show that 15d-PGJ_2 also exerts a variety of PPARγ-independent cellular responses, e.g. activation of MAPKs [Kim et al., 2008b; Lim et al., 2007], induction of apoptosis [Cho et al., 2006; Lee et al., 2008], inactivation of p53 [Kim et al., 2010], and modulation of Cox-2 expression [Kim et al., 2008a].

1.3.1.3 15d-PGJ_2 and NF-κB

NF-κB is an inducible and ubiquitously expressed transcription factor responsible for the regulating the expression of genes involved in cell survival, cell adhesion, inflammation, cell differentiation, and growth. Active NF-κB complexes are dimers of various combinations of the Rel family of polypeptides consisting of p50 (NF-κB1), p52 (NF-κB2), c-Rel, v-Rel, Rel A (p65), and Rel B. In most resting cells, NF-κB is retained in the cytoplasm by binding to one of the inhibitory IκB proteins, which blocks the nuclear localization sequences of NF-κB. NF-κB is activated in response to a wide variety of stimuli that promote the dissociation of IκBα through

phosphorylation by an IKK complex followed by ubiquitination and degradation. Thus unmasking of the nuclear localization sequence of NF-κB allows NF-κB to enter the nucleus and bind to κB-regulatory elements [Chun and Surh, 2004].

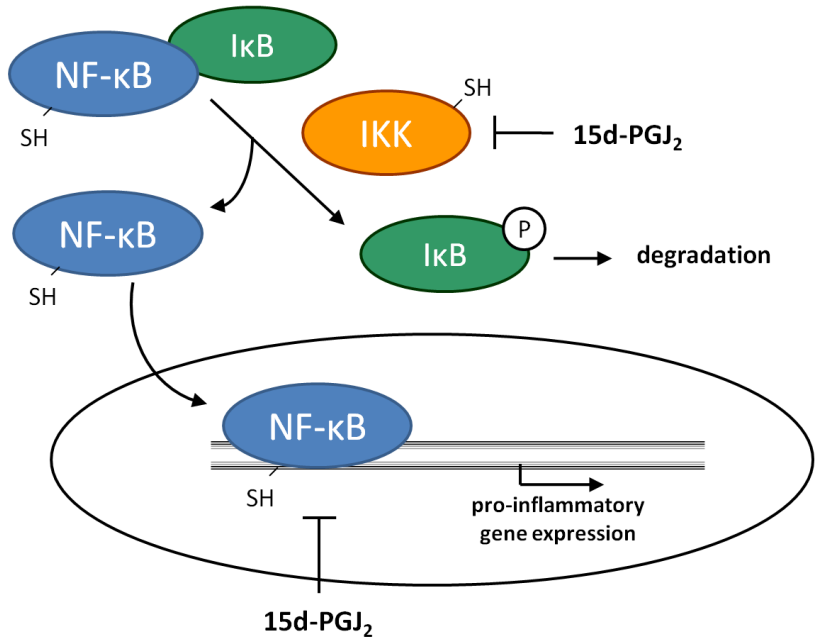

Scheme 4: Proposed mechanisms responsible for NF-κB inhibition by 15d-PGJ$_2$. 15d-PGJ$_2$ inhibits NF-κB-dependent gene expression either by inactivation of IKK activity, thereby preventing IκB degradation and nuclear entry of NF-κB, or direct interference with binding of NF-κB to a target DNA sequence. The electrophilic carbonyl group of 15d-PGJ$_2$ may cause thiol modifications in IKK and the p50/p65 subunit of NF-κB, leading to suppression of NF-κB activation. The scheme was adapted from [Na and Surh, 2003].

It has been reported that 15d-PGJ$_2$ strongly inhibits NF-κB-dependent transcription by two distinct mechanisms (Scheme 4). First, 15d-PGJ$_2$ can interrupt NF-κB-dependent gene expression through covalent modifications of critical cysteine residues in IKK with subsequent prevention of IκBα degradation and nuclear entry of NF-κB [Rossi et al., 2000; Straus et al., 2000]. Second, 15d-PGJ$_2$ interferes with NF-κB binding to target DNA sequences without blocking IκB degradation and nuclear translocation of NF-κB. This is more likely to be achieved by alkylation of a conserved cysteine residue located in the DNA binding domain of Rel proteins [Cernuda-Morollon et al., 2001; Straus et al., 2000].

1.3.1.4 Redox Alterations and Antioxidant Response by 15d-PGJ_2

15d-PGJ_2 can affect the intracellular redox regulation by various mechanisms. 15d-PGJ_2 reacts via the electrophilic carbonyl group of the cyclopentenone ring with free sulfhydryl groups of cysteine residues located in reduced glutathione (GSH) [Brunoldi et al., 2007; Paumi et al., 2003] or cellular proteins that are involved in the intracellular redox regulation [Straus and Glass, 2001]. Within the vascular wall, there are several sources of ROS generation, including NADPH oxidases, cytochrome *P*-450, xanthine oxidase, uncoupled nitric oxide synthase, and mitochondria. 15d-PGJ_2 induced xanthine oxidase activity in a cell free system; in human lymphocytes, the xanthine oxidase inhibitor allopurinol reversed 15d-PGJ_2-mediated induction of HO-1 expression [Alvarez-Maqueda et al., 2004]. Landar and coworkers [Landar et al., 2006] showed that fluorescently labeled 15d-PGJ_2 was localized in mitochondria and increased intracellular ROS levels. 15d-PGJ_2-mediated mitochondrial dysregulation is related to a direct inhibition of mitochondrial complex I [Martinez et al., 2005; Pignatelli et al., 2005]. Furthermore, 15d-PGJ_2 increases superoxide anion production by the membrane NADPH oxidase enzyme complex [Huang et al., 2002]. In addition to a reduction of intracellular GSH levels, 15d-PGJ_2 decreases the activity of GSH peroxidase [Kondo et al., 2001], an important enzyme involved in the protection from oxidative stress by reducing H_2O_2 to water. Furthermore, the production of lipid peroxidation derived aldehydes such as acrolein and 4-hydroxy-2-noneal as well as accumulation of oxidized proteins was observed as a consequence of elevated intracellular ROS levels in response to 15d-PGJ_2 [Kondo et al., 2001].

Under oxidative stress conditions, cells respond with the induction of redox-regulated and/or stress-responding genes. Beside the upregulation of cellular defensive enzymes such as heme oxygenase 1 (HO-1) [Alvarez-Maqueda et al., 2004; Diers et al., 2009; Oh et al., 2008], peroxiredoxin [Itoh et al., 2004], and heat shock proteins [Ianaro et al., 2003; Zhang et al., 2004], 15d-PGJ_2 induces the synthesis of phase II detoxification enzymes including γ-glutamyl cysteine ligase (GCL) [Brechbuhl et al., 2009; Chen et al., 2006; Levonen et al., 2001], glutathione *S*-transferase [Kawamoto et al., 2000; Kobayashi et al., 2009], GSH peroxidase [Kondo et al., 2002], and NAD(P)H:quinine oxidoreductase [Hosoya et al., 2005; Yu et al., 2006]. Redox sensitive transcription factors which might be involved in the regulation of these stress-inducible proteins and which have been shown to be

activated by 15d-PGJ_2 are Nrf-2, NF-κB, AP-1, STAT, p53, and hypoxia inducible factor 1 [Kim and Surh, 2006].

1.3.1.5 15d-PGJ_2 and Nrf-2

The transcriptional activation of the chemoprotective response genes by cyclopentenone PGs has been traced to a *cis*-acting transcriptional enhancer called the antioxidant/electrophile response element (ARE/EpRE). Nuclear erythroid factor 2-related factor 2 (Nrf-2), a basic-leucine zipper transcription factor, has been reported to positively regulate the ARE/EpRE-mediated expression [Na and Surh, 2003]. Under normal physiological conditions, Nrf-2 is sequestered by the cytoplasmic Kelch-like ECH-associated protein 1 (Keap1) [Itoh et al., 1999] which directs Nrf-2 to cullin 3-dependent ubiquitination and degradation (Scheme 5). Keap1 is an extremely thiol-rich protein and thought to act as an electrophilic stress sensor. Under oxidative or electrophilic stress conditions, critical cysteine residues of Keap1 are modified, allowing Nrf-2 to escape the degradation pathway and translocate to the nucleus [Cullinan et al., 2004; Kobayashi et al., 2004]. Nrf-2 forms heterodimers with small Maf proteins which regulate ARE/EpRE-driven gene expression [Itoh et al., 1997].

The cyclopentenone 15d-PGJ_2 forms adducts with Keap1 [Hosoya et al., 2005] and modifies at least two cysteine residues (Cys273 and Cys288) permitting Nrf-2-driven expression of stress enzymes [Kobayashi et al., 2009]. In addition to 15d-PGJ_2, other lipid oxidation products such as 15-A_{2t}-isoprostane and 4-hydroxy-2-nonenal activate ARE/EpRE activities by modification of Keap1 allowing Nrf-2 translocation [Levonen et al., 2004]. Next to Keap1 modifications, signalling pathways have been proposed to participate in Nrf-2-dependent gene expression. Several protein kinases, such as PKC, PI3K, p42/44 MAPK, p38 MAPK, and RNA-activated protein kinase-like ER kinase have been shown to be activated after treatment with Nrf-2-activating agents [Kansanen et al., 2009].

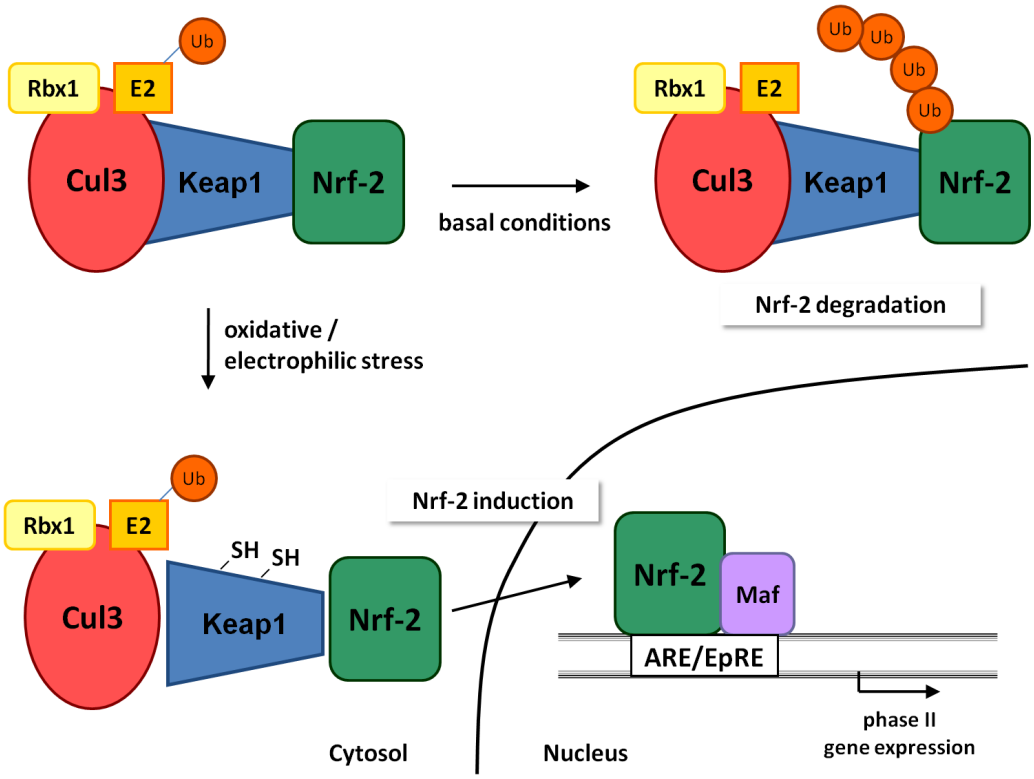

Scheme 5: Proposed model for Nrf-2-mediated phase II enzyme activation.
Under basal conditions, Keap1 functions as an adaptor protein in the cullin 3 (Cul3)-based E3 ligase system, mediating ubiquitination and proteasomal degradation of Nrf-2. In the presence of electrophiles such as 15d-PGJ_2, modifications of Keap1 cysteines lead to conformational changes in Keap1 resulting in the detachment of Keap1 from Cul3. In this setting, the ubiquitination and degradation of Nrf-2 is disturbed. Nrf-2 translocates to the nucleus and forms heterodimers with Maf proteins. The Nrf-2-Maf complexes bind to AREs/EpREs and drive phase II genes expression. The scheme was adapted from [Kansanen et al., 2009].

1.3.1.6 15d-PGJ_2 and HO-1

Heme oxygenases (HOs) are key enzymes in heme catabolism that catalyze the conversion of heme to carbon monoxide (CO) and bilirubin with a concurrent release of iron. Two HO isoforms, HO-1 and HO-2, are encoded by different genes. HO-1 is barely expressed under basal conditions and can be induced by oxidative stress-causing agents such as UV, LPS, ROS, and reactive nitrogen species [Kim and Surh, 2008]. Oxidative stress in response to heavy metals such as Co^{2+}, Cr^{3+}, and Zn^{2+} caused increased HO-1 expression in MG-63 cells [Aina et al., 2007; Fleury

et al., 2006]. HO-1 is also upregulated by cyclopentenone PGs such as Δ^{12}-PGJ_2 and 15d-PGJ_2 [Na and Surh, 2003]. HO-2 is constitutively expressed in most tissues, and its levels are relatively unaffected by factors inducing HO-1 [Kim and Surh, 2008].

HO-1 expression is mainly mediated via AREs/EpREs present in the promoter regions of many antioxidant or detoxifying enzymes, which are under the control of Nrf-2 [Kim and Surh, 2008]. Moreover, regulatory elements such as the AP-1 site, NF-κB site, heme- and cadmium-response elements, phorbol ester-response elements as well as an early growth response (Egr)-1 binding site have been identified in the regulatory regions of the HO-1 gene [Ryter et al., 2006]. Egr-1 is an immediate early response gene that is rapidly expressed in response to various stress stimuli including hypoxia [Khachigian, 2006]. Egr-1 contributes to elevated HO-1 expression in human lung tissue [Chen et al., 2010] and mouse fibroblasts [Yang et al., 2001]. It has also been reported that PPARγ activation upregulates HO-1 expression [Kronke et al., 2007; Lin et al., 2006; Ptasinska et al., 2007]. PPARγ knock-down and pharmacological inhibition of PPARγ by T0070907 abolished HO-1 protein induced by nitric oxide [Ptasinska et al., 2007]. Furthermore, Kronke et al. identified a PPRE motif in the HO-1 promoter located at -623 bp which is transcriptionally activated by PPARγ agonists. It was further demonstrated that mutations of AREs/EpREs did not affect PPARγ-induced HO-1 promoter activity, which implies that expression of HO-1 is directly regulated by PPARγ [Kronke et al., 2007].

The biological functions of HO-1 are believed to be associated with a fundamental adaptive and defensive response to oxidative stress and other cellular injuries. This might be beneficial in normal cells but might account for an association between HO-1 induction and tumorigenesis under certain conditions. Indeed, elevated HO-1 expression was associated with increased cancer cell growth because of its anti-oxidative and anti-apoptotic effects [Kim and Surh, 2008]. The angiogenic potential of HO-1 is linked to increased expression of VEGF [Kim et al., 2006a] and MMP-1 [Kim et al., 2009] which have been identified as downstream targets of HO-1. It is proposed that the anti-apoptotic action of HO-1 in cancerous cells is mostly attributable to its heme degradation products [Brouard et al., 2002; Fang et al., 2003]. HO-1/CO has been shown to be involved in the downregulation of inducible nitric oxide synthase, an inducer of oxidative stress by release of nitric oxide [Hong et al., 2008; Lee et al., 2003]. Conversely, HO-1 activity may also contribute to intracellular

ROS production by release of iron in course of the conversion of heme. Zinc protophorphyrin, an inhibitor of HO-1 activity, and iron chelators reversed a delayed increase of ROS mediated by 15d-PGJ_2 in human breast cancer cells [Kim et al., 2009].

In primary osteoblasts, upregulated HO-1 expression resulted in impaired maturation and mineralization by its downstream products bilirubin, CO, and iron. In this case upregulation of HO-1 during oxidative or inflammatory processes is suggested to be involved in bone loss [Lin et al., 2010].

1.4 Apoptosis

Apoptosis or programmed cell death is a regulated physiological process that plays a critical role in controlling the number of cells in development and throughout an organism's life by removal of infected, injured or aged cells at the appropriate time. Apoptosis is characterized by specific biochemical and morphological changes including cellular and nuclear shrinking, membrane blebbing, formation of apoptotic bodies, chromatin condensation, DNA fragmentation, and phosphatidylserine externalization. Apoptotic cells are rapidly phagocytosed prior to the release of intracellular contents without induction of an inflammation response. These features are distinct from those observed in cells undergoing necrotic cell death [Hengartner, 2000; Movassagh and Foo, 2008; Zimmermann et al., 2001]. However, a dysregulation of apoptosis is involved in a wide range of pathological conditions, including cancer. Therefore, the knowledge of the mechanisms involved in apoptosis may be important for the design of new therapeutic approaches [Zimmermann et al., 2001].

1.4.1 Caspases

Caspases are central regulators of apoptotic cell death. Caspases are aspartate-specific cysteine proteases conducting the proteolytic cleavage by a conserved cysteine side chain after aspartate residues in a number of intracellular

substrates. These enzymes are activated consecutively as initiator caspases (caspase-2, -8, -9, and -10) act usually upstream of effectors (also known as executioner) caspases (caspase-3, -6, and -7). The zymogens (precursors) of effector caspases are present as inactive dimers which are activated by a proteolytic cleavage of intersubunit linkers allowing the rearrangement of catalytic chains to form an active site. In contrast, inactive initiator caspases exist as monomers and are activated by dimerization regardless if they are cleaved or uncleaved [Riedl and Salvesen, 2007].

1.4.2 Apoptotic Pathways

There are three principal routes described that lead to the activation of caspases and induction of apoptotic cell death [Hengartner, 2000; Movassagh and Foo, 2008].

(i) The extrinsic or receptor-mediated pathway involves transmembrane death receptors which are activated upon ligand binding and recruit adapter proteins and procaspases to form a so-called death-inducing signalling complex (DISC).

(ii) The intrinsic or mitochondrial pathway initiates cell death following intracellular or extracellular signals. Members of the Bcl-2 family are involved in the permeabilization of the outer mitochondrial membrane leading to a release of pro-apoptotic proteins like caspases and cytochrome C and subsequent formation of the apoptosome. Crosstalk and integration between the death-receptor and mitochondrial pathways is provided by Bid, a pro-apoptotic Bcl-2 family member.

(iii) The third pathway involves the activation of caspase-12 in the ER in response to impaired protein folding or Ca^{2+} signalling.

Finally, all three pathways converge on the level of effector caspase activation and subsequent targeting of various intracellular molecules provoking structural alterations and DNA degradation resulting in irreversible loss of viability. More than 100 caspase targets have been identified that are involved in the regulation of programmed events leading to morphological changes and finally cell death [Hengartner, 2000; Mallat and Tedgui, 2000]. Well-studied caspase targets are the intermediate filament of the nuclear envelope lamin [Cuvillier et al., 1998], the DNA-repair enzyme poly(ADP-ribose) polymerase (PARP) [Tewari et al., 1995], and the inhibitor of caspase-activated deoxyribonuclease [Sakahira et al., 1998].

1.4.2.1 Death Receptor-mediated Apoptosis

The TNF receptor (TNFR) family is a group of type I transmembrane receptors containing characteristic cysteine-rich extracellular domains and conserved intracellular regions, called “death domains” (DD). Death receptors of the TNFR family include TNFR1, Fas (CD95/Apo-1), DR3/WSL, and the TNF-related apoptosis-inducing ligand (TRAIL)/Apo-2L receptors also designated as death receptor (DR)4 and DR5, respectively. The death receptors are constitutively expressed in many tissues whereas ligand expression is often restricted to cell type or certain stimuli. The most extensively studied signal transduction leading to induction of apoptosis is initiated by binding of the FasL to the Fas receptor (Scheme 6). Upon activation, Fas receptors oligomerize and form a DISC by recruiting adapter proteins to the receptor’s DD [Zimmermann et al., 2001]. In case of the Fas receptor and the DR3, the Fas-associated DD (FADD) protein is required [Chinnaiyan et al., 1995]. DR4 signalling can also occur in the absence of FADD [Yeh et al., 1998]. Signalling from TNFR1 needs an additional adapter protein, TNFR-1-associated DD (TRADD) [Hsu et al., 1996] as prerequisite for FADD binding. Through this adapter proteins, procaspase-8 [Ahmad et al., 1997; Muzio et al., 1996] or procaspase-10 [Fernandes-Alnemri et al., 1996] are recruited to the DISC and activated by dimerization and/or autocatalytic cleavage [Riedl and Salvesen, 2007; Zimmermann et al., 2001]. Caspase-8 activation can be blocked by the degenerated caspase homologue FADD-like IL-1β-converting enzyme-like inhibitory protein (FLIP) [Irmler et al., 1997]. Initiator caspases can stimulate apoptosis via two cascades: (1) they directly activate effector caspases [Fernandes-Alnemri et al., 1996], or (2) they influence the mitochondrial pathway via cleavage of the pro-apoptotic BH3-only molecule Bid into truncated Bid (tBid) [Luo et al., 1998]. tBid translocates to the mitochondria where it is involved in the membrane permeabilization process when other pro-apoptic proteins, Bak or Bax, are present [Korsmeyer et al., 2000].

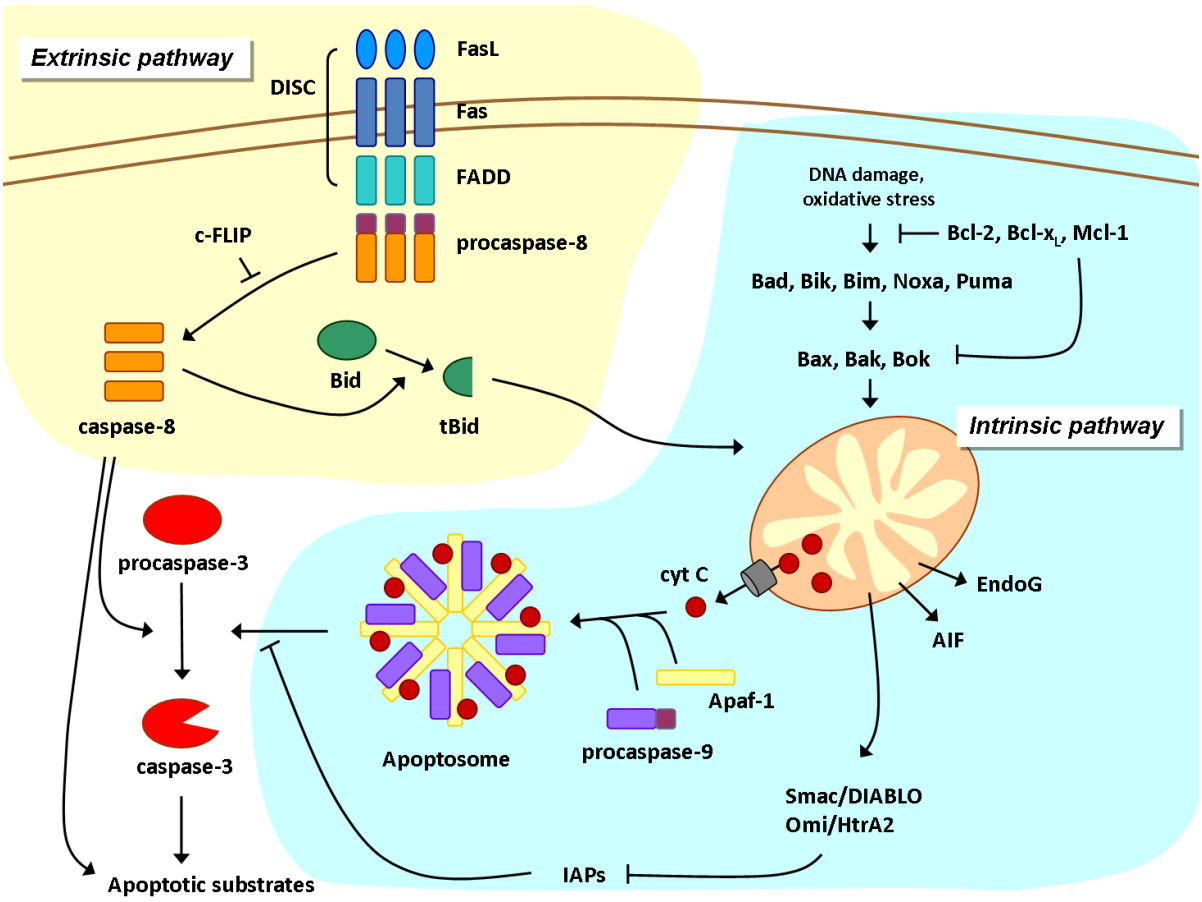

Scheme 6: Apoptosis overview.

The scheme provides important regulators involved in the death-receptor-mediated extrinsic pathway and mitochondria-mediated intrinsic pathway leading to programmed cell death. The scheme was adapted from [Hengartner, 2000].

1.4.2.2 Mitochondria-mediated Pathway

The mitochondrial pathway is activated in response to extracellular and intracellular stimuli such as toxins, radiation, oxidative stress, and DNA damage. Members of the Bcl-2 family are potent regulators of this pathway by controlling the mitochondrial permeability and the release of apoptotic factors such as cytochrome C to the cytoplasm [Movassagh and Foo, 2008; Zimmermann et al., 2001] (Scheme 6).

The Bcl-2 family members have generally been grouped into three classes depending on their activities and the particular Bcl-2 homology (BH) domains conserved within the protein. The class I comprises of anti-apoptotic molecules that contain BH domains 1, 2, 3, and 4; members are Bcl-2, Bcl-x_L, and myeloid cell leukemia 1 (Mcl-1). The class II (also known as Bax family) promotes apoptosis, and

contains BH domains 1, 2, and 3; these include Bax, Bak and Bok. The third class also displays a pro-apoptotic activity and is often referred to as BH3-only proteins; class III members such as Bad, Bik, Bid, Bim, Noxa, and Puma contain just BH domain 3 [Pradelli et al., 2010]. Both groups of pro-apoptotic proteins are required to initiate apoptosis: the BH3-only proteins seem to act as damage sensors and direct antagonists of the pro-survival proteins, whereas the Bax-like proteins act further downstream, probably in mitochondrial disruption [Cory and Adams, 2002]. In their active state, Bcl-2 family members form homodimers, but pro- and anti-apoptotic proteins can also heterodimerize and neutralize or potentiate each other's functions [Hengartner, 2000; Zimmermann et al., 2001].

A critical apoptotic event is the permeabilization of mitochondria. This process is under tight control of Bcl-2 family members and is most likely regulated by protein-protein interactions. Upon cellular stress signals, pro-apoptotic Bcl-2 proteins such as Bax and Bak shuttle from the cytosol to mitochondria where they are involved in the mitochondrial pore formation [Movassagh and Foo, 2008]. However, the exact mechanism is still under investigation. One model proposes that Bak and Bax oligomerize and form channels by their own [Antignani and Youle, 2006]. Alternatively, these molecules might interact with components of the existing mitochondrial permeability transition pore – for example, the voltage-dependent anion channel – to create a larger channel [Narita et al., 1998]. The anti-apoptotic proteins Bcl-2 and Bcl-x_L prevent the permeabilization of the mitochondrial membrane by attaching to the pore-forming pro-apoptotic proteins [Cory and Adams, 2002]. In contrast, pro-apoptotic BH-3-only class members such as Bid, Bim, Puma, and Noxa promote mitochondrial disruption either by direct activation of Bax and Bak or interference with anti-apoptotic Bcl-2 proteins [Desagher et al., 1999; Nakano and Vousden, 2001; Oda et al., 2000; Zong et al., 2001]. The BH3-only protein Bad is phosphorylated in its inactive state; upon dephosphorylation, Bad binds to class I Bcl-2 familiy members, thus inactivating their anti-apoptotic character [Wang et al., 1999; Yang et al., 1995].

The mitochondrial disruption is linked to a dissipation of the mitochondrial inner transmembrane potential and increased generation of ROS [Zamzami et al., 1995]. Consequently, procaspases and the key pro-apoptotic factor cytochrome C are irreversibly released from the mitochondria intermembrane compartment into the cytosol [Hengartner, 2000; Zimmermann et al., 2001]. In the presence of cytochrome

C, the apoptosis activating factor 1 (Apaf-1) oligomerizes which allows the recruitment of procaspase-9 [Li et al., 1997]. This wheel-shaped complex is called apoptosome and can be seen as the (soluble) receptor of the intrinsic pathway [Riedl and Salvesen, 2007]. Other caspase-regulating pro-apoptotic proteins released by mitochondria are Smac/DIABLO [Du et al., 2000] and Omi/HtrA2 [Suzuki et al., 2001]; both block the activity of cytosolic caspase inhibitory proteins (IAPs). Caspase-independent mitochondrial factors include apoptosis-inducing factor (AIF) [Daugas et al., 2000] and endonuclease G (EndoG) [Li et al., 2001b], which translocate to the nucleus and are involved in DNA fragmentation.

1.4.2.3 Other pathways

Another organelle involved in the regulation of apoptosis is the ER. At least two different mechanisms are involved: unfolded protein response and Ca^{2+} signalling [Movassagh and Foo, 2008]. During ER stress, ER-localized kinases such as RNA-activated protein kinase-like ER kinase [Ma et al., 2002] as well as mitochondria-associated kinases such as Apoptosis signal-regulating kinase-1 (Ask-1) [Nishitoh et al., 2002] are activated and involved in induction of apoptosis. Increased Ca^{2+} release may directly induce Bax- and Bak-mediated permeabilization of the mitochondrial membrane and release of apoptotic factors [Oakes et al., 2005]. The before mentioned processes influence the mitochondrial pathway, whereas activation of procaspase-12 is an ER-specific event. Once activated, caspase-12 translocates from the ER to the cytoplasm, cleaves and activates procaspase-9 independently of apoptosome formation [Morishima et al., 2002; Nakagawa et al., 2000; Yoneda et al., 2001].

2 OBJECTIVES

PGs are important regulators of oncogenesis and might also be involved in the induction and progression of human osteosarcoma. PGE_2 is considered the major PG in bone metabolism, however, recent evidence suggests that PGD_2 contributes to cellular migration and matrix calcification of bone tissue. PGD_2 is released by osteoblasts and may therefore be present in bone tumor surrounding areas. Spontaneous dehydration of PGD_2 during inflammatory events leads to the formation of the cyclopentenone 15d-PGJ_2 which is often designated as an anti-inflammatory PG. 15d-PGJ_2 elicits various cellular responses via PPARγ-dependent and PGD_2-receptor-dependent mechanisms, however, recent evidence suggests that many cellular events are related to its electrophilic character. 15d-PGJ_2 has also been identified to differently regulate Cox-2 expression in several cell types. This represents an interesting mechanism in PG feedback regulation as Cox-2 is a rate-limiting enzyme in PG metabolism.

In the first part of the thesis, it was aimed at investigating 15d-PGJ_2-mediated activation of signalling cascades and Cox-2 expression in human osteosarcoma MG-63 cells with respect to following aspects:

- Cox-2 expression in response to 15d-PGJ_2 should be followed in a concentration- and time-dependent manner.
- The phosphorylation status of the main MAPK routes – p38 MAPK, p42/44 MAPK and JNK – should be determined by phospho-specific antibodies.
- The activation of the EGFR and potential downstream activation of MAPKs should be elucidated.
- The participation of activated signalling pathways in elevated Cox-2 expression and prolonged Cox-2 mRNA half-life should be clarified by pretreatment of cells with specific inhibitors of the respective proteins.
- The involvement of PPARγ and PGD_2 receptors in the observed events should be elucidated by knock-down strategies and pharmacological inhibitors.
- Alterations in the intracellular redox status should be analyzed by detections of ROS and GSH levels. A contribution of ROS accumulation to 15d-PGJ_2-mediated events should be studied by pretreatment with antioxidant GSH

precursors. As redox alterations are related to the electrophilic carbon centre of 15d-PGJ_2, it should be tested if the non-electrophilic structural analogue 9,10-dihydro-15d-PGJ_2 fails to mimic the observed effects.

- Functional activity of Cox-2 should be determined by synthesis of PGE_2 and $PGF_{2\alpha}$ from AA as the basic substrate.

There is evidence that many of the cellular events mediated by 15d-PGJ_2 are related to the ability to modulate the intracellular redox status. Increased ROS levels were connected to cytotoxic and apoptotic responses as well as to the regulation of phase II detoxification enzymes. Thus, in the second part of the thesis, it was aimed at exploring the impact of the cyclopentenone on cell viability, apoptosis, and cytoprotective events in MG-63 cells considering following investigations:

- The time- and concentration-dependent impact of 15d-PGJ_2 on cell viability and the regulation of well-described apoptotic markers, caspase-3 and PARP, should be followed.
- A potential contribution of MAPKs, PPARγ, PGD_2 receptors and imbalanced redox status should also be documented in this part.
- To clarify if 15d-PGJ_2-mediated cell death occurs in receptor- or mitochondria-dependent manner, the activation of caspase-8 and expression profiles of Bcl-2 family members such as Bcl-2, Bax, and Puma should be investigated.
- It should be elucidated if 15d-PGJ_2 triggers cytoprotective events such as elevated intracellular GSH concentrations and induction of stress-responsive genes like HO-1 after long-termed incubation periods.
- The nuclear translocation of the stress-related transcription factors Nrf-2 and Egr-1, as potential regulators of HO-1 expression, should be followed.
- To investigate if increased GSH levels influence the stage of cell viability and apoptosis markers, experiments should be performed in the presence of the GSH synthesis inhibitor BSO.

3 MATERIALS AND METHODS

3.1 Materials

3.1.1 Cell Culture Materials

Fetal calf serum (FCS) and trypsin/EDTA were from PAA (Linz, Austria). Gentamycin, α-minimum essential medium (α-MEM), and Oligofectamine® were from Gibco Invitrogen (Lofer, Austria). Tissue culture flasks (75 cm^2) were from Greiner Bio-One (Frickenhausen, Germany), 100 mm culture dishes, 6-well plates and 12-well plates were from Corning Incorporated (New York, NY, USA).

3.1.2 RNA Isolation Materials

QIAshredder and RNeasy® Mini Kit were from QIAGEN (Hilden, Germany). DNase-I was from Gibco Invitrogen (Lofer, Austria). Recombinant RNasin® Ribonuclease Inhibitor was from Promega (Mannheim, Germany).

3.1.3 RT-PCR Materials

OneStep RT-PCR Kit was purchased from QIAGEN (Hilden, Germany). Agarose LE and DNA Molecular Weight Marker IX (0.072 - 1.35 kbp) were from Roche Diagnostics (Mannheim, Germany). Ethidium bromide solution was from Invitrogen™ life technologies (Carlsbad, CA, USA) and 5x TBE buffer was from Eppendorf (Hamburg, Germany). All primers used in RT-PCR analysis were purchased by TIB MOLBIOL (Berlin, Germany).

3.1.4 Quantitative PCR Materials

High-Capacity cDNA Reverse Transcription Kit and MicroAmp® Optical 96-well Reaction Plates were from Applied Biosystems (Foster City, CA, USA). QuantiFast™ SYBR® Green PCR mastermix and QuantiTect® Primer Assays were from QIAGEN (Hilden, Germany).

3.1.5 Protein Isolation and Western Blot Materials

Lysis buffer components HEPES, EDTA, glycerol, Triton X-100, $Na_4P_2O_7$ and Na_3VO_4 were from Sigma-Aldrich (Saint Louis, MO, USA), and NaF was from Fluka (Buchs, Switzerland). Complete Mini protease inhibitor cocktail tablets were from Roche Applied Science (Vienna, Austria). Bovine serum albumin (BSA) and non-fat dry milk were from Sigma-Aldrich (Saint Louis, MO, USA).

NuPAGE® 4-12% Bis-Tris Gels (1 mm and 1.5 mm), NuPAGE® MES and MOPS SDS running Buffer, NuPAGE® LDS sample buffer, NuPAGE® sample reducing agent, SeeBlue® Plus prestained standard, and nitrocellulose membranes (0.45 µm pore size) were from Gibco Invitrogen (Lofer, Austria). Hyperfilm™ MP was from GE Healthcare (Vienna, Austria). Restore™ Western Blot Stripping Buffer, SuperSignal® West Pico chemiluminescent substrate and BCA™ Protein Assay Kit were from Pierce Biotechnology, Inc. (Rockford, IL, USA). Immobilon Western Chemiluminescent HRP substrate was from Millipore (Billerica, MA, USA).

3.1.6 Antibodies

3.1.6.1 Primary Antibodies

Phospho-specific anti-p38 MAPK antibody (Tyr180/Tyr182; pp38), phospho-specific anti-p42/44 MAPK antibody (Tyr202/Tyr204; E10; pp42/44), anti-SAPK/JNK antibody (JNK1/2), anti-caspase-3 antibody, anti-Puma antibody, and anti-Bax antibody were from Cell Signaling Technology (Beverly, MA, USA). Anti-ERK1 antibody (K23; p42/44), anti-Cox-2 antibody (C20), anti-p-Tyr antibody (PY99), anti-EGFR antibody (1005), anti-NF-κB p65 antibody (C-20), anti-lamin A/C antibody (H-110), anti-caspase-8 (4H46), anti-Bcl-x_L antibody (S-18) and anti-β-actin antibody (C4) were from Santa Cruz Biotechnology, Inc. (Santa-Cruz, CA, USA). Anti-p38 MAPK antibody was from Sigma-Aldrich (Saint Louis, MO, USA). Anti-Cox-1 antibody (ALX-804-030) was from Enzo Life Sciences (Lörrach, Germany). Phospho-specific anti-SAPK/JNK antibody (Tyr183/Tyr185; pJNK1/2) was from BD Biosciences Pharmingen (San Diego, CA, USA). Anti-PARP antibody (C-2-10) was from BIOMOL (Hamburg, Germany). Anti-Bcl-2 antibody was from Calbiochem (La Jolla, CA, USA).

3.1.6.2 Secondary Antibodies

Horseradish-peroxidase (HRP)-conjugated goat anti-rabbit IgG and HRP-conjugated donkey anti-goat IgG were from Jackson Immunoresearch Laboratories (West Grove, PA, USA). HRP-conjugated goat anti-mouse IgG was from Rockland (Gilbertsville, PA, USA).

3.1.7 Agonists, Antagonists and Inhibitors

15d-PGJ_2, 9,10-dihydro-15d-PGJ_2, PGD_2, AG1478, AG1296, FR-122047, T0070907, manumycin A, CAY10512, MK-0524, dihydro-keto-(DK)-PGD_2, BW 245c, CAY10471, D_4-PGE_2, and D_4-$PGF_{2\alpha}$ were from Cayman Chemical Company (Ann Arbor, MI, USA). PD098059, PD169316, SB203580, JNK inhibitor II, Akt inhibitor, LY294002, and IKK inhibitor VII were from Calbiochem (La Jolla, CA, USA). NS-398, 9-*cis* retinoic acid (RA) and Z-VAD-FMK were from BIOMOL (Hamburg, Germany). ET-1, N-2-mercaptopropionyl-glycine (MPG), GSH ethyl ester, L-buthionine sulfoximine (BSO), actinomycin D (ActD), cycloheximide, EGF, AA and bradykinin were from Sigma-Aldrich (Saint Louis, MO, USA). LPA was from Avanti Polar Lipids (Alabaster, AL, USA).

3.1.8 Buffers

Table 1: Buffers

Buffer	Components	pH
HANKS/Hepes Buffer	$CaCl_2$ 0.95 mM, KCl 5.3 mM, KH_2PO4 0.44 mM, $MgSO_4$ 0.8 mM, NaCl 136.8 mM, $NaHCO_3$ 4.16 mM, Na_2HPO_4 0.27 mM, *D*-glucose 5.5 mM, HEPES 10 mM	7.4
Lysis Buffer	HEPES 50 mM, NaCl 150 mM, EDTA 1 mM, $Na_4P_2O_7$ 10 mM, Na_3VO_4 2 mM, NaF 10 mM, Triton X-100 1% (*v/v*), glycerol 10% (*v/v*), Complete Mini protease inhibitor	7.4
TBS-T	Tris 20 mM, NaCl 137 mM, Tween-20 0.1% (*v/v*)	7.6
Blotting buffer	Tris 2.5 mM, glycin 19.2 mM, SDS 0.01% (*w/v*)	

3.2 Methods

3.2.1 Cell Culture

3.2.1.1 Cell Model for human Osteosarcoma

MG-63 [Billiau et al., 1977], a human osteosarcoma cell line (ATCC, Manassas, VA, USA), was maintained in α-MEM, supplemented with 5% (*v/v*) FCS, 50 µg/ml (*w/v*) gentamycin and 2 mM *L*-glutamine at 37°C in a humidified atmosphere of 5% CO_2. Cells were used between the 10^{th} and 20^{th} passage counted from the day of receipt. The cells were cultured in 75 cm^2 tissue culture flasks and seeded prior to the experiments in 100 mm dishes ($8x10^5$ cells), in 6-well plates ($1x10^5$ or $2x10^5$ cells per well) or in 12-well plates ($4x10^4$ or $5x10^4$ cells per well). Experiments were performed four to six days after seeding.

3.2.1.2 Control Cell Lines

The mouse osteoblast-like cell line **MC3T3-E1** (named MC3T3-E1 "B" in our laboratory, [Leis et al., 1997]) was kindly provided by Dr. Klaushofer (Hanusch Hospital, Vienna). The cells were cultured in α-MEM supplemented with 5% (*v/v*) FCS and 2 mM *L*-glutamine at 37°C in a humidified atmosphere of 5% CO_2. Cells were used between the 7^{th} and 20^{th} passages counted from the day of receipt. For experiments, cells were seeded at a density of $2x10^5$ in 6-well dishes and fed with fresh medium at day four. Experiments were performed with confluent cells at day six. MC3T3-E1 cells were used as a control cell line for Cox-1/Cox-2 expression. For induction of Cox-2 expression, MC3T3-E1 cells were stimulated with 20 nM ET-1 for 3 h [Leis et al., 1998].

Human hepatocellular **HepG2** cells were maintained in low-glucose DMEM supplemented with 10% (*v/v*) FCS and 1% (*v/v*) penicillin/streptavidin. HepG2 cells were used as control cell line for expression of PPARγ1 and PPARγ2 transcripts. RNA of HepG2 cells was kindly provided by Prof. Ernst Malle (Institute of Molecular Biology and Biochemistry, Medical University of Graz, Austria).

3.2.2 Agonists, Antagonists and Inhibitors

All chemicals were dissolved and stored according to manufacturer's suggestions. As DMSO was used as solvent for the various water-insoluble substances, it was applied as vehicle control in the respective experiments. Freeze-thaw cycles were avoided to prevent a loss of substance activities. It is important to note that for 15d-PGJ_2 even one freeze-thaw cycle was sufficient to detect highly diminished responses, especially in short termed experiments. An overview of the compounds, their solvents and applied concentrations is listed in Table 2.

3.2.3 Cell Stimulation

For the following set of experiments, MG-63 cells were plated at a density of $2x10^5$ cells per well in 6-well plates and grown to confluency. Experiments were performed four to six days after seeding and analyzed by qPCR (see section 3.2.6) or Western blot (see section 3.2.8).

3.2.3.1 Stimulation for Studying MAPK Activation

To study time-dependent activation of MAPK/JNK pathways, MG-63 cells were incubated in medium containing 20 µM 15d-PGJ_2 up to 48 h.

To study concentration-dependent activation of MAPK/JNK pathways, MG-63 cells were incubated for 10 min (pp38 MAPK) or 4 h (pp42/44 MAPK, pJNK1/2) in medium containing 1 to 50 µM 15d-PGJ_2.

To study concentration-dependent activation of pp38 MAPK in the absence of FCS, the standard growth medium of MG-63 cells was exchanged to α-MEM without FCS or HANKS/Hepes buffer (Table 1) before addition of 1 to 50 µM 15d-PGJ_2 for 10 min.

To study concentration-dependent activation of MAPK/JNK pathways in response to H_2O_2, MG-63 cells were incubated for 10 min (pp38 MAPK) or 4 h (pp42/44 MAPK, pJNK1/2) in medium containing 100 to 800 µM H_2O_2.

Table 2: Compounds used in the study.

Compound	Description	Applied Concentration	Solvent
15d-PGJ_2	Cyclopentenone PG	1 – 50 µM	DMSO
9,10-dihydro-15d-PGJ_2	Structural analogue of 15d-PGJ_2 lacking the electrophilic carbon group	20 – 50 µM	DMSO
PGD_2	Cox product	20 – 50 µM	DMSO
ActD	Inhibitor of transcription	0.5 µM	DMSO
Cycloheximide	Inhibitor of translation	0.5 µM	DMSO
PD169316	p38 kinase inhibitor	1 µM	DMSO
SB203580	p38 kinase inhibitor	10 µM	DMSO
PD098059	MAPK kinase inhibitor	20 µM	DMSO
JNK inhibitor II	JNK inhibitor	1 µM	DMSO
AG1296	PDGF receptor tyrosine kinase inhibitor	20 µM	DMSO
AG1478	EGF receptor tyrosine kinase inhibitor	20 µM	DMSO
EGF	Agonist of EGF receptors	50 ng/ml	1% BSA/H_2O
LY294002	PI3K inhibitor	20 µM	DMSO
Akt inhibitor	Akt inhibitor	20 µM	DMSO
Manumycin A	Ras inhibitor	10 µM	DMSO
CAY10512	NF-κB inhibitor	20 µM	DMSO
IKK inhibitor VII	IKK inhibitor	20 µM	DMSO
T0070907	PPARγ inhibitor	1 – 20 µM	DMSO
DK-PGD2	CRTH2 agonist	10 – 20 µM	DMSO
CAY10471	CRTH2 antagonist	10 – 20 µM	DMSO
BW 245c	DP agonist	10 – 20 µM	DMSO
MK-0524	DP antagonist	10 – 20 µM	DMSO
Apocynin	NAPDH oxidase inhibitor	1 µM	DMSO
Rotenone	Mitochondrial complex I inhibitor	1 µM	DMSO
MPG	Antioxidant, GSH precursor	5 mM	H_2O
GSH ethyl ester	Antioxidant, GSH precursor	10 mM	H_2O
BSO	Inhibitor of GSH synthesis	20 µM	H_2O
AA	Substrate for Coxs	10 µM	0.1 M NaOH
Bradykinin	Agonist of bradykinin receptors	1 µM	DMSO
FR-122047	Cox-1 inhibitor	100 nM	DMSO
NS-398	Cox-2 inhibitor	100 - 250 nM	DMSO
Z-FAD-FMK	pan caspase inhibitor	1 µM	DMSO
ET-1	Agonist of ET receptors	20 nM	H_2O
LPA	Agonist of LPA receptors	20 µM	H_2O
9-*cis*-RA	Ligand of RXRs	1 – 20 µM	DMSO

To reveal specific pathways involved in MAPK/JNK activation in response to 15d-PGJ_2, a diverse set of agonists and antagonists was used. The relevant agonists (PGD_2, DK-PGD_2, BW 245C, 9,10-dihydro-15d-PGJ_2; see Table 2) were added directly into the medium of MG-63 cells for 10 min (pp38 MAPK) or 4 h (pp42/44 MAPK, pJNK1/2). The respective antagonists (CAY10471, MK-0524, T0070907, AG1296, AG1478; see Table 2) were added directly into the medium of MG-63 cells for 30 min prior to stimulation with 15d-PGJ_2 for 10 min (pp38 MAPK) or 4 h (pp42/44 MAPK, pJNK1/2).

To reveal specific effects of antioxidants/GSH precursors on MAPK/JNK activation in response to 15d-PGJ_2, MG-63 cells were preincubated for 1 h in medium with 5 mM MPG or 10 mM GSH ethyl ester prior to stimulation with 20 µM 15d-PGJ_2 for 10 min (pp38 MAPK) or 4 h (pp42/44 MAPK, pJNK1/2).

3.2.3.2 Stimulation for Studying Cox-2 Expression

To study time-dependent induction of Cox-2 expression, MG-63 cells were incubated in medium containing 20 µM 15d-PGJ_2 up to 48 h.

To study concentration-dependent induction of Cox-2 expression, MG-63 cells were incubated for 6 h (mRNA expression) or 8 h (protein expression) in medium containing 1 to 50 µM 15d-PGJ_2.

To study the molecular mechanisms of Cox-2 mRNA and protein expression, MG-63 cells were preincubated for 30 min with 0.5 µM ActD and 0.5 µM cycloheximide, respectively, prior to stimulation with 20 µM 15d-PGJ_2 for 6 h (mRNA expression) or 8 h (protein expression).

To reveal specific signal transduction pathways involved in Cox-2 mRNA and protein expression in response to 15d-PGJ_2, a diverse set of inhibitors was used. The MAPK/JNK inhibitors (PD169316, PD098580, JNK inhibitor II; see Table 2) were added directly into the medium of MG-63 cells for 30 min followed by stimulation with 20 µM 15d-PGJ_2 for 6 h (mRNA) or 8 h (protein). Other kinase inhibitors (LY294002, manumycin A, Akt inhibitor, CAY10512, IKK inhibitor, AG1296, AG1478; see Table 2) were added directly into the medium of MG-63 cells for 30 min followed by stimulation with 20 µM 15d-PGJ_2 for 8 h to analyze Cox-2 protein expression.

To reveal other specific pathways involved in Cox-2 protein expression, a diverse set of agonists and antagonists/inhibitors was used. The relevant agonists

(PGD_2, DK-PGD_2, BW 245C, 9,10-dihydro-15d-PGJ_2; see Table 2) were added directly into the medium of MG-63 cells for 8 h. The respective antagonists/inhibitors (CAY10471, MK-0524, T0070907; see Table 2) were added directly into the medium of MG-63 cells for 30 min prior to stimulation with 15d-PGJ_2 for 8 h.

To study concentration-dependent induction of Cox-2 expression in response to H_2O_2, MG-63 cells were incubated for 8 h in medium containing 100 to 800 µM H_2O_2.

To reveal specific effects of antioxidants/GSH precursors on Cox-2 expression in response to 15d-PGJ_2, MG-63 cells were preincubated for 1 h in medium with 5 mM MPG or 10 mM ethyl ester prior to stimulation with 20 µM 15d-PGJ_2 for 8 h.

To study the effect of 9-*cis*-RA on Cox-2 expression, MG-63 cells were pretreated for 10 min with 9-*cis*-RA prior to 8 h stimulation with 20 µM 15d-PGJ_2 and 20 µM LPA.

3.2.3.3 Stimulation for Studying Cox-2 mRNA Stability

MG-63 cells were treated for 4 h with DMSO or 20 µM 15d-PGJ_2 to induce Cox-2 mRNA expression followed by addition of 0.5 µM ActD for up to 2 h.

To reveal specific MAPK/JNK pathways involved in Cox-2 mRNA stability, MG-63 cells were treated for 4 h with DMSO or 20 µM 15d-PGJ_2 followed by addition of 0.5 µM ActD in the absence or presence of MAPK/JNK inhibitors (PD169316, PD098580, JNK inhibitor II; see Table 2) for 2 h.

3.2.3.4 Stimulation for Studying EGFR Tyrosine Phosphorylation

To study time-dependent induction of EGFR tyrosine phosphorylation, MG-63 cells were incubated in medium containing 20 µM 15d-PGJ_2 up to 8 h.

To reveal that the tyrosine phosphorylation signal is specific for EGFR, MG-63 cells were pretreated for 30 min with 20 µM of the EGFR inhibitor AG1478 and the PDGFR inhibitor AG1296 followed by stimulation with 20 µM 15d-PGJ_2 for 8 h. Furthermore, MG-63 cells were treated with 50 ng/ml EGF for 15 min. Cell lysates were analyzed by Western blot (see section 3.2.8.3) and immunoprecipitation (see section 3.2.9).

To reveal specific MAPK/JNK pathways involved in EGFR tyrosine phosphorylation, MAPK/JNK inhibitors (PD169316, SB203580, PD098580, JNK

inhibitor II; see Table 2) were added directly into the medium of MG-63 for 30 min followed by stimulation with 15d-PGJ_2 for 8 h.

To reveal specific effects of antioxidants/GSH precursors on EGFR tyrosine phosphorylation, MG-63 cells were preincubated for 1 h in medium with 5 mM MPG or 10 mM GSH ethyl ester prior to stimulation with 20 µM 15d-PGJ_2 for 8 h.

3.2.3.5 Stimulation for Studying HO-1 Expression

To study time-dependent induction of HO-1 expression, MG-63 cells were incubated in medium containing 20 µM 15d-PGJ_2 up to 48 h.

To study concentration-dependent induction of HO-1 expression, MG-63 cells were incubated for 6 h (mRNA expression) and 8 h (protein expression), respectively, in medium containing 1 to 50 µM 15d-PGJ_2.

3.2.3.6 Stimulation for Studying Expression of p65, Nrf-2 and Egr-1

To study the expression levels and nuclear translocation of NF-κB subunit p65, Nrf-2, and Egr-1, MG-63 cells were treated with 20 µM 15d-PGJ_2 up to 8 h.

3.2.3.7 Stimulation of MG-63 Cells with knocked-down PPARγ Expression

MG-63 cells were transfected with specific siRNAs for PPARγ and a scrambled control siRNA for 66 h (see section 3.2.10). After this transfection period, 20 µM 15d-PGJ_2 were added directly into the medium of confluent cells for 10 min (pp38 MAPK), 4 h (pp42/44 MAPK, pJNK1/2), 8 h (Cox-2 expression), or 24 h (PARP cleavage and caspase-3 activation).

3.2.3.8 Stimulation for Studying Apoptosis-relevant Proteins

For this set of experiments, MG-63 cells were plated at a density of $1x10^5$ cells per well in 6-well plates and grown to confluence. Experiments were performed four days after seeding followed by Western blot analysis (see section 3.2.8).

To study time-dependent induction of caspase-3 activation and PARP cleavage and expression levels of early apoptotic proteins, MG-63 cells were incubated in medium containing 20 µM 15d-PGJ_2 up to 48 h.

To study concentration-dependent induction of caspase-3 activation and PARP cleavage, MG-63 cells were incubated for 24 h in medium containing 1 to 50 µM 15d-PGJ_2. Furthermore, MG-63 cells were incubated in medium with 20 to 50 µM PGD_2 and 9,10-dihydro-15d-PGJ_2.

To reveal MAPK/JNK pathways involved in caspase-3 activation and PARP cleavage, MAPK/JNK inhibitors (PD169316, PD098580, JNK inhibitor II; see Table 2) were added directly into the medium of MG-63 cells for 30 min followed by stimulation with 20 µM 15d-PGJ_2 for 24 h.

To study if PPARγ is involved in 15d-PGJ_2-induced caspase-3 activation and PARP cleavage, 1 to 20 µM of the PPARγ antagonists T0070907 were added directly into the medium of MG-63 cells for 30 min prior to stimulation with 20 µM 15d-PGJ_2 for 24 h.

To reveal specific effects of antioxidants/GSH precursors on caspase-3 activation and PARP cleavage, MG-63 cells were preincubated for 1 h in medium with 5 mM MPG or 10 mM GSH ethyl ester prior to stimulation with 20 µM 15d-PGJ_2 for 24 h.

To explore specific effects of caspase inhibitors on alterations in apoptotic cell death, MG-63 cells were preincubated for 30 min in medium with 1 µM of the pan-caspase inhibitor prior to stimulation with 20 µM 15d-PGJ_2 for 24 h.

To study the effect of GSH depletion on caspase-3 activation and PARP cleavage, MG-63 cells were incubated for 20 h with 10 µM BSO prior to stimulation with 20 µM 15d-PGJ_2 for 24 h.

To study the effect of Cox-2 inhibition on caspase-3 activation and PARP cleavage, MG-63 cells were incubated for 30 min with 250 nM NS-398 prior to stimulation of MG-63 cells with 1 to 50 µM 15d-PGJ_2 for 24 h.

3.2.3.9 Stimulation for the Detection of intracellular DCF Fluorescence

For this set of experiments, MG-63 cells were plated at a density of $5x10^4$ cells per well in 12-well plates and grown to confluence. Experiments were performed in triplicates four days after seeding followed by ROS assay procedure (see section 3.2.12).

To study time-dependent induction of DCF fluorescence, MG-63 cells were incubated in medium containing 20 µM 15d-PGJ_2 up to 60 min. Furthermore, MG-63 cells were stimulated with 20 µM 9,10-dihydro-15d-PGJ_2 for 1 h.

To reveal specific signal transduction pathways involved in elevated DCF fluorescence, signal transduction inhibitors (PD169316, PD098580, JNK inhibitor II, AG1478; see Table 2) were added directly into the medium of MG-63 cells for 30 min followed by stimulation with 20 µM 15d-PGJ_2 for 1 h.

To study if specific oxidases are involved in enhanced DCF fluorescence, MG-63 cells were preincubated for 30 min with 1 µM apocynin or rotenone prior to stimulation with 20 µM 15d-PGJ_2 for 1 h.

To reveal specific effects of antioxidants/GSH precursors on elevated DCF fluorescence, MG-63 cells were preincubated for 1 h in medium with 5 mM MPG or 10 mM ethyl ester prior to stimulation with 20 µM 15d-PGJ_2 for 1 h.

3.2.3.10 Stimulation for Studying intracellular GSH Concentrations

To study time-dependent alterations in intracellular GSH concentrations, MG-63 cells were incubated in medium containing 20 µM 15d-PGJ_2 up to 48 h or with 10 µM BSO up to 24 h.

3.2.3.11 Stimulation for Studying Cell Viability

For this set of experiments, MG-63 cells were plated at a density of $4x10^4$ cells per well in 12-well plates. Experiments were performed with confluent, but still spindle-shaped cells, four days after seeding followed by determination of cell viability by MTT test (see section 3.2.14).

To study time-dependent alterations in cell viability, MG-63 cells were treated in triplicate in medium containing 20 µM 15d-PGJ_2 up to 48 h.

To study concentration-dependent alterations in cell viability, MG-63 cells were incubated for 24 h in medium containing 1 to 50 µM 15d-PGJ_2.

To reveal specific effects of antioxidants/GSH precursors on cell viability, MG-63 cells were preincubated for 1 h in medium with 5 mM MPG or 10 mM GSH ethyl ester prior to stimulation with 20 µM 15d-PGJ_2 for 24 h.

To explore specific effects of caspase inhibitors on cell viability, MG-63 cells were preincubated for 30 min in medium with 1 µM of the pan-caspase inhibitor prior to stimulation with 20 µM 15d-PGJ_2 for 24 h.

To study the effect of GSH depletion on cell viability, MG-63 cells were incubated for 20 h with 10 µM BSO prior to stimulation with 20 µM 15d-PGJ_2 for 24 h.

3.2.3.12 Stimulation for Studying PG Synthesis

To study time-dependent synthesis of PGE_2 and $PGF_{2\alpha}$, MG-63 cells were incubated in triplicates in medium containing 20 µM 15d-PGJ_2 up to 24 h followed by addition of 10 µM AA or 1 µM bradykinin for 10 min after each incubation period.

To block Cox-1 and Cox-2 activity, MG-63 cells were stimulated in triplicates in medium containing 20 µM 15d-PGJ_2 for 24 h followed by 15 min incubation with 100 nM FR-122047 and NS-398 prior to addition of 10 µM AA for 10 min.

3.2.4 RNA Isolation

MG-63 cells were plated in 6-well plates, grown to confluence and treated with agonists, in the presence or absence of respective inhibitors/antagonists, added directly into the medium (see section 3.2.3). The experiments were terminated by aspiration of the medium and washing of the cells with chilled PBS/EDTA (pH 7.4) followed by washing with PBS (pH 7.4). Total RNA was isolated using QIAshredder and RNeasy® Mini Kit according to the manufacturer's protocol. The RNA concentration was determined photometrically at 260 nm (Multiscan® FC microplate photometer, Thermo Scientific, Vantaa, Finland); the stock solutions (containing approx. 40 µg RNA) were supplemented with 1 µl of Recombinant RNasin® Ribonuclease Inhibitor and stored at -70°C.

3.2.5 RT-PCR

RT-PCR was performed to detect expression levels of PPARγ1 and PPARγ2 transcripts. The samples were analyzed with QIAGEN® OneStep RT-PCR Kit as recommended by the manufacturer in 50 µl reactions containing template RNA (100 ng of total RNA) and Master Mix (400 µM each dNTP, 10 µl 5x QIAGEN OneStep RT-PCR Buffer, 2 µl QIAGEN OneStep RT-PCR Enzyme Mix and gene-specific

primers in a final concentration of 0.6 µM). The reverse transcription reaction was conducted for 1 h at 42°C followed by an initial step (15 min at 95°C) to activate HotStarTaq DNA Polymerase and inactivate Omniscript and Sensiscript Reverse Transcriptases. The conditions of PCR-amplification were as follows: denaturation step 10 sec at 94°C, 30 sec at annealing temperature, extension step 30 sec at 72°C; followed by a final 7 min elongation at 72°C. The primer sequences as well as the respective annealing temperature, amplicon size and number of amplification cycles are listed in Table 3. 15 µl aliquots of the RT-PCR products were mixed with 5 µl DNA loading buffer (50% (*v/v*) glycerol, bromphenol blue and xylene cyanol) and separated on a 1% agarose gel supplemented with 0.1% (*v/v*) ethidium bromide solution in 1x TBE buffer for 1 h at 100 V and visualised on UV transilluminator (Herolab, Wiesloch, Germany). To ensure equal RNA loading, RT-PCR for GAPDH was performed for each experiment.

Table 3: PPARγ1/2-specific primers used for RT-PCR analysis.
The expected amplicon size in basepairs (bp) and unique PCR properties (cycle number and annealing temperature) are listed.

Gene Accession No.	**Primers** F – forward, R - reverse	**Amplicon size (bp)**	**Anneal temp. (°C)**	**Cycle No.**	**Reference**
PPARγ1 NM_138712	F 5' CCATTCTGGCCCACAAC 3' R 5' CTTATTGTAGAGCTGAGTCTTCTC 3'	267	55	35	[Jackson et al., 1999]
PPARγ2 NM_015869	F 5' ACTCTGGGAGATTCTCCTATT 3' R 5' CTTATTGTAGAGCTGAGTCTTCTC 3'	366	55	35	[Yanase et al., 1997]
GAPDH M17851	F 5' ACAGTCCATGCCATCACTGCC 3' R 5' GCCTGCTTCACCACCTTCTTG 3'	265	58	30	[Iochmann et al., 1999]

3.2.6 Quantitative Real-Time PCR (qPCR)

qPCR was performed to quantify mRNA levels of Cox-2, HO-1 and PPARγ, normalized to the housekeeping gene GAPDH. Therefore, equal amounts of RNA (1 to 3 µg) were treated with DNase-I as recommended by the manufacturer and were reverse transcribed using the High-Capacity cDNA Reverse Transcription Kit according to the supplier's manual. The amplified cDNA was stored at -20°C.

For qPCR reactions, cDNA was diluted to final concentrations of 5 ng/µl for Cox-2 and HO-1 mRNA detection, and 20 ng/µl for PPARγ mRNA expression. 2 µl of diluted cDNA were amplified using QuantiFast™ SYBR® Green PCR mastermix supplemented with validated QuantiTect® Primer Assays for Cox-2, PPARγ and GAPDH and analyzed in duplicate in 10 µl reactions in 96-well plates in a LightCycler® 480 Real-time PCR device (Roche Diagnostics GmbH, Vienna, Austria). The thermal profile initiates with a 5 min step at 95°C followed by 40 cycles of 15 sec at 95°C and 30 sec at 60°C. The amplification period was followed by a melting curve analysis with a temperature gradient of 0.1°C/sec from 70 to 95°C to exclude amplification of unspecific products. A non-template control was included in each experiment.

For the calculation of the relative expression levels of Cox-2, HO-1 and PPARγ mRNA normalized to GAPDH mRNA, the ΔΔCt based method [Livak and Schmittgen, 2001] was used according to following formula:

$$\text{fold change expression}_{\text{TARGET GENE}} = 2^{-\Delta\Delta Ct}$$

where ΔΔCt = ΔCt of treated samples – ΔCt of untreated samples; ΔCt = Ct of target gene (Cox-2/HO-1/PPARγ) – Ct of reference gene (GAPDH).

3.2.7 Protein Isolation

MG-63 cells were plated in 6-well plates, grown to confluence and treated with agonists, in the presence or absence of respective inhibitors/antagonists, added directly into the medium (see section 3.2.3). The experiments were terminated by aspiration of the medium and washing of the cells with chilled PBS (pH 7.4). Cell lysis was performed with 100 µl lysis buffer (Table 1) for 15 min on ice on with shaking. Insoluble cell debris was removed by centrifugation at 13,000 *g* (4°C; 5 min). Protein contents of cell lysates were determined using the BCA™ protein assay (Pierce Biotechnology, Rockford, IL, USA) according to the manufacturer's suggestions using BSA as standard. The measurement was performed at 540 nm using the Multiscan® FC microplate photometer (Thermo Scientific, Vantaa, Finland). Protein samples were stored at -70°C.

3.2.8 Western Blot Analysis

3.2.8.1 Detection of MAPK Phosphorylation

Aliquots of cell lysates (approx. 30 µg for pp42/44 MAPK detection, approx. 100 µg of protein for pp38 MAPK/pJNK1/2 detection) were supplemented with 4x NuPAGE® LDS sample buffer and 10x NuPAGE® sample reducing agent. The protein samples were heated for 10 min at 70°C and subjected to electrophoresis on 4-12% gradient SDS-PAGE gels (1 mm for pp42/44 MAPK detection, 1.5 mm for pp38 MAPK/pJNK1/2 detection) in NuPAGE® MES SDS Running Buffer (35 min at 200 V for 1 mm gels; 1.5 h at 130 V for 1.5 mm gels). Proteins were transferred to nitrocellulose membranes using blotting buffer (Table 1) supplemented with 20% (*v/v*) methanol (1.5 h at 0.3 mA for 1 mm gels; 2 h at 0.3 mA for 1.5 mm gels).

Membranes were blocked with 5% (*w/v*) non-fat dry milk powder in TBS-T (Table 1) for 30 min at room temperature followed by incubation with primary antibodies diluted in 3% (*w/v*) BSA in TBS-T. Dilutions and incubation times of anti-pp38 MAPK, anti-pp42/44 MAPK, and anti-pJNK1/2 antibodies are displayed in Table 4. The membranes were washed three times for 5 min in TBS-T, followed by incubation for 1 h with HRP-conjugated secondary antibodies (Table 4) diluted in 5% (*w/v*) non-fat dry milk in TBS-T. After another washing sequence (three times for 5 min with TBS-T), immunodetection was performed with SuperSignal® West Pico chemiluminescent substrate or Immobilon Western Chemiluminescent HRP substrate. For normalization of phosphorylated immunoreactive bands, the membranes were stripped with Restore™ Western Blot Stripping Buffer and re-probed with the respective antibodies (anti-p38 MAPK, anti-p42/44 MAPK, and anti-JNK1/2; see Table 4) recognizing total expression levels of MAPKs.

3.2.8.2 Detection of Cox-1, Cox-2, HO-1, Nrf-2, Egr-1, p65 Expression

Aliquots of cell lysates (approx. 100 µg of protein) were supplemented with 4x NuPAGE® LDS sample buffer and 10x NuPAGE® sample reducing agent. The protein samples were heated for 10 min at 70°C and subjected to electrophoresis on 1.5 mm 4-12% gradient SDS-PAGE gels in NuPAGE® MES SDS Running Buffer (1.5 h at 130 V). Proteins were transferred to nitrocellulose membranes using blotting buffer (Table 1) supplemented with 20% (*v/v*) methanol (2 h at 0.3 mA).

Membranes were blocked with 5% (*w/v*) non-fat dry milk powder in TBS-T (Table 1) for 30 min at room temperature followed by incubation with primary antibodies diluted in 3% (*w/v*) BSA in TBS-T. Dilutions and incubation times of anti-Cox-1, anti-Cox-2, anti-NF-κB p65, anti-HO-1, anti-Nrf-2, and anti-Egr-1 antibodies are displayed in Table 4. The membranes were washed three times for 5 min in TBS-T, followed by incubation for 1 h with HRP-conjugated secondary antibodies (Table 4) diluted in 5% (*w/v*) non-fat dry milk in TBS-T. Washing steps, immunodetection and incubation with the respective secondary antibodies (anti-β-actin, and anti-lamin A/C; see Table 4) was done as described above (section 3.2.8.1).

3.2.8.3 Detection of EGFR and phospho-Tyrosines

Aliquots of cell lysates (approx. 100 µg of protein) were supplemented with 4x NuPAGE® LDS sample buffer and 10x NuPAGE® sample reducing agent. The protein samples were heated for 10 min at 70°C and subjected to electrophoresis on 1.5 mm 4-12% gradient SDS-PAGE gels in NuPAGE® MOPS SDS Running Buffer (2 h at 130 V). Proteins were transferred to nitrocellulose membranes using blotting buffer (Table 1) supplemented with 20% (*v/v*) methanol (3 h at 0.3 mA).

Membranes were blocked with 5% (*w/v*) non-fat dry milk powder in TBS-T (Table 1) for 30 min at room temperature followed by incubation with anti-EGFR and anti-p-Tyr antibodies (Table 4), respectively, diluted in 3% (*w/v*) BSA in TBS-T. The membranes were washed three times for 5 min in TBS-T, followed by incubation for 1 h with HRP-conjugated secondary antibodies (Table 4) diluted in 5% (*w/v*) non-fat dry milk in TBS-T. Washing steps, immunodetection and incubation with the respective secondary antibody (anti-β-actin; see Table 4) was done as described above (section 3.2.8.1).

Table 4:

Dilutions and incubation times of primary antibodies.

Antibody	Source	Dilution in 3% BSA/TBS-T	Incubation time
anti-pp38 MAPK	rabbit	1:1000	over night, 4°C
anti-p38 MAPK	rabbit	1:1000	1 h, room temperature
anti-pp42/44 MAPK	mouse	1:1000	1 h, room temperature
anti-p42/44 MAPK	rabbit	1:2000	1 h, room temperature
anti-pJNK1/2 MAPK	mouse	1:200	1 h, room temperature
anti-JNK1/2 MAPK	rabbit	1:200	over night, 4°C
anti-Cox-1	mouse	1:200	over night, 4°C
anti-Cox-2	goat	1:200	over night, 4°C
anti-HO-1	rabbit	1:500	over night, 4°C
anti-β-actin	mouse	1:1000	1 h, room temperature
anti-p-Tyr	mouse	1:2000	1 h, room temperature
anti-EGFR	rabbit	1:200	2 h, room temperature
anti-NF-κB p65	rabbit	1:1000	1 h, room temperature
anti-Nrf-2	rabbit	1:200	over night, 4°C
anti-Egr-1	rabbit	1:500	2 h, room temperature
anti-lamin A/C	rabbit	1:1000	1 h, room temperature
anti-PARP	mouse	1:2000	1 h, room temperature
anti-caspase-3	rabbit	1:500	over night, 4°C
anti-caspase-8	mouse	1:500	2 h, room temperature
anti-Puma	rabbit	1:500	over night, 4°C
anti-Bax	rabbit	1:500	over night, 4°C
anti-Bcl-x_L	rabbit	1:200	over night, 4°C
anti-Bcl-2	rabbit	1:200	over night, 4°C

Dilutions and incubation times of secondary antibodies.

Antibody	Source	Dilution in 5% milk /TBS-T	Incubation time
anti-rabbit IgG	goat	1:200,000	1 h, room temperature
anti-goat IgG	donkey	1:200,000	1 h, room temperature
anti-mouse IgG	goat	1:100,000	1 h, room temperature

3.2.8.4 Detection of Apoptosis Markers

Aliquots of cell lysates (approx. 60 µg of protein) were supplemented with 4x NuPAGE® LDS sample buffer and 10x NuPAGE® sample reducing agent. The protein samples were heated for 10 min at 70°C and subjected to electrophoresis on 1.5 mm 4-12% gradient SDS-PAGE gels in NuPAGE® MES SDS Running Buffer (1.5 h at 130 V). Proteins were transferred to nitrocellulose membranes using blotting buffer (Table 1) supplemented with 20% (*v/v*) methanol (2 h at 0.3 mA).

Membranes were blocked with 5% (*w/v*) non-fat dry milk powder in TBS-T (Table 1) for 30 min at room temperature followed by incubation with primary antibodies diluted in 3% (*w/v*) BSA in TBS-T. Dilutions and incubation times of anti-caspase-3, and anti-PARP antibodies are listed in Table 4. The membranes were washed three times for 5 min in TBS-T, followed by incubation for 1 h with HRP-conjugated secondary antibodies (Table 4) diluted in 5% (*w/v*) non-fat dry milk in TBS-T. Washing steps, immunodetection and incubation with the respective secondary antibody (anti-β-actin; see Table 4) was done as described above (section 3.2.8.1).

3.2.9 Immunoprecipitation

MG-63 cells were seeded at a density of $8x10^5$ cells per 100 mm culture dish and treated as described above (see section 3.2.3.4). After cell lysis in 1 ml RIPA buffer (Santa Cruz Biotechnology, CA, USA), 400 µl aliquots were incubated with 20 µl agarose-conjugated antibodies against EGFR (1005, Santa Cruz Biotechnology, CA, USA) or p-Tyr (PY99, Santa Cruz Biotechnology, CA, USA), respectively, overnight at 4°C on a rotation device. Precipitates were washed twice with RIPA buffer, resuspended in 30 µl 2x electrophoresis sample buffer, and heated for 3 min at 95°C. After brief centrifugation, the supernatant was electrophoresed on 4-12% gradient SDS-PAGE gels and Western blot analysis was performed as described by using anti-p-Tyr and anti-EGFR antibodies as primary antibodies (see section 3.2.8.3).

3.2.10 siRNA Transfection

MG-63 cells were transfected with two siRNAs specific for PPARγ (si-1 = *Silencer*® Select siRNA against PPARG, siRNA ID #: s10888, Ambion®, Applied Biosystems; si-2 = HP GenomeWide siRNA Hs_PPARG_1_HP siRNA, catalogue number: SI00071673, Qiagen) or with a scrambled negative control siRNA (si-scr = Allstars Negative Control siRNA, Qiagen). The siRNA transfection was performed with Oligofectamine® according to the supplier's manual. MG-63 cells were plated at a density of $5x10^4$ in 6-well plates and grown over night to 30-50% confluency. MG-63 cells were transfected in 1 ml α-MEM without FCS containing 4 µl Oligofectamine® and 50 nM of the respective siRNA. As a mock control, cells were treated with the transfection reagent alone. After an incubation period of 6 h at 37°C (5% CO_2), the transfection mix was removed and replaced by the standard growth medium (α-MEM containing 5% FCS). Experiments were performed after a 66 h cultivation period (see section 3.2.3.7).

3.2.11 Isolation of Cytosolic and Nuclear Fractions

Nuclear and cytosolic protein fractions were separated after treatment with 15d-PGJ_2 to follow the nuclear translocation of Nrf-2, Egr-1 and NF-κB subunit p65. MG-63 cells were seeded at a density of $2x10^5$ cells per well in 6-well plates. Confluent cells were treated with 15d-PGJ_2 as described in section 3.2.3.6. Then, cells were washed twice with cold PBS (pH 7.4) and scraped in 500 µl PBS (pH 7.4). Cells were pelleted by centrifugation at 500 *g* (4°C, 3 min) and the supernatant was removed. The packed cell volume was estimated to be approx. 20 µl. Nuclear and cytosolic proteins were isolated by using NE-PER® Nuclear and Cytoplasmic Extraction Reagents (Pierce Biotechnology, Inc., Rockford, IL, USA) with additional protease inhibitors (Complete Mini protease inhibitor cocktail-tablets) according to the manufacturer's suggestions. Shortly, the addition of CER I and NER reagents caused disruption of cell membranes and release of cytoplasmic contents. After recovering the intact nuclei from the cytoplasmic extract by centrifugation (16,000 *g* for 5 min at 4 °C), the nuclei were lysed with CER II reagent to yield the nuclear extracts.

Protein concentrations in nuclear and cytosolic extracts were determined using BCA™ Protein Assay Kit according to the manufacturer's instructions using BSA as standard. Extracts were aliquoted and stored at -70 °C until use.

3.2.12 Intracellular ROS Measurement

Intracellular levels of ROS were assessed by using carboxy-H_2DCF-DA (DCF-DA; Molecular Probes, Invitrogen), a cell-permeable dye that becomes fluorescent upon oxidation by ROS. MG-63 cells were seeded in 12-well plates at a density of $5x10^4$ in α-MEM containing 5% FCS. Confluent cells were stimulated in triplicates as indicated (see section 3.2.3.9). After treatment, cells were washed once with pre-warmed PBS (37°C) and exposed to 600 µl of a pre-warmed 20 µM DCF-DA/PBS solution per well for 20 min at 37°C. Afterwards, cells were washed twice with ice-cold PBS (pH 7.4) and subjected to fluorescence microscopy (Zeiss Axiovert 35, Zurich, Switzerland with Olympus XM10 camera). Alternatively, cells were lysed with 200 µl PBS containing 1% (*v/v*) Triton X-100 per well for 1 h with shaking at 4°C. For the last 10 min, 40 µl ethanol were added to the lysis solution to improve the solubilization of the fluorescence dye. DCF fluorescence was measured in 100 µl duplicates in white 96-well Optiplates™ (PerkinElmer Life Sciences Wallac, Turku, Finland) at excitation and emission wavelengths of 485 and 530 nm, respectively, with a Wallac Victor^2 multilabel counter (PerkinElmer Life Sciences Wallac, Turku, Finland). Fluorescent counts detected with vehicle-treated cells were set as 100%.

3.2.13 Glutathione Assay

Intracellular glutathione concentrations were determined in MG-63 cells by using a commercial Glutathione Assay Kit (Cayman Chemical Company, Ann Arbor, MI, USA) according to the manufacturer's protocol. The assay is based on the reaction of reduced GSH with the substrate 5,5′-dithio-bis-2-nitrobenzoic acid (DTNB, also known as Ellman's reagent) [Ellman, 1959] to form a yellow derivative that can be measured photometrically. Experiments were performed in duplicate on the fourth day after seeding $2x10^5$ cells per well in 6-well plates. Cells were washed twice with cold PBS and harvested by scraping in 1 ml PBS containing 1 mM EDTA (pH 7.0). Cells were homogenized by sonication followed by deproteination with 5% (*w/v*) metaphosphoric acid by adding an equal volume of 10% (*w/v*) metaphosphoric acid. Before assaying, triethanolamine was added to a final concentration of 0.2 M (50 µl of 4 M triethanolamine per ml sample) to increase pH stability of the samples. 50 µl duplicates of each sample were incubated for 20 min with 150 µl of the assay cocktail containing 1x MES buffer, a cofactor mixture ($NADP^+$ and glucose-6-phosphate), an

enzyme mixture (glutathione reductase and glucose-6-phosphate dehydrogense), and DTNB. The formation of the yellow DTNB derivative was measured at 405 nm (Multiscan® FC microplate photometer, Thermo Scientific, Vantaa, Finland). A standard curve was included in every measurement. The results are reported as µmoles of total GSH normalized to 10^6 cells.

3.2.14 MTT Viability Assay

The cell viability was determined using 3-(4,5-dimethylthiozol-2-yl)-2,5-dipheyltetrazolium bromide (MTT; Sigma-Aldrich, Saint Louis, MO, USA) which is reduced by intact cells to an insoluble dark blue formazan product. MG-63 cells were plated in 12-well plates at a density of $4x10^4$ cells in α-MEM containing 5% FCS and were grown until cells were confluent, but still spindle-shaped. After treatments (see section 3.2.3.11), cells were washed with pre-warmed PBS (pH 7.4) and were incubated for 1 h with 400 µl MTT solution (0.5 mg/ml in α-MEM) per well. After a washing step with pre-chilled PBS, the dark blue formazan crystals were dissolved with 600 µl ice-cold acidic isopropanol (absolute isopropanol containing 0.04 M HCl) per well. After a short centrifugation step (2 min at 13,000 *g*) to remove cell debris, the absorbance of reduced MTT was read in 100 µl duplicates at 570 nm with background subtraction at 630 nm using a microplate reader (Multiscan® FC microplate photometer, Thermo Scientific, Vantaa, Finland). The percentage of viable cells were expressed as the percentage of MTT reduction obtained in treated cells, assuming that the absorbance of untreated control cells was 100% according to following formula:

$$\text{Viable cells (\%)} = \frac{(A_{570nm}\ \text{treated} - A_{630nm}\ \text{treated})}{(A_{570nm}\ \text{untreated} - A_{630nm}\ \text{untreated})} \cdot 100$$

3.2.15 Quantification of Prostaglandins

The release of PGE_2 and $PGF_{2\alpha}$ was followed in cell culture supernatants of MG-63 cells that were incubated in triplicate with the respective compounds as described in section 3.2.3.12. Cell culture supernatants were collected and acidified to pH 3.2 with formic acid. After addition of 10 ng deuterated PGE_2 and $PGF_{2\alpha}$

standards, PGs were extracted with ethyl acetate. PGE_2 and $PGF_{2\alpha}$ were analyzed as trimethyl silyl ether pentafluorobenzyl ester methoxime derivative by negative ion chemical ionization-gas chromatography/mass spectrometry (NICI-GC/MS) [Leis et al., 1987; Malle et al., 1989]. Quantitative measurements were performed by comparing the calculated peak areas of the corresponding PG derivatives (PGE_2 and $PGF_{2\alpha}$) at m/z 524 and 569 with the peak areas of deuterated PG derivatives (m/z 528 and 573). A TRACE GC-MS system (Thermo Scientific) quadrupole MS was used. GC was performed on a 15 m DB5-MS fused silica capillary column. The temperature of the splitless Grob injector was kept at 280°C, initial column temperature was 160°C for 1 min, followed by an increase of 40°C min^{-1} to 310°C. NICI was done in the single ion recording mode using methane as moderating gas.

3.2.16 Statistical Analysis

Data of representative experiments (qPCR, MTT test, ROS assay, GSH assay) are expressed as mean ± SD. Statistical significance of the individual treatments was analyzed by one-way analysis of variance (ANOVA) followed by a Bonferroni post-test to compare differences between all groups of data (GraphPad Prism®, Version 5.0). To compare differences between two selected groups a standard *t* test was used.

4 RESULTS

4.1 Signalling Cascades and Cox-2 Expression in Response to 15d-PGJ_2

4.1.1 15d-PGJ_2 upregulates Cox-2 Expression in human Osteosarcoma Cells

The human osteosarcoma cell line MG-63 elicits only low levels of Cox-2 expression on mRNA and protein level (Figure 1). Addition of 15d-PGJ_2 to cells increased Cox-2 expression on both, mRNA and protein level in a concentration-dependent manner (Figure 1 A, B). As 20 µM 15d-PGJ_2 led to a pronounced Cox-2 induction, this concentration was used in further experiments. Higher concentrations of the compound did not induce Cox-2 protein expression (Figure 1 B) whereas Cox-2 mRNA was still significantly induced (Figure 1 A). Furthermore, time-dependent induction of Cox-2 mRNA and protein expression up to 48 h is shown (Figure 1 C, D).

In order to study the molecular mechanisms contributing to Cox-2 expression, MG-63 cells were treated with ActD or cycloheximide prior to stimulation with 15d-PGJ_2. ActD, an inhibitor of transcription [Bailey et al., 1993], blocked expression of Cox-2 mRNA and protein to baseline levels (Figure 1 E, F). Cycloheximide, an inhibitor of translation [Obrig et al., 1971], diminished Cox-2 mRNA expression by approx. 50% while Cox-2 protein expression was almost completely blocked (Figure 1 E, F). These data demonstrate that *de novo* protein synthesis is required for 15d-PGJ_2-induced Cox-2 expression.

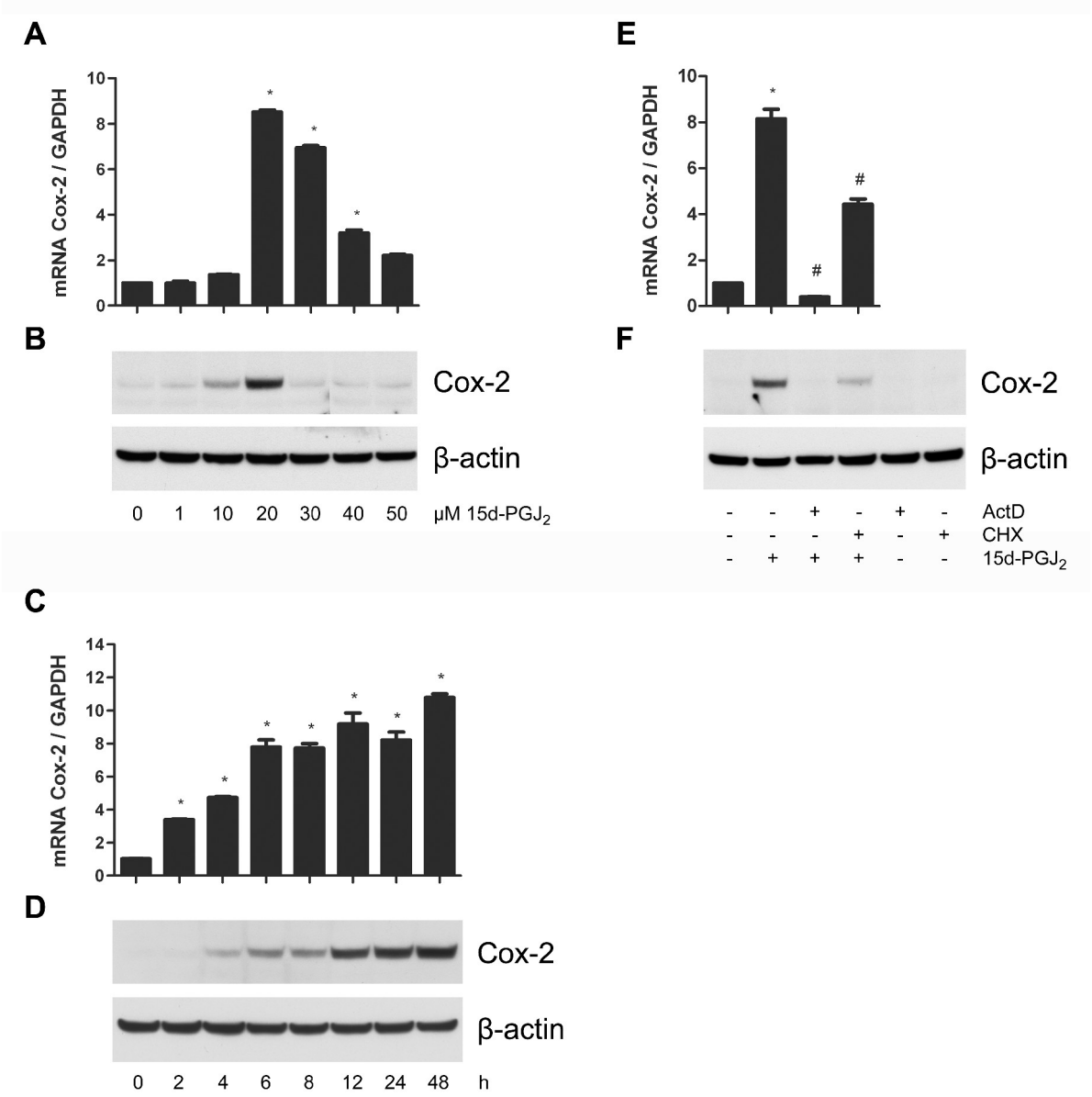

Figure 1: Upregulation of Cox-2 expression by 15d-PGJ$_2$.

(A, B) MG-63 cells were treated at increasing concentrations of 15d-PGJ$_2$ for 6 h to follow Cox-2 mRNA expression (A) and for 8 h to explore Cox-2 protein expression (B). (C, D) MG-63 cells were treated with 20 µM 15d-PGJ$_2$ at indicated time periods. (E, F) MG-63 cells were pretreated for 30 min with 0.5 µM ActD or 0.5 µM cycloheximide (CHX) prior to 8 h treatment with 15d-PGJ$_2$. As a control, cells were treated with the respective inhibitors alone for 8.5 h (F, lanes 5, 6). (A, C, E) For determination of Cox-2 mRNA expression, cDNA was generated and subjected to qPCR using specific primers for Cox-2. Cox-2 expression was normalized to GAPDH and values are expressed as mean ± SD. *P<0.001 versus vehicle-treated cells. $^{\#}P$<0.001 versus 15d-PGJ$_2$-treated cells. (B, D, F) For detection of Cox-2 protein, cell lysates were subjected to Western blot analysis using a specific anti-Cox-2 antibody. For normalization, membranes were stripped and reprobed with an anti-β-actin antibody. One representative experiment out of three is shown.

4.1.2 15d-PGJ_2-induced Activation of MAPK Signalling Pathways

As 15d-PGJ_2-mediated Cox-2 expression might be coupled to intracellular signalling cascades, the involvement of MAPK pathways was studied. Time-dependent incubation of cells with 15d-PGJ_2 resulted in activation of three main MAPK routes, indicated by phosphorylation of p38 MAPK, p42/44 MAPK and JNK1/2 in a time- (Figure 2 A) and concentration-dependent (Figure 2 B) manner. Activation of p38 MAPK was rapid and transient between 5 and 60 min, reaching a maximum at approx. 10 min after treatment. In contrast, phosphorylation of p42/44 MAPK was observed after 1 h and remained consistent up to 48 h. A weak induction of JNK1/2 was detected between 5 to 30 min which increased at longer incubation periods and was - similarly to pp42/44 MAPK - induced up to 48 h (Figure 2 A). It can be excluded that the observed late time point activations of p42/44 MAPK and JNK1/2 are mediated by the solvent DMSO as these effects were not detected in vehicle-treated cells (Figure 2 C).

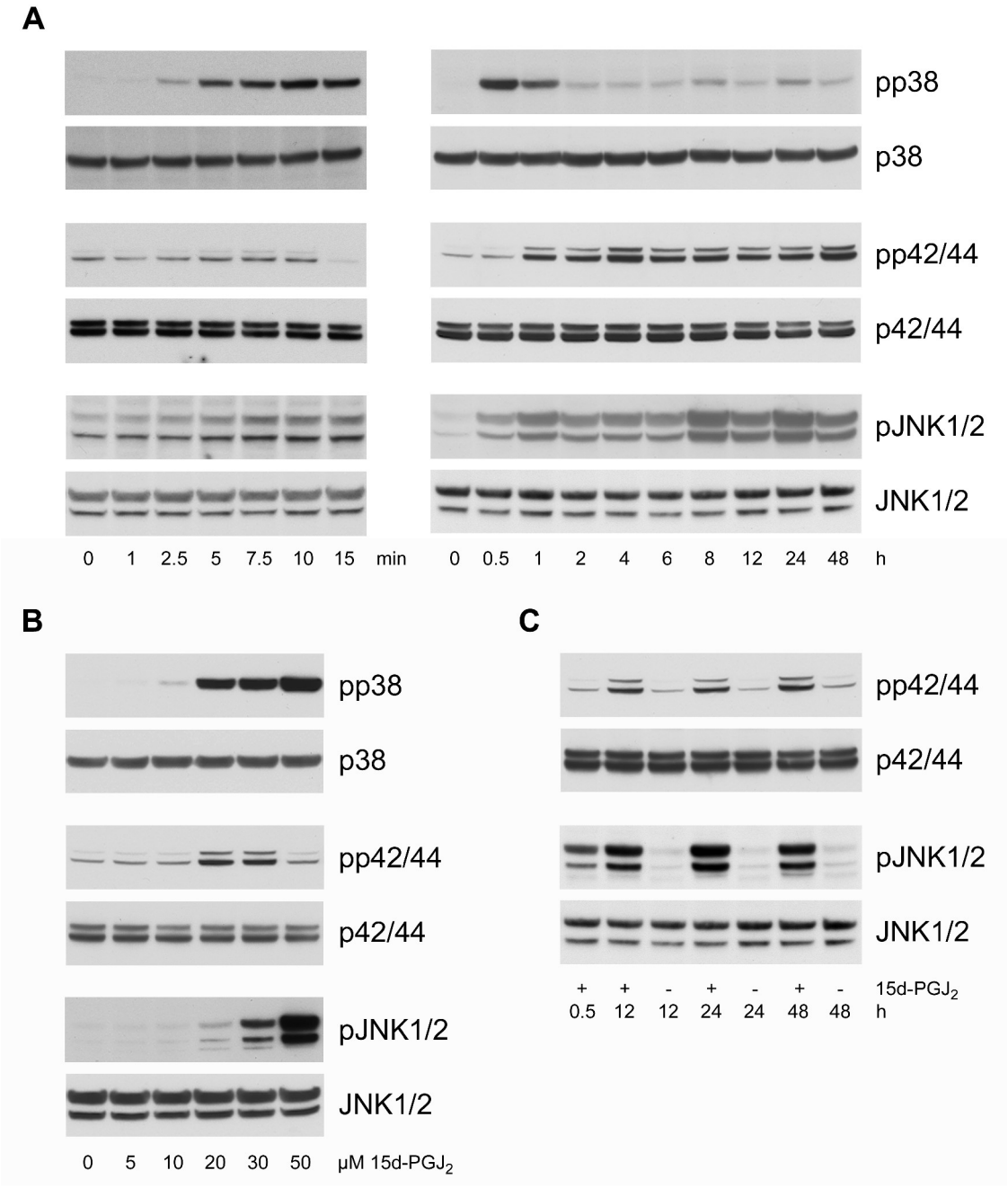

Figure 2: 15d-PGJ$_2$ activates p38 MAPK, p42/44 MAPK and JNK1/2.

(A) MG-63 cells were stimulated for indicated time periods with 20 µM 15d-PGJ$_2$. Cell lysates were subjected to Western blot analysis using phospho-specific anti-p38 MAPK (pp38), anti-p42/44 MAPK (pp42/44) and anti-JNK1/2 (pJNK1/2) antibodies. For normalization, membranes were stripped and reprobed with anti-p38 MAPK, anti-p42/44 MAPK and anti-JNK1/2 antibodies. (B) MG-63 cells were treated with indicated concentrations of 15d-PGJ$_2$ for 10 min (pp38 MAPK) and 4 h (pp42/44 MAPK and pJNK1/2). Cell lysates were subjected to Western blot analysis (see above). (C) MG-63 cells were treated for indicated time periods with 20 µM 15d-PGJ$_2$ (+) or DMSO as a vehicle control (-). Cell lysates were subjected to Western blot analysis (see above). (A-C) One representative experiment out of three is shown.

To explore if a significant proportion of 15d-PGJ_2 is metabolized by components of the standard growth medium, the medium was exchanged for HANKS/Hepes buffer before MG-63 cells were stimulated with 15d-PGJ_2 for short time periods. A significant phosphorylation of p38 MAPK was already obtained with 5 µM of 15d-PGJ_2 (Figure 3 A). However, 20 µM 15d-PGJ_2 was necessary to induce p38 MAPK activation in standard growth medium containing 5% FCS (Figure 2 B). It is likely to assume that a certain FCS component might be responsible for the metabolization of 15d-PGJ_2 as pp38 MAPK was also recorded at much lower concentrations of 15d-PGJ_2 in α-MEM without FCS (Figure 3 B) compared to the standard medium (Figure 3 B, last lane). However, all other experiments were performed in standard growth medium as the presence of FCS is essential for long-term cultivations of this cell line and represents physiological conditions.

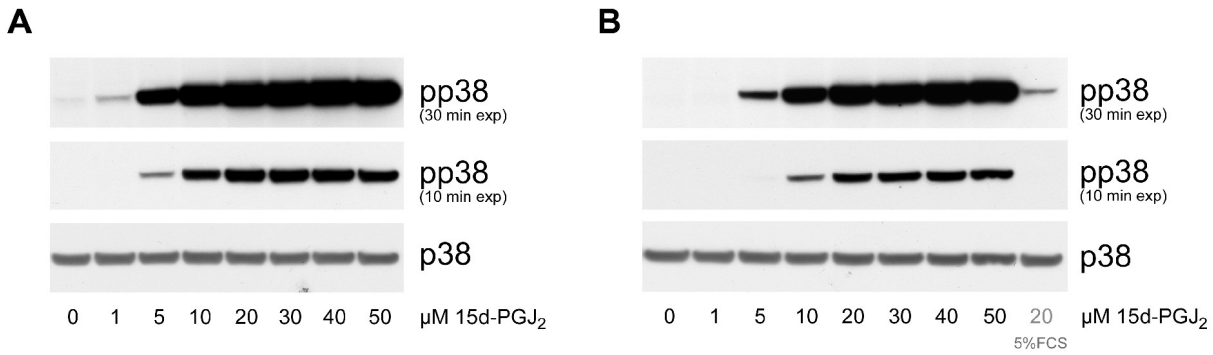

Figure 3: 15d-PGJ_2-mediated p38 MAPK activation in the absence of FCS.
MG-63 cells were treated with indicated concentrations of 15d-PGJ_2 for 10 min in HANKS/Hepes buffer (A) and in α-MEM without FCS (B). As a control, MG-63 cells were treated with 20 µM 15d-PGJ_2 in standard growth medium (α-MEM containing 5% FCS) (B, last lane). Cell lysates were subjected to Western blot analysis using a phospho-specific anti-p38 MAPK antibody (pp38). Different film exposure times (exp) are indicated for pp38 detection. For normalization, membranes were stripped and reprobed with an anti-p38 antibody. One representative experiment out of two is shown.

4.1.3 Signalling Pathways involved in 15d-PGJ_2-induced Cox-2 Expression

To prove a direct involvement of MAPK signalling in Cox-2 expression, inhibitors of the different MAPK routes were added prior to stimulation of cells with 15d-PGJ_2. While the JNK inhibitor II had no effect on Cox-2 mRNA and protein expression, pre-treatment of MG-63 cells with PD169316 (a p38 MAPK inhibitor) or PD098059 (a MAPK kinase inhibitor upstream of p42/44), either alone or in combination potently blocked Cox-2 expression on mRNA and protein level (Figure 4 A, B). These results led us conclude that 15d-PGJ_2-induced Cox-2 expression is mediated by upstream signalling events including p38 and p42/44 MAPK activation.

Upstream of MAPK activation, PI3K, Ras and Akt are frequently involved in the regulation of Cox-2 expression [Surh and Kundu, 2005; Telliez et al., 2006]. To investigate if any of these factors is mediating enhanced Cox-2 expression in the human osteosarcoma model, MG-63 cells were incubated with inhibitors of PI3K (LY294002), Ras (manumycin A), and Akt prior to stimulation with 15d-PGJ_2. Inhibition of PI3K and Ras, alone or in combination, resulted in highly diminished Cox-2 expression whereas inhibition of Akt had no effect. It should be noted that the Ras inhibitor manumycin A alone induced Cox-2 expression (Figure 4 C).

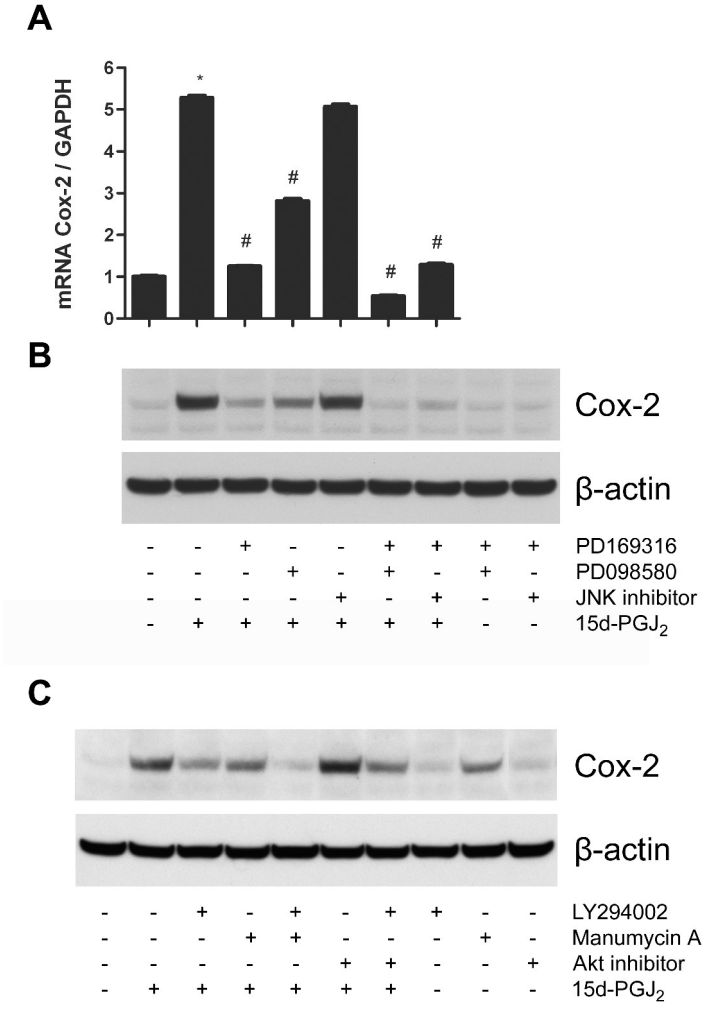

Figure 4: Signalling pathways in 15d-PGJ_2-induced Cox-2 expression.

(A, B) MG-63 cells were pretreated for 30 min with p38 MAPK inhibitor PD169316 (1 µM), MAPK kinase inhibitor PD098059 (20 µM), JNK inhibitor II (1 µM), and combinations of inhibitors, followed by stimulation with 20 µM 15d-PGJ_2 for 6 h to detect Cox-2 mRNA (A) or for 8 h to follow Cox-2 protein expression (B). As a control, cells were treated with the respective inhibitors alone for 8.5 h (B, lanes 8, 9). (A) For determination of Cox-2 mRNA expression, cDNA was generated and subjected to qPCR using specific primers for Cox-2. Cox-2 expression was normalized to GAPDH and values are expressed as mean ± SD. **P*<0.001 versus vehicle treated cells. #*P*<0.001 versus 15d-PGJ_2-treated cells. (B) For detection of Cox-2 protein, cell lysates were subjected to Western blot analysis using a specific anti-Cox-2 antibody. For normalization, membranes were stripped and reprobed with an anti-β-actin antibody. (A, B) One representative experiment out of three is shown. (C) MG-63 cells were pretreated for 30 min with PI3K inhibitor LY294002 (20 µM), Ras inhibitor manumycin A (10 µM), Akt inhibitor (20 µM), and combinations of inhibitors prior to stimulation with 20 µM 15d-PGJ_2 for 8 h. As a control, cells were treated with the respective inhibitors alone for 8.5 h (lanes 8-10). Cell lysates were subjected to Western blot analysis for Cox-2 detection (see above). One representative experiment out of two is shown.

4.1.4 15d-PGJ_2-mediated Cox-2 Expression is PPARγ-independent

15d-PGJ_2 is a potent ligand of the nuclear receptor PPARγ [Kliewer et al., 1995]. However, recent studies reported on a variety of cellular responses by 15d-PGJ_2 that may occur independently of PPARγ activation (see Introduction, section 1.3.1). MG-63 cells express PPARγ1 on mRNA level whereas just traces of the PPARγ2 isoform could be detected by RT-PCR (Figure 5). To reveal whether 15d-PGJ_2-induced intracellular signalling leading to Cox-2 expression is PPARγ-dependent or PPARγ-independent, MG-63 cells were pretreated with the PPARγ antagonist T0070907. Figure 6 A shows that stimulation of p38 and p42/44 MAPK and Cox-2 expression by 15d-PGJ_2 was not affected by T0070907 at indicated concentrations. To confirm these data, PPARγ expression was knocked down using two different PPARγ-specific siRNAs. Each siRNA diminished PPARγ mRNA expression by about 80% (Figure 6 B) without influencing MAPK activation and Cox-2 expression in MG-63 cells (Figure 6 C).

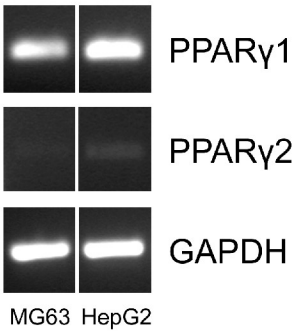

Figure 5: Expression of PPARγ isoforms in MG-63 cells.
RNA was isolated of MG-63 cells and HepG2 cells (= positive control) and subjected to RT-PCR using specific primer pairs for the detection of PPARγ1, PPARγ2 and GAPDH. The RT-PCR products were separated on a 1% agarose gel. One representative experiment out of two is shown.

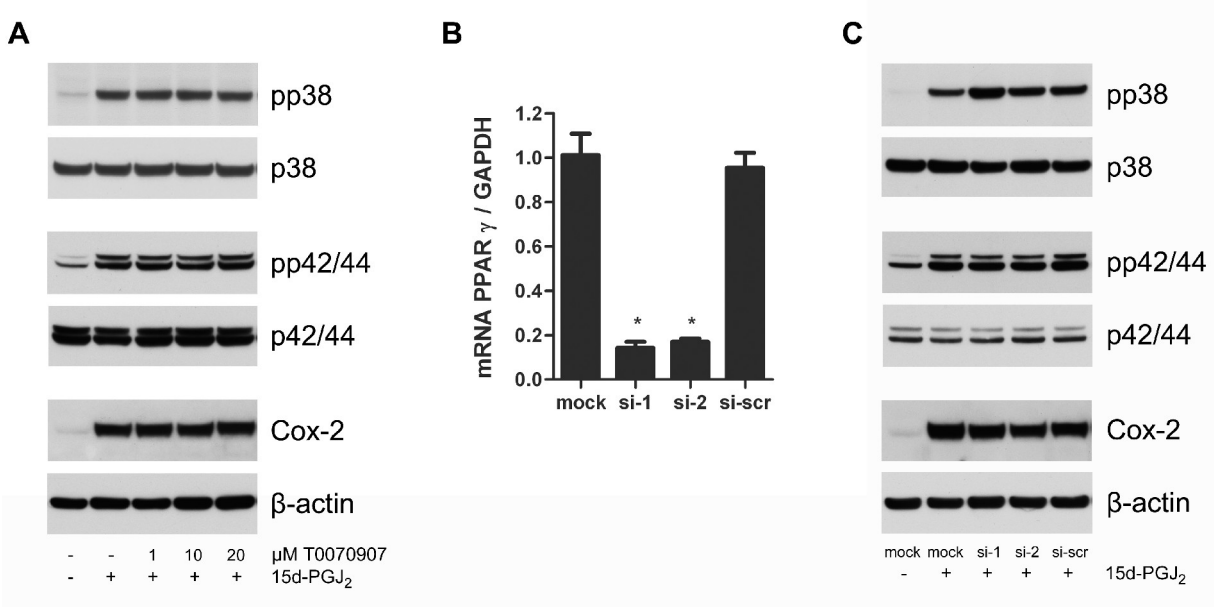

Figure 6: 15d-PGJ$_2$-mediated effects are PPARγ-independent.

(A) MG-63 cells were pretreated for 30 min with indicated concentrations of the PPARγ blocker T0070907 prior to stimulation with 20 µM 15d-PGJ$_2$. To follow activation of MAPKs, cells were incubated for 10 min (pp38 MAPK) or 4 h (pp42/44 MAPK), respectively. Cox-2 expression was determined after 8 h. For detection of the respective proteins, cell lysates were subjected to Western blot analysis using specific antibodies against pp38 MAPK, pp42/44 MAPK or Cox-2. For normalization, membranes were stripped and reprobed with antibodies against p38 MAPK, p42/44 MAPK and β-actin. (B) MG-63 cells were transfected with siRNAs specific for PPARγ (si-1 and si-2) or with a scrambled negative control siRNA (si-scr), each at a concentration of 50 nM. Mock transfected cells (mock) were treated with the transfection reagent Oligofectamine® alone. After a transfection period of 66 h, RNA was isolated and the expression level of PPARγ was determined by qPCR. PPARγ expression was normalized to GAPDH and values are expressed as mean ± SD. **P*<0.001 versus mock-treated cells. (C) MG-63 cells were transfected with siRNAs specific for PPARγ (si-1 and si-2) or with a scrambled negative control siRNA (si-scr), each at a concentration of 50 nM. Mock transfected cells (mock) were treated with the transfection reagent Oligofectamine® alone. After a transfection period of 66 h, MG-63 cells were treated with 20 µM 15d-PGJ$_2$. To follow the activation of MAPKs, the cells were incubated for 10 min (p38 MAPK) or 4 h (p42/44 MAPK). Cox-2 expression was determined after 8 h. For detection of the respective proteins, cell lysates were subjected to Western blot analysis (see above). (A-C) One representative experiment out of two is shown.

4.1.5 15d-PGJ_2-mediated Cox-2 Expression occurs independently of PGD_2 Receptor Subtypes

The rapid activation of p38 MAPK raised the question if 15d-PGJ_2 might activate intracellular signalling cascades through the activation of GPCRs which are frequently involved in fast signal transduction from extracellular stimuli. Candidate GPCRs are the PGD_2 receptors DP and CRTH2 which can also be activated by 15d-PGJ_2 [Scher and Pillinger, 2005] (see Introduction, section 1.3.1.1). Hence, MG-63 cells were treated with PGD_2 as well as synthetic agonists and antagonists of DP and CRTH2 to clarity if these receptors regulate 15d-PGJ_2-mediated cellular responses. PGD_2 did not induce activation of p38 MAPK, p42/44 MAPK, and JNK1/2 (Figure 7 A). High concentrations (50 µM) of PGD_2 slightly increase Cox-2 expression (Figure 7 B) which rather argues for receptor-independent effects as these receptors are likely to be stimulated by low nanomolar PGD_2 concentrations [Sawyer et al., 2002]. In concordance, agonists of DP and CRTH2 did not induce MAPK/JNK activation and Cox-2 expression (Figure 8 A), and 15d-PGJ_2-induced MAPK/JNK phosphorylation and Cox-2 expression is not impaired in the presence of PGD_2 receptor antagonists (Figure 8 B).

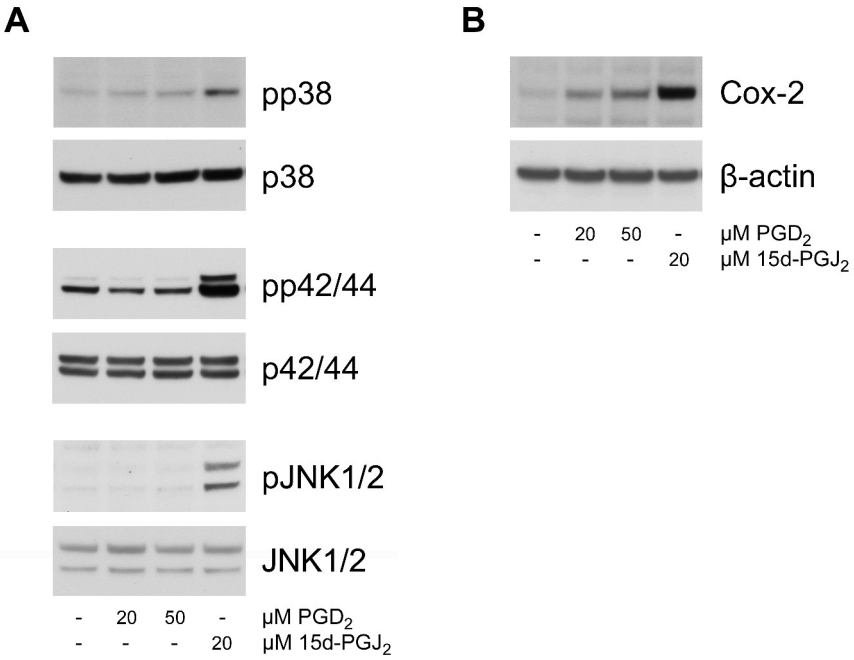

Figure 7: PGD_2 does not mimic 15d-PGJ_2-induced cellular responses.

MG-63 cells were treated with indicated concentrations of PGD_2 and 15d-PGJ_2. (A) To follow the activation of MAPKs, the cells were incubated for 10 min (pp38 MAPK) and 4 h (pp42/44 MAPK, pJNK1/2), respectively. (B) Cox-2 expression was determined after 8 h. For detection of the respective proteins, cell lysates were subjected to Western blot analysis using specific antibodies against pp38 MAPK, pp42/44 MAPK, pJNK1/2, and Cox-2. For normalization, membranes were stripped and reprobed with antibodies against p38 MAPK, p42/44 MAPK, JNK1/2, and β-actin. One representative experiment out of three is shown.

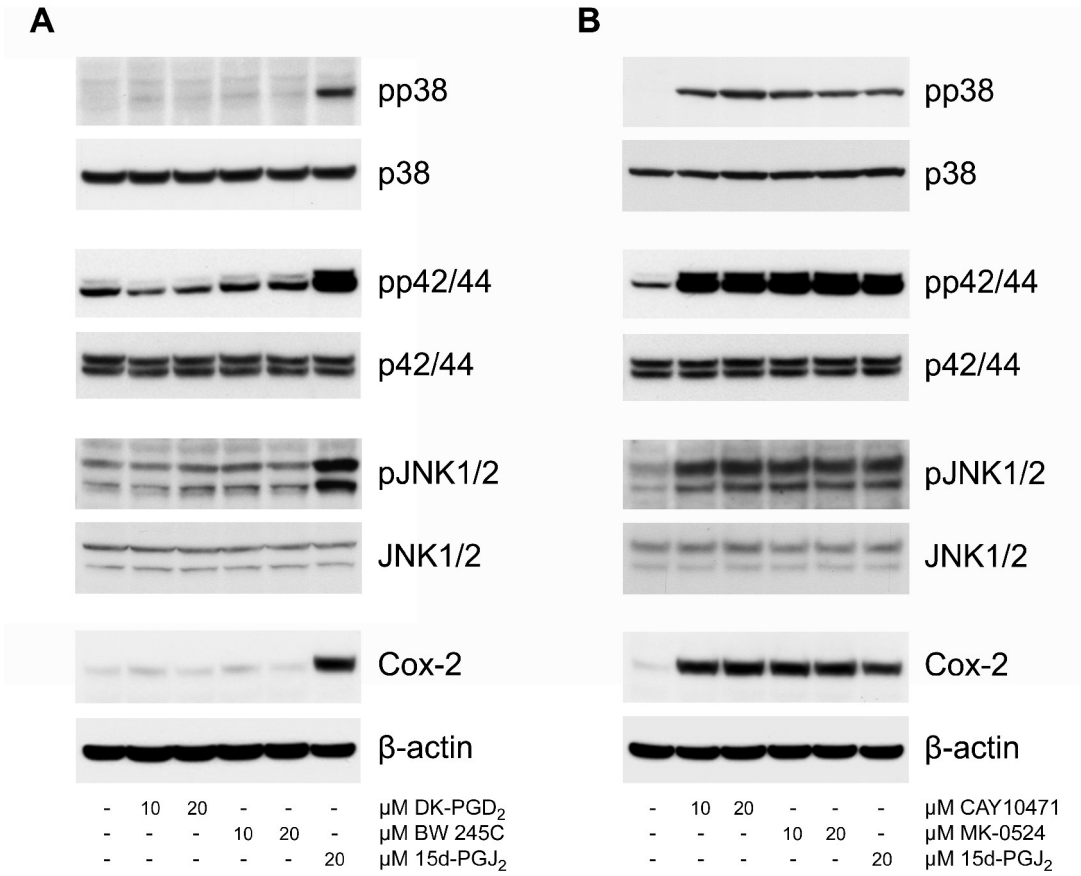

Figure 8: PGD_2 receptor subtype analogues do not influence 15d-PGJ_2-mediated effects.

(A) MG-63 cells were incubated with indicated concentrations of the CRTH2 agonist DK-PGD_2, the DP agonist BW 245C, or 20 µM 15d-PGJ_2. To follow the activation of MAPKs, the cells were incubated for 10 min (pp38 MAPK) or 4 h (pp42/44 MAPK, pJNK1/2), respectively. Cox-2 expression was determined after 8 h. For detection of the respective proteins, cell lysates were subjected to Western blot analysis using specific antibodies against pp38 MAPK, pp42/44 MAPK, pJNK1/2, and Cox-2. For normalization, membranes were stripped and reprobed with antibodies against p38 MAPK, p42/44 MAPK, JNK1/2, and β-actin. (B) MG-63 cells were preincubated for 30 min with indicated concentrations of CRTH2 antagonist CAY-10471 or DP antagonist MK-0524 followed by addition of 20 µM 15d-PGJ_2. Incubation periods for 15d-PGJ_2 and Western blot analysis see above. One representative experiment out of two is shown.

4.1.6 15d-PGJ_2 induced Cox-2 Expression is NF-κB-independent

The transcription factor NF-κB is activated under inflammatory conditions and regulates Cox-2 expression in response to various stimuli [Inoue and Tanabe, 1998; Newton et al., 1997; Yamamoto et al., 1995]. It is not likely that 15d-PGJ_2-induced Cox-2 expression in MG-63 cells is NF-κB-dependent as neither the NF-κB inhibitor CAY10512 nor an IKK inhibitor affected Cox-2 expression levels (Figure 9 A, B). This is supported by findings that the NF-κB subunit p65 did not translocate to the nucleus in response to 15d-PGJ_2 (Figure 9 C).

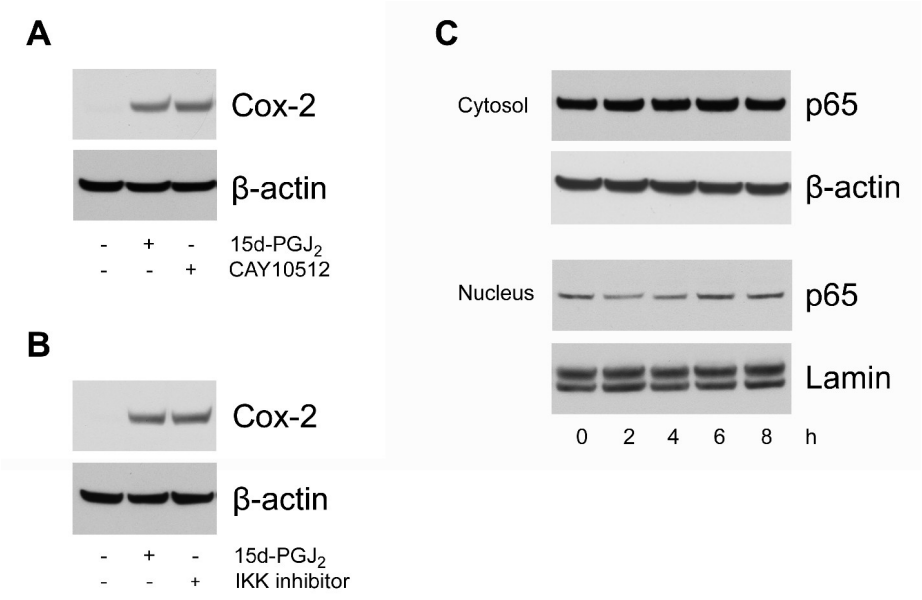

Figure 9: 15d-PGJ_2-induced Cox-2 expression is NF-κB-independent

(A) MG-63 cells were pretreated for 30 min with 10 µM CAY10512 (NF-κB blocker) prior to stimulation with 20 µM 15d-PGJ_2 for 8 h. For detection of Cox-2 protein, cell lysates were subjected to Western blot analysis using a specific anti-Cox-2 antibody. For normalization, membranes were stripped and reprobed with an anti-β-actin antibody. (B) MG-63 cells were pretreated for 30 min with 10 µM IKK inhibitor prior to stimulation with 20 µM 15d-PGJ_2 for 8 h. Cox-2 expression was followed by Western blot experiments as described above. (C) MG-63 cells were treated for indicated time periods with 20 µM 15d-PGJ_2 followed by isolation of nuclear and cytosolic proteins. Equal amounts of proteins were subjected to Western blot analysis using a specific antibody for the NF-κB subunit p65. For normalization of the cytosolic fraction β-actin was used. For normalization of the nuclear fraction Lamin A/C was used. (A-C) One representative experiment out of two is shown.

4.1.7 15d-PGJ_2 induces Cox-2 mRNA Stability

Cox-2 is usually transiently expressed under stress conditions; however, prolonged elevation of Cox-2 expression can be regulated by increased mRNA stability [Harper and Tyson-Capper, 2008]. As 15d-PGJ_2-induced Cox-2 mRNA and protein expression was increased in MG-63 cells up to 24 h (Figure 1 B), we hypothesized that 15d-PGJ_2 could play a role in both, increased Cox-2 mRNA transcription and stabilization. To clarify, cells were incubated with vehicle control (DMSO) in the absence or presence of 15d-PGJ_2 prior to addition of ActD (to inhibit transcription). Time-course experiments revealed decreased degradation of 15d-PGJ_2-induced Cox-2 mRNA compared to vehicle control (Figure 10 A).

As an increased mRNA stability could underlie various signalling events [Cao et al., 2007; Monick et al., 2002; Sheng et al., 2001], Cox-2 mRNA stability was investigated in 15d-PGJ_2-treated cells in the presence of combinations of ActD and various MAPK inhibitors. Addition of the p38 MAPK inhibitor PD169316 reversed the impaired Cox-2 mRNA degradation caused by 15d-PGJ_2 to levels obtained with vehicle control (Figure 10 B). Both, the MAPK kinase inhibitor PD098059 and the JNK inhibitor had no effect. These data suggest that 15d-PGJ_2 induces Cox-2 mRNA stability via a p38 MAPK sensitive route.

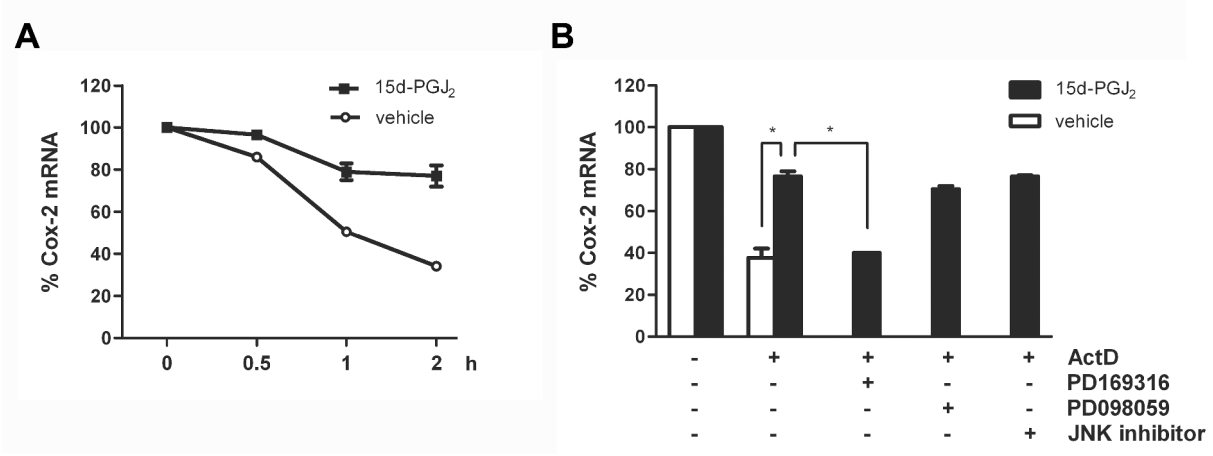

Figure 10: 15d-PGJ$_2$ induces Cox-2 mRNA stability via p38 MAPK activation.
(A) MG-63 cells were treated for 4 h with 20 µM 15d-PGJ$_2$ or vehicle (DMSO) followed by incubation with 0.5 µM ActD for indicated time periods. For determination of Cox-2 mRNA expression, cDNA was generated and subjected to qPCR using specific primers for Cox-2. Cox-2 expression was normalized to GAPDH and values are expressed as mean ± SD. Cox-2 levels after the 15d-PGJ$_2$ incubation period without ActD (time point 0) are set 100%. (B) MG-63 cells were incubated for 4 h with 15d-PGJ$_2$ or vehicle (DMSO) followed by 2 h treatment with 0.5 µM ActD in the absence or presence of p38 MAPK inhibitor PD169316 (1 µM), MAPK kinase inhibitor PD098059 (20 µM), or JNK inhibitor II (1 µM). For determination of Cox-2 mRNA expression see above. Cox-2 levels after the 15d-PGJ$_2$ incubation period without ActD are set 100%. *P<0.001 indicates significant differences between two groups. (A, B) One representative experiment out of three is shown.

4.1.8 15d-PGJ$_2$-induced Cox-2 Expression is mediated by EGFR Activation

As 15d-PGJ$_2$-induced activation of p42/44 MAPK can be coupled to transactivation of the EGFR and the platelet-derived growth factor receptor (PDGFR), respectively [Ichiki et al., 2004], MG-63 cells were treated with specific blockers for these receptors prior to stimulation with 15d-PGJ$_2$. Western blot analysis revealed that phosphorylation of p42/44 MAPK as well as Cox-2 expression was nearly reduced to basal levels in the presence of the EGFR inhibitor AG1478 (Figure 11 A). In contrast, the PDGFR blocker AG1296 only slightly diminished phosphorylation of p42/44 MAPK without influencing Cox-2 expression. Phosphorylation of p38 MAPK and JNK1/2 was unaffected by both inhibitors (Figure 11 A).

To confirm 15d-PGJ_2-mediated activation of EGFRs, two phospho-specific antibodies against Tyr1068 and Tyr1173 were used. However, I failed to detect the phosphorylation status of EGFR with these antibodies (data not shown). Therefore, an antibody recognizing phospho-tyrosine-modified epitopes was used to detect other potential phosphorylation sites on EGFRs. Time-dependent stimulation of MG-63 cells with 15d-PGJ_2 increased tyrosine phosphorylation of a protein of approx. 170 kDa (Figure 11 B) that comigrated with EGFR. Most importantly, this phosphorylation signal is blocked specifically by the EGFR inhibitor AG1478 but not by the PDGFR inhibitor (Figure 11 C, lanes 3, 4) and could be mimicked by EGF treatment (Figure 11 C, last lane). To finally prove that the immunoreactive 170 kDa EGFR-like band is the EGFR that becomes phosphorylated, immunoprecipitation was performed. For these experiments, an agarose-conjugated EGFR antibody was used and precipitated proteins were subjected to SDS-PAGE and immunoblotting using an antibody specific for phospho-tyrosine epitopes. Figure 11 D shows that treatment with 15d-PGJ_2 leads to an increased EGFR tyrosine-phosphorylation, which is blocked by the EGFR inhibitor AG1478 but not affected by the PDGFR inhibitor AG1296.

To elucidate whether 15d-PGJ_2-mediated activation of MAPKs (Figure 2 A) may directly contribute to phosphorylation of EGFR, MG-63 cells were preincubated with several MAPK/JNK inhibitors prior to stimulation. However, no reduction in the phosphorylation status of the EGFR could be detected (Figure 12 A). Additionally, we can exclude a crosslink between rapidly activated p38 MAPK and delayed phosphorylation of p42/44 MAPK as inhibitors of p38 MAPK did not block the pp42/44 signal (Figure 12 B).

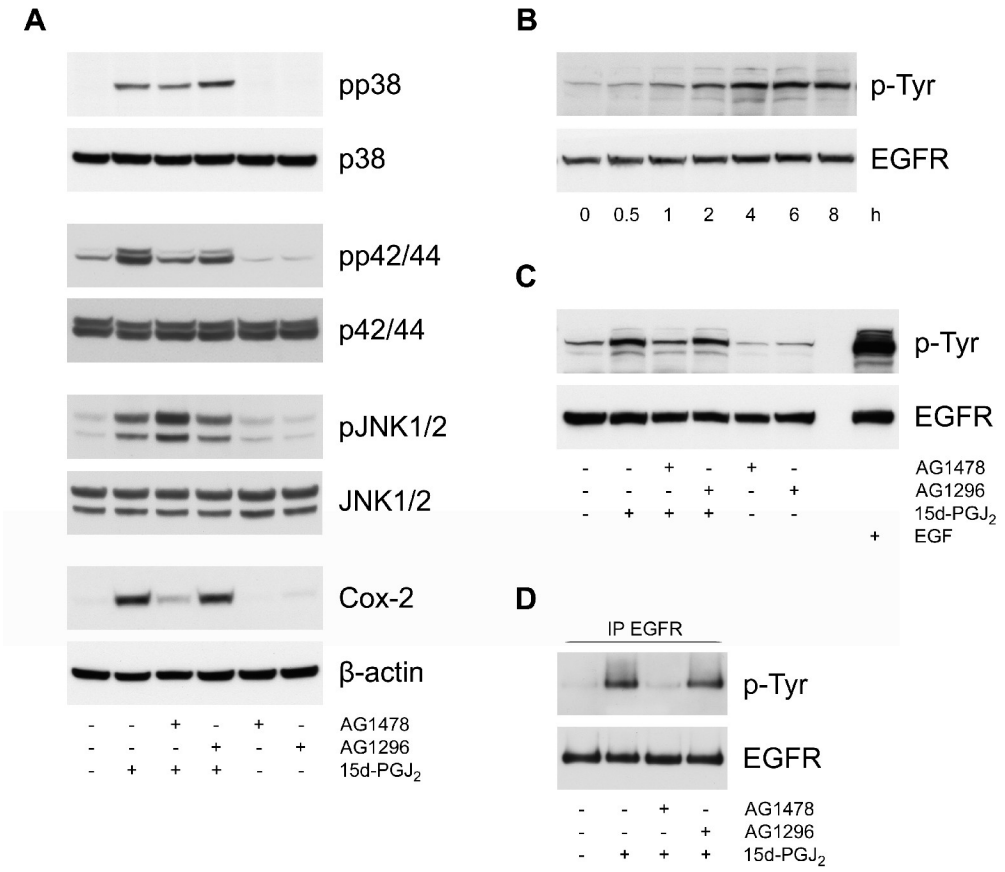

Figure 11: 15d-PGJ_2-induced Cox-2 expression is mediated by EGFR activation.
(A) MG-63 cells were pretreated for 30 min with EGFR blocker AG1478 (20 µM) or PDGFR blocker AG1296 (20 µM) prior to stimulation with 20 µM 15d-PGJ_2. To follow activation of p38 or p42/44 MAPK, cells were incubated for 10 min or 4 h, respectively. Cox-2 expression was followed after 8 h. As a control, cells were treated with inhibitors alone. For detection of the respective proteins, cell lysates were subjected to Western blot analysis using specific antibodies against pp38 MAPK, pp42/44 MAPK, pJNK1/2, and Cox-2. For normalization, membranes were stripped and reprobed with antibodies against p38 MAPK, p42/44 MAPK, JNK1/2, and β-actin, respectively. (B) MG-63 cells were incubated with 20 µM 15d-PGJ_2 at indicated time periods. Cell protein lysates were subjected to Western blot analysis using an antibody specifically recognizing phospho-tyrosine-modified proteins (p-Tyr). For normalization, membranes were stripped and reprobed with an anti-EGFR antibody. (C) MG-63 cells were pretreated for 30 min with AG1478 (20 µM) or AG1296 (20 µM) prior to stimulation with 20 µM 15d-PGJ_2 for 8 h to detect p-Tyr. As a control, cells were treated with inhibitors alone. EGF (50 ng/ml) treatment was performed for 15 min. Cell lysates were subjected to Western blot analysis as described above. (D) MG-63 cells were pretreated for 30 min with AG1478 (20 µM) or AG1296 (20 µM) prior to stimulation with 20 µM 15d-PGJ_2 for 8 h. Cell lysates were immunoprecipitated with an agarose-conjugated anti-EGFR antibody followed by Western blot analysis using anti-p-Tyr and anti-EGFR antibodies. (A-D) One representative experiment out of three is shown.

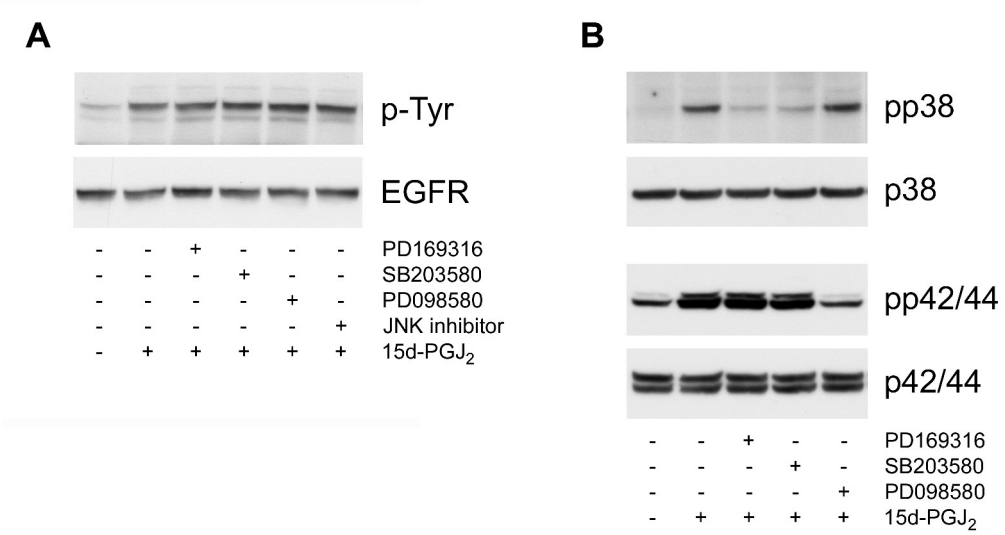

Figure 12: Activation of p42/44 MAPK occurs independently of p38 MAPK.
(A) MG-63 cells were pretreated for 30 min with p38 MAPK inhibitors PD169316 (1 µM) or SB203580 (20 µM), MAPK kinase inhibitor PD098059 (20 µM), and JNK inhibitor II (1 µM) followed by 8 h stimulation with 20 µM 15d-PGJ_2. Cell lysates were subjected to Western blot analysis using specific antibodies against p-Tyr and EGFR. (B) MG-63 cells were pretreated for 30 min with p38 MAPK inhibitors PD169316 (1 µM) and SB203580 (10 µM), and MAPK kinase inhibitor PD098059 (20 µM) followed by stimulation with 20 µM 15d-PGJ_2 for 10 min (pp38 MAPK) and 4 h (pp42/44 MAPK). Cell lysates were subjected to Western blot analysis using specific antibodies against pp38 and pp42/44 MAPK. For normalization, membranes were stripped and reprobed with antibodies against p38 MAPK and p42/44 MAPK. (A, B) One representative experiment out of three is shown.

4.1.9 15d-PGJ_2 generates intracellular ROS Accumulation

Cyclopentenone PGs have been reported to alter the intracellular redox state and to generate ROS, which in turn could mediate a wide range of activities including alterations in intracellular signalling cascades [Na and Surh, 2003; Uchida and Shibata, 2008]. Detection of intracellular ROS levels was performed with the cell-permeable dye H_2DCF-DA which becomes fluorescent upon oxidation (see Materials and Methods, section 3.2.12). To confirm intracellular fluorescence signals, H_2DCF-DA-labeled cells were stimulated with increasing 15d-PGJ_2 concentrations and were subjected to fluorescence microscopy (Figure 13). All further readouts of DCF fluorescence were performed spectrofluorometrically.

Stimulation of MG-63 cells with 15d-PGJ_2 caused a fast, time-dependent increase in DCF fluorescence (Figure 14 A). As pretreatment of cells with both, MAPK inhibitors and the EGFR inhibitor did not block increased ROS levels (Figure 14 C), it is reasonable to assume that this effect occurs upstream of these signal transduction events. Furthermore, elevated ROS levels in MG-63 cells were not changed in the presence of the mitochondrial complex I inhibitor rotenone or the NADPH oxidase inhibitor apocynin (Figure 14 D).

Measurements of intracellular GSH contents showed a significant decrease after 10 min treatment with 15d-PGJ_2. Decreased GSH levels remained stable up to 60 min (Figure 14 B) and returned to baseline levels after additional 5 h (Figure 30 A). GSSG levels were widely unchanged up to 60 min after addition of 15d-PGJ_2 although after 10 and 20 min treatment GSSG levels were significantly decreased (Figure 14 B).

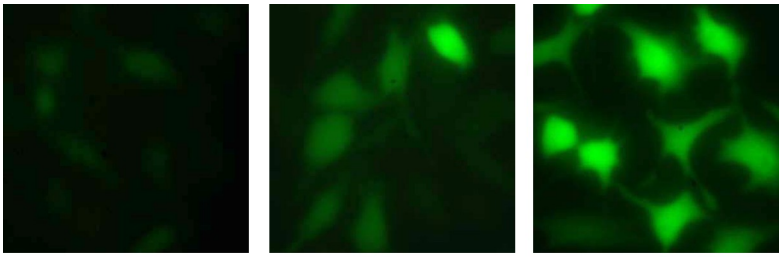

Figure 13: Intracellular DCF fluorescence upon 15d-PGJ_2 treatment.
MG-63 cells were treated with DMSO or indicated concentrations of 15d-PGJ_2 for 1 h followed by loading of 20 µM DCF-DA for 20 min. DCF fluorescence was recorded by microscopy.

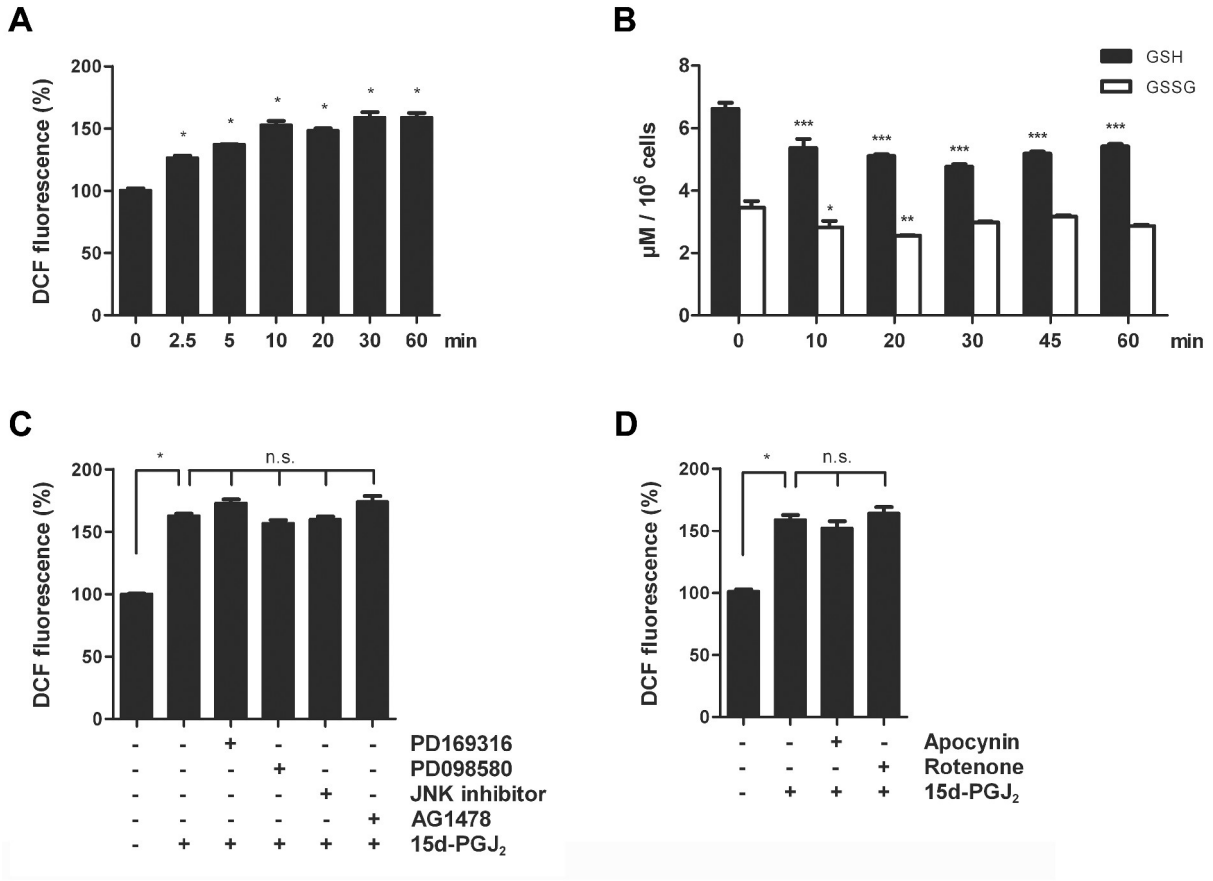

Figure 14: 15d-PGJ_2 induces intracellular ROS levels.

(A) MG-63 cells were treated with 20 µM 15d-PGJ_2 at indicated time periods followed by loading of 20 µM DCF-DA for 20 min. After cell lysis, DCF fluorescence was recorded spectrofluorometrically. Vehicle-treated cells are set 100%. Data are expressed as mean ± SD. **P*<0.001 versus vehicle-treated cells. (B) MG-63 cells were treated with 20 µM 15d-PGJ_2 at indicated time periods. Intracellular GSH and GSSG concentrations were determined with a commercial Glutathione Assay Kit (Cayman Chemical) according to the supplier's manual. The results are reported as µM reduced GSH (total GSH minus GSSG) and GSSG per 10^6 cells. Data are expressed as mean ± SD. ****P*<0.001, ***P*<0.01, **P*<0.05 versus vehicle-treated cells. (C) MG-63 cells were pretreated for 30 min with p38 MAPK inhibitor PD169316 (1 µM), MAPK kinase inhibitor PD098059 (20 µM), JNK inhibitor II (1 µM), and EGFR inhibitor AG1478 (20 µM) prior to stimulation for 1 h with 20 µM 15d-PGJ_2. Detection of DCF fluorescence was performed as above. Vehicle-treated cells are set 100%. **P*<0.001 versus vehicle-treated cells; n.s. indicates not significant versus 15d-PGJ_2-treated cells. (D) MG-63 cells were pretreated for 30 min with 5 µM of the NAPDH oxidase inhibitor apocynin or 5 µM of the mitochondrial complex I inhibitor rotenone prior to stimulation with 20 µM 15d-PGJ_2 for 1 h. Detection of DCF fluorescence was performed as above. Vehicle-treated cells are set 100%. **P*<0.001 versus vehicle-treated cells; n.s. indicates not significant versus 15d-PGJ_2-treated cells. (A-D) One representative experiment out of three is shown.

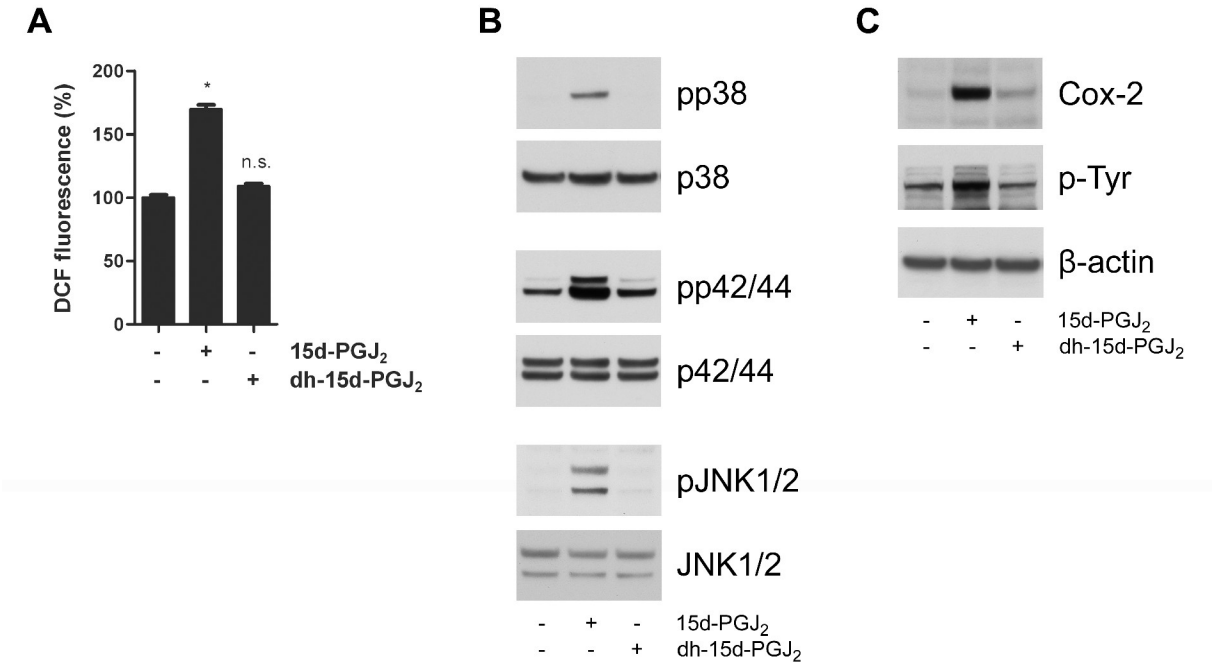

Figure 15: 15d-PGJ$_2$-mediated effects are related to its reactive carbon group.

(A) MG-63 cells were treated with 20 µM 15d-PGJ$_2$ or 9,10-dihydro-15d-PGJ$_2$ (dh-15d-PGJ$_2$) for 1 h to follow ROS levels. After DCF-DA loading and cell lysis, DCF fluorescence was measured spectrofluorometrically. Vehicle-treated cells are set 100%. **P*<0.001 versus vehicle-treated cells, n.s. indicates not significant versus vehicle-treated cells. (B) MG-63 cells were treated with 20 µM 15d-PGJ$_2$ or dh-15d-PGJ$_2$ for 10 min to follow p38 MAPK activation and for 4 h to follow p42/44 MAPK and pJNK1/2 activation. For the detection of the respective proteins, cell lysates were subjected to Western blot analysis using specific antibodies against pp38 MAPK, pp42/44 MAPK, and pJNK1/2. For normalization, membranes were stripped and reprobed with antibodies against p38 MAPK, p42/44 MAPK, and JNK1/2. (C) MG-63 cells were treated with 20 µM 15d-PGJ$_2$ or dh-15d-PGJ$_2$ for 8 h to follow Cox-2 protein expression and EGFR tyrosine phosphorylation. Cell lysates were subjected to Western blot analysis using an anti-Cox-2 antibody or an antibody against phospho-tyrosine-modified proteins (p-Tyr). For normalization, membranes were stripped and reprobed with an anti-β-actin antibody. (A-C) One representative experiment out of three is shown.

Cyclopentenones are characterized by the presence of a reactive α,β-unsaturated carbonyl group which can react with various nucleophiles [Uchida and Shibata, 2008]. To proof that the electrophilic carbon group of 15d-PGJ_2 is a prerequisite for increased intracellular ROS levels and subsequent downstream events, the structural analogue 9,10-dihydro-15d-PGJ_2 was tested. This compound, which lacks the α,β-unsaturated carbonyl group, did not show any effect observed with 15d-PGJ_2 such as increased DCF fluorescence (Figure 15 A), phosphorylation of MAPKs (p38, p42/44), JNK1/2 (Figure 15 B) and the EGFR (Figure 15 C) as well as Cox-2 expression (Figure 15 C). These data indicate that the polar carbon group of 15d-PGJ_2 is essential for its reactivity.

4.1.10 15d-PGJ_2-induced Cox-2 Expressions is modulated by intracellular GSH

As the intracellular redox balance is under tight control of GSH [Forman et al., 2009; Winterbourn and Hampton, 2008] and 15d-PGJ_2 modulates GSH levels in MG-63 cells (Figure 14 C), the next set of experiments aimed at investigating whether exogenously added antioxidative GSH precursor molecules could reverse 15d-PGJ_2-induced ROS accumulation and downstream events. Indeed, pretreatment of MG-63 cells with MPG and cell-permeable GSH ethyl ester suppressed 15d-PGJ_2-induced DCF fluorescence to basal levels (Figure 16 A). Similarly to Cox-2 expression (Figure 16 B), also 15d-PGJ_2-induced activation of p38 MAPK, p42/44 MAPK, JNK1/2 and the EGFR were inhibited by MPG and GSH ethyl ester (Figure 16 C). These data confirm that the rapid activation of p38 MAPK is a GPCR-independent effect but is regulated by alterations in the intracellular redox balance.

Next, it was aimed to figure out if the induction of Cox-2 expression could be mimicked generally under oxidative stress conditions. To confirm that ROS are likely formed during 15d-PGJ_2 treatments, cells were incubated with H_2O_2, an oxidant previously reported to elevate intracellular ROS levels in MG-63 cells [Bai et al., 2005]. Here it is shown that H_2O_2 induced both MAPK/JNK phosphorylation and Cox-2 expression in a concentration-dependent manner (Figure 17) similarly as observed with 15d-PGJ_2 (Figure 1 A).

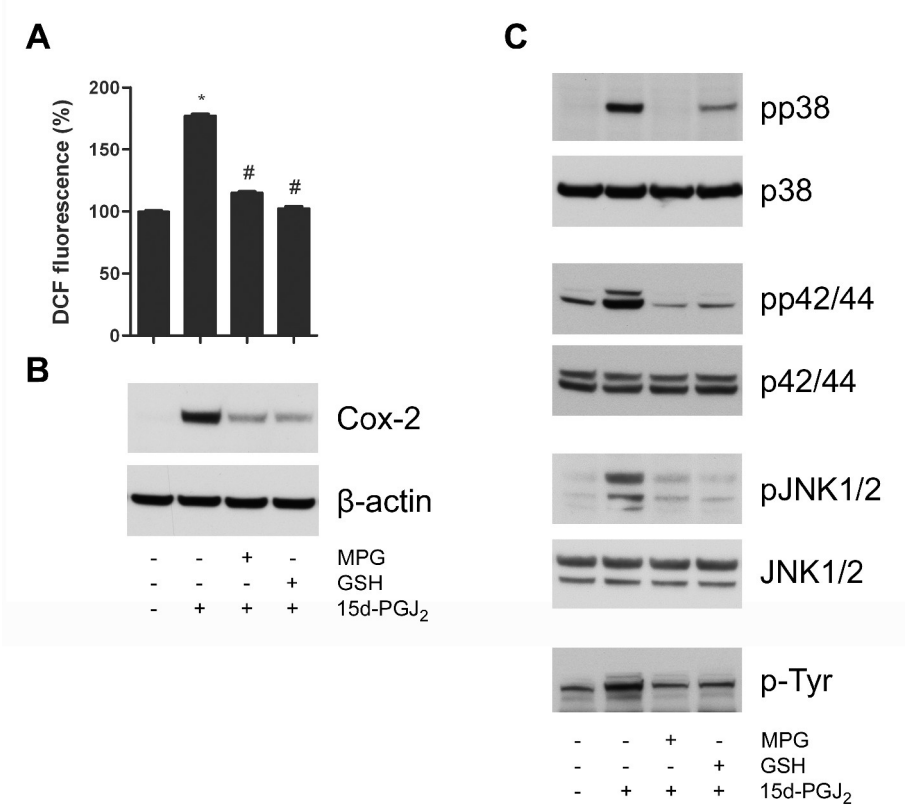

Figure 16: Cox-2 expression is modulated by the intracellular redox balance.

(A, B) MG-63 cells were pretreated for 60 min with 5 mM MPG or 10 mM GSH ethyl ester (GSH). Then, the cells were treated with 20 µM 15d-PGJ_2 for 1 h to follow ROS levels (A) and for 8 h to follow Cox-2 protein expression (B). (A) For ROS detection, treated cells were loaded for 20 min with 20 µM DCF-DA. After cell lysis, DCF fluorescence was measured spectrofluorometrically. The fluorescence counts detected with vehicle-treated cells are set 100%. Data are expressed as mean ± SD. **P*<0.001 versus vehicle-treated cells. $^{\#}P$<0.001 versus 15d-PGJ_2-treated cells. (B) For detection of Cox-2 protein, cell lysates were subjected to Western blot analysis using a specific anti-Cox-2 antibody. For normalization, membranes were stripped and reprobed with an anti-β-actin antibody. (C) MG-63 cells were pretreated for 60 min with 5 mM MPG or 10 mM GSH ethyl ester (GSH) followed by addition of 20 µM 15d-PGJ_2 for 10 min to follow p38 MAPK activation, for 4 h to detect p42/44 MAPK and JNK1/2 activation and for 8 h to identify EGFR tyrosine phosphorylation (p-Tyr). For detection of the respective proteins, cell lysates were subjected to Western blot analysis using antibodies against pp38 MAPK, pp42/44 MAPK, pJNK1/2 and p-Tyr. For normalization, membranes were stripped and reprobed with antibodies against p38 MAPK, p42/44 MAPK, and JNK1/2, respectively. (A-C) One representative experiment out of three is shown.

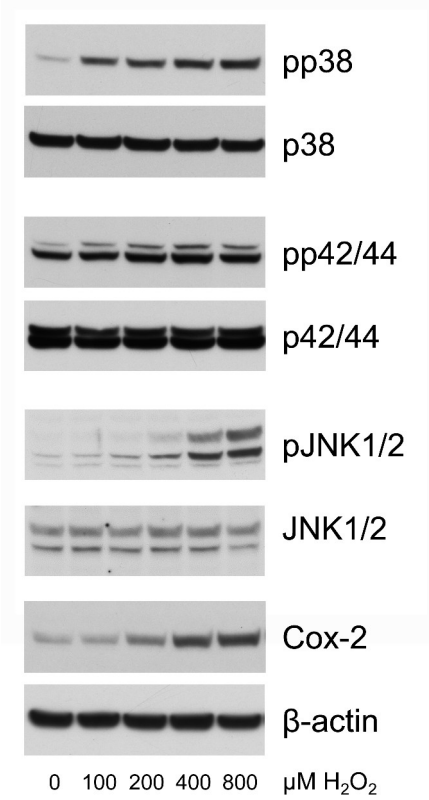

Figure 17: 15d-PGJ_2-induced effects are mimicked by H_2O_2.

MG-63 cells were incubated with H_2O_2 at indicated concentrations for 10 min to follow p38 MAPK activation, for 4 h to detect p42/44 MAPK and JNK1/2 activation and for 8 h to follow Cox-2 expression. For Western blot analysis, cell lysates were subjected to Western blot analysis using specific antibodies against pp38 MAPK, pp42/44 MAPK, pJNK1/2 and Cox-2. For normalization, membranes were stripped and reprobed with antibodies against p38 MAPK, p42/44 MAPK, JNK1/2, and β-actin. One representative experiment out of two is shown.

4.1.11 Prostaglandin Production by 15d-PGJ_2-treated Cells

To elucidate whether 15d-PGJ_2-induced Cox-2 is enzymatically active, exogenous AA was added as a substrate for PG synthesis. PGs were extracted from cellular supernatants and analyzed by GC/MS after suitable derivatization (see Material and Methods, section 3.2.15). Figure 18 A shows time-dependent synthesis of PGE_2 and $PGF_{2\alpha}$. The release of PGs increased constantly after 6 h, data that parallel 15d-PGJ_2-mediated expression of Cox-2 (Figure 1 B).

Next we studied whether PG synthesis could also occur due to the presence of Cox-1. Figure 18 B displays high Cox-2 expression in MG-63 cells under 15d-PGJ_2-stimulated conditions while no immunoreactive band became apparent for Cox-1 under non-stimulated and 15d-PGJ_2-stimulated conditions. As positive control for Cox-1 expression MC3T3-E1 cells were used [Leis et al., 1998]. Furthermore, the Cox-2 inhibitor NS-398 completely blocked PG biosynthesis from exogenous AA while the Cox-1 inhibitor FR-122047 did not block PGE_2 and $PGF_{2\alpha}$ synthesis (Figure 18 C).

To examine whether endogenous AA can be metabolized via 15d-PGJ_2-induced Cox-2 expression, MG-63 cells were treated with bradykinin, a hormone that promotes receptor-mediated signalling leading to release of phospholipid-associated AA [Brechter and Lerner, 2007; Hong and Levine, 1976]. Addition of bradykinin after 15d-PGJ_2 treatment led to pronounced PGE_2 synthesis (Figure 18 D) indicating that PG biosynthesis may occur under physiological conditions in MG-63 cells.

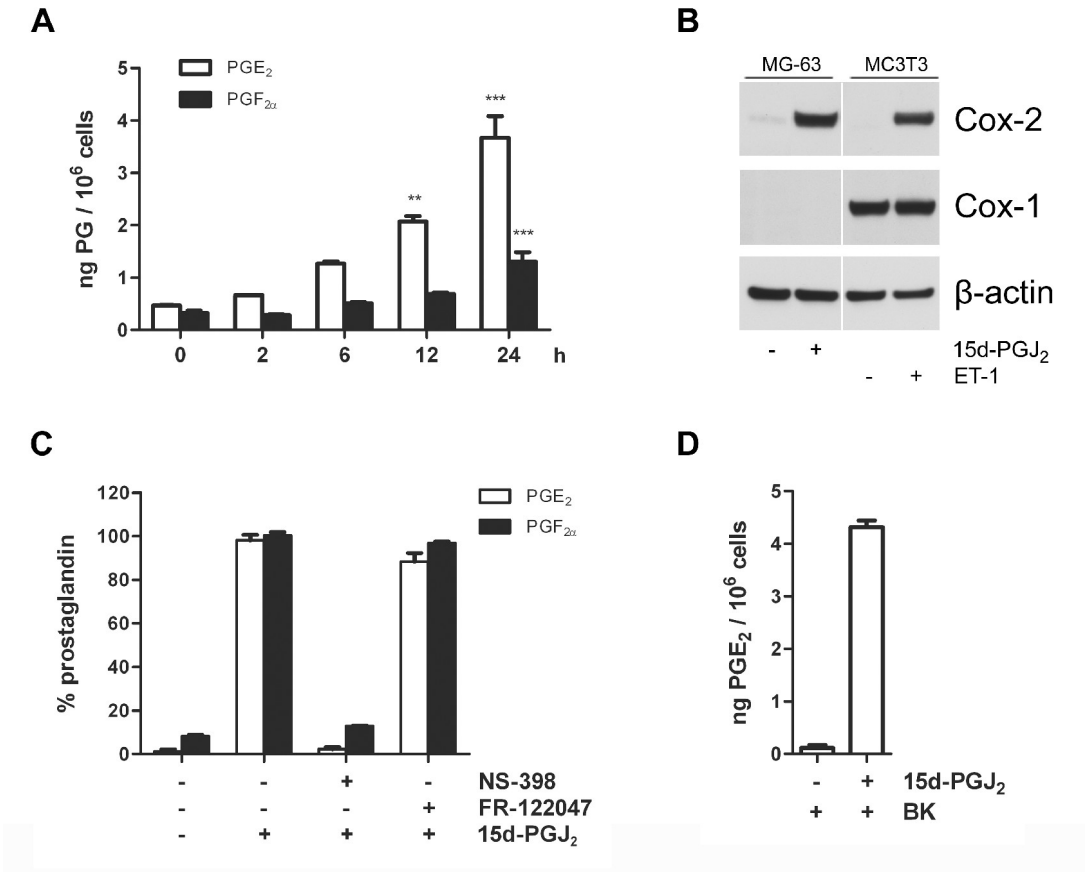

Figure 18: PG synthesis by 15d-PGJ$_2$-induced Cox-2.

(A) MG-63 cells were treated with 20 µM 15d-PGJ$_2$ up to 24 h to induce Cox-2 expression. Then, cells were incubated for 10 min with 10 µM AA after each indicated incubation period. PGE$_2$ and PGF$_{2\alpha}$ released into the cell culture supernatant were extracted, derivatized and estimated by GC/MS. PG levels were normalized to 10^6 cells. Values are expressed as mean ± SD. ***P*<0.01, ****P*<0.001 versus vehicle-treated cells. (B) MG-63 cells were treated with 20 µM 15d-PGJ$_2$ for 8 h. MC3T3 osteoblast-like cells, used as controls, were treated with 20 nM ET-1 for 3 h. Cell lysates were subjected to Western blot analysis using anti-Cox-1 and anti-Cox-2 antibodies. For normalization, membranes were stripped and reprobed with an anti-β-actin antibody. (C) MG-63 cells were treated with 20 µM 15d-PGJ$_2$ for 24 h to induce Cox-2 expression. Then, cells were incubated with 100 nM of FR-122047 (Cox-1 inhibitor) or NS-398 (Cox-2 inhibitor) for 15 min prior to addition of 10 µM AA for 10 min. PGE$_2$ and PGF$_{2\alpha}$ released into the cell culture supernatant were measured by GC/MS. PG levels were normalized to 10^6 cells. PG concentrations measured after treatment with 15d-PGJ$_2$ are set 100%. Values are expressed as mean ± SD. One representative experiment (performed in triplicate) is shown; 100% PGE$_2$ levels correspond to 6.14 ± 0.35 ng/10^6 cells while 100% PGF$_{2\alpha}$ levels corresponds to 2.47 ± 0.12 ng/10^6 cells. (D) MG-63 cells were treated with 20 µM 15d-PGJ$_2$ for 24 h. Then, cells were incubated for 10 min with 1 µM bradykinin (BK). PGE$_2$ levels were measured by GC/MS and normalized to 10^6 cells. Values are expressed as mean ± SD. (A-D) One representative experiment out of three is shown.

4.1.12 9-*cis*-RA reversed the Induction of Cox-2 Expression in a ROS-independent Manner

9-*cis*-RA is a ligand of RXR subtypes [Wolf, 2006] which form homodimers or heterodimerize with other nuclear transcription factors such as PPARγ and act as transcriptionally active complexes. Various studies report that retinoids reduce Cox-2 expression levels in different cell systems (see Discussion, section 5.4.4). In MG-63 cells, 15d-PGJ_2 failed to induce Cox-2 expression in the presence of 9-*cis*-RA (Figure 19 A). It is reasonable that 9-*cis*-RA modulates Cox-2 expression by a ROS-independent mechanism as 15d-PGJ_2-induced DCF fluorescence was not blocked by 9-*cis*-RA (Figure 19 C). This suggestion is supported by the finding that a similar effect was observed when Cox-2 expression was induced by LPA (Figure 19 B), a lipid that did not influence DCF fluorescence (Figure 19 C). The molecular mechanisms underlying 9-*cis*-RA-modulated Cox-2 expression in MG-63 cells are under construction.

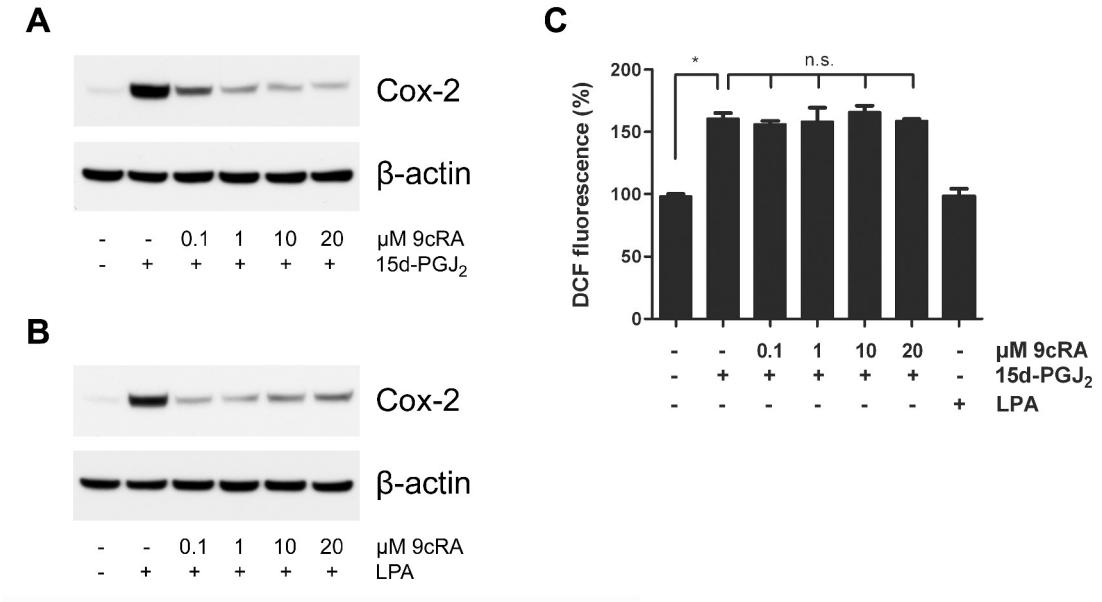

Figure 19: 9-*cis*-RA reversed 15d-PGJ$_2$- and LPA-induced Cox-2 expression.

MG-63 cells were pretreated for 10 min with indicated concentrations of 9-*cis*-RA (9cRA) prior to stimulation with 20 µM 15d-PGJ$_2$ (A) or 20 µM LPA (B) for 8 h. For detection of Cox-2 protein, cell lysates were subjected to Western blot analysis using a specific anti-Cox-2 antibody. For normalization, membranes were stripped and reprobed with an anti-β-actin antibody. (C) MG-63 cells were pretreated for 10 min with indicated concentrations of 9cRA prior to stimulation with 20 µM 15d-PGJ$_2$ for 1 h. Furthermore, cells were treated with 20 µM LPA for 1 h. For the detection of intracellular ROS levels, treated cells were loaded for 20 min with 20 µM DCF-DA. After cell lysis, the fluorescence counts were detected spectro-fluorometrically. Vehicle-treated cells are set 100%. Data are expressed as mean ± SD. **P*<0.001 versus vehicle-treated cells. n.s. indicates not significant versus 15d-PGJ$_2$-treated cells. (A-C) One representative experiment out of two is shown.

4.2 Apoptotic Cell Death in Response to 15d-PGJ_2

4.2.1 15d-PGJ_2 impairs the Viability of MG-63 Cells

The cyclopentenone 15d-PGJ_2 exerts cytotoxic effects in several cell types, particularly when administered at high concentrations (> 20 µM). The impaired cell viability is often paralleled with induction of apoptotic markers (see Discussion, section 5.5). In MG-63 cells, 15d-PGJ_2 decreased the number of viable cells in a time- and concentration dependent manner (Figure 20). The cell viability was decreased by approx. 40% after 24 h. This incubation period was used in further experiments.

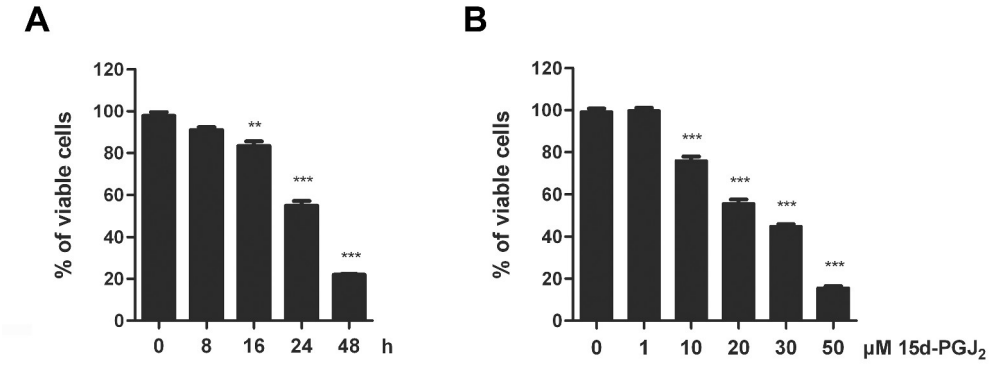

Figure 20: 15d-PGJ_2 impairs cell viability of MG-63 cells.
MG-63 cells were treated with 20 µM 15d-PGJ_2 for indicated time periods (A) or at indicated concentrations of 15d-PGJ_2 for 24 h (B). Cell viability was determined by MTT assay. The bar charts display the amount of viable cells after treatment (% of vehicle-treated cells). Data are expressed as mean ± SD. ***P*<0.01, ****P*<0.001 versus vehicle-treated cells. (A, B) One representative experiment out of three is shown.

4.2.2 15d-PGJ_2 induces apoptotic Cell Death Markers

Reduced cell viability could be a consequence of impaired cell proliferation or increased cell death in an apoptotic or necrotic manner. To elucidate if apoptotic cell death is induced in MG-63 cells, the status of the well-described apoptotic markers caspase-3 and PARP was followed. PARP plays a crucial role in DNA repair and

replication (Soldani, 2002). Administration of 15d-PGJ_2 provoked proteolytic cleavage of the effector caspase-3 and its downstream target PARP in a time- and concentration-dependent manner (Figure 21). The proform of caspase-3 (32 kDa) is cleaved upon activation to a 14 kDa and a 17 kDa fragment. Intact PARP (116 kDa) is cleaved to inactive 89 kDa and 27 kDa fragments.

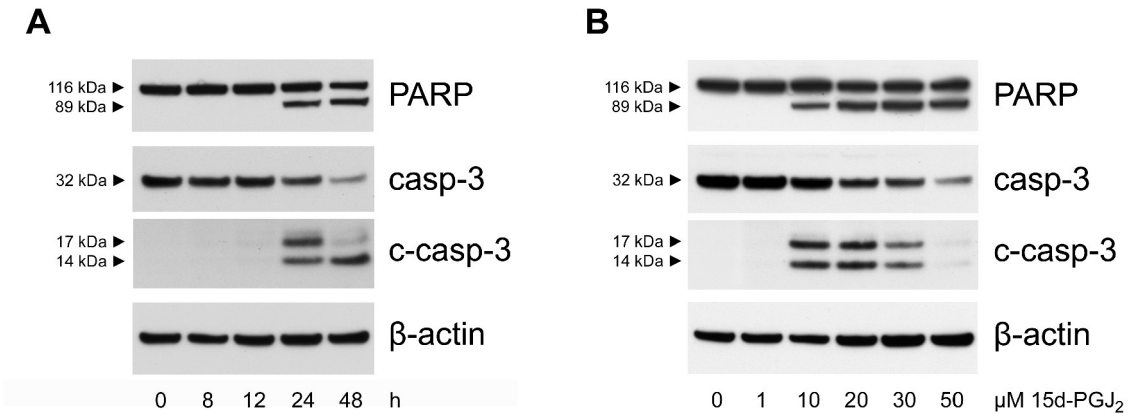

Figure 21: 15d-PGJ_2 induces caspase-3 activation and PARP cleavage.
MG-63 cells were treated for indicated time periods with 20 µM 15d-PGJ_2 (A) or at indicated concentrations of 15d-PGJ_2 for 24 h (B). Cells lysates were subjected to Western blot analysis using specific antibodies against PARP and caspase-3. The proform of caspase-3 (casp-3; 32 kDa) is cleaved upon activation to a 14 kDa and a 17 kDa fragment (c-casp-3). For normalization, membranes were stripped and reprobed with an anti-β-actin antibody. (A, B) One representative experiment out of three is shown.

4.2.3 15d-PGJ_2-induced Apoptosis is MAPK-independent

To investigate if MAPK activation plays regulatory roles in 15d-PGJ_2-induced apoptotic cell death, different MAPK/JNK inhibitors were added prior to stimulation of cells with the cyclopentenone. As none of these blockers inhibited PARP cleavage or caspase-3 activation (Figure 22), it is likely to assume that MAPK signalling is not involved in these events.

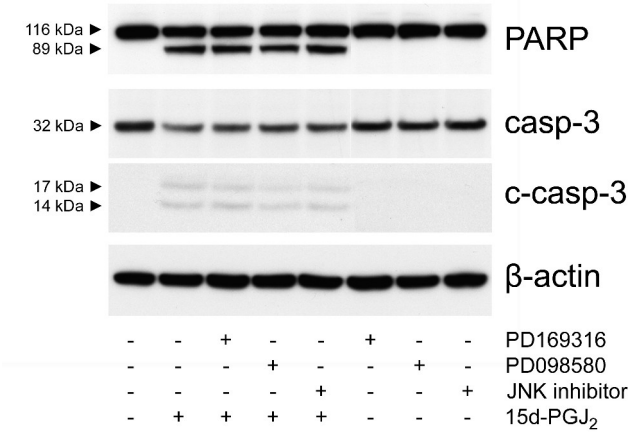

Figure 22: 15d-PGJ$_2$-induced apoptosis is MAPK-independent.
MG-63 cells were pretreated for 30 min with p38 MAPK inhibitor PD169316 (1 µM), MAPK kinase inhibitor PD098059 (20 µM), and JNK inhibitor II (1 µM) followed by stimulation with 20 µM 15d-PGJ$_2$ for 24 h. As a control, cells were incubated with inhibitors alone (lanes 6-8). Cells lysates were subjected to Western blot analysis using specific antibodies against PARP and caspase-3. The proform of caspase-3 (casp-3; 32 kDa) is cleaved upon activation to a 14 kDa and a 17 kDa fragment (c-casp-3). For normalization, membranes were stripped and reprobed with an anti-β-actin antibody. One representative experiment out of two is shown.

4.2.4 15d-PGJ$_2$-induced Apoptosis is PPARγ- and PGD$_2$ Receptor-independent

In the first part of the study it was documented that 15d-PGJ$_2$-induced signalling events and Cox-2 expression occurred independently of PPARγ and PGD$_2$ receptor subtypes. Similarly, 15d-PGJ$_2$-induced procaspase-3 activation and PARP cleavage were not affected by the PPARγ antagonist T0070907 at indicated concentrations (Figure 23 A) and by a knock-down of PPARγ mRNA expression (Figure 23 B) in MG-63 cells. Furthermore, treatment of the human osteosarcoma cells with PGD$_2$, even at a concentration of 50 µM, did not mimic 15d-PGJ$_2$-induced caspase-3 activation and PARP cleavage (Figure 24). Therefore, it is not likely that PPARγ or PGD$_2$ receptor subtypes are involved in these events.

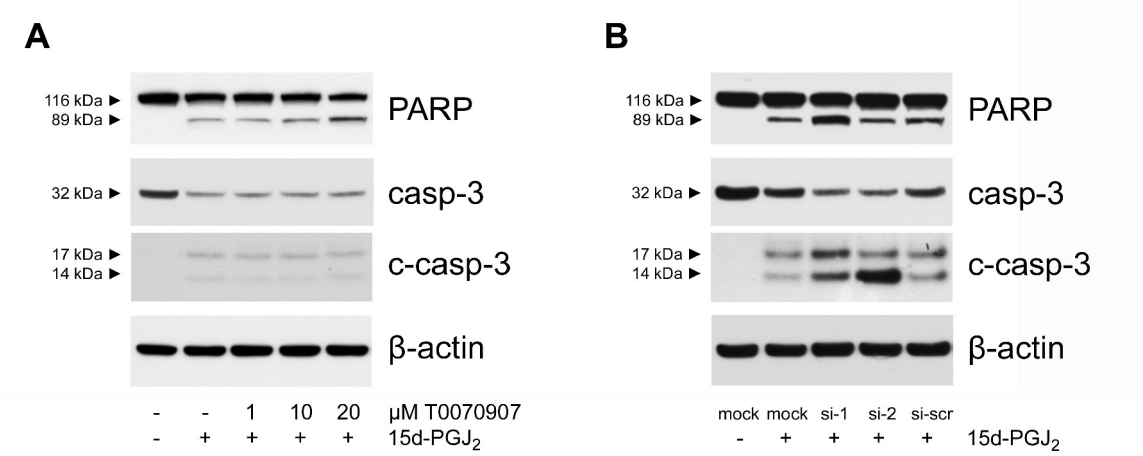

Figure 23: 15d-PGJ$_2$-induced apoptosis occurs independently of PPARγ.

(A) MG-63 cells were pretreated for 30 min at indicated concentrations of the PPARγ blocker T0070907 prior to stimulation with 20 µM 15d-PGJ$_2$ for 24 h. (B) MG-63 cells were transfected with 50 nM siRNAs specific for PPARγ (si-1 and si-2) or with a scrambled negative control siRNA (si-scr). Mock transfected cells (mock) were treated with the transfection reagent Oligofectamine® alone. After a transfection period of 66 h, MG-63 cells were treated with 20 µM 15d-PGJ$_2$ for 24 h. (A, B) Cells lysates were subjected to Western blot analysis using specific antibodies against PARP and caspase-3. The proform of caspase-3 (casp-3; 32 kDa) is cleaved upon activation to a 14 kDa and a 17 kDa fragment (c-casp-3). For normalization, membranes were stripped and reprobed with an anti-β-actin antibody. (A, B) One representative experiment out of two is shown.

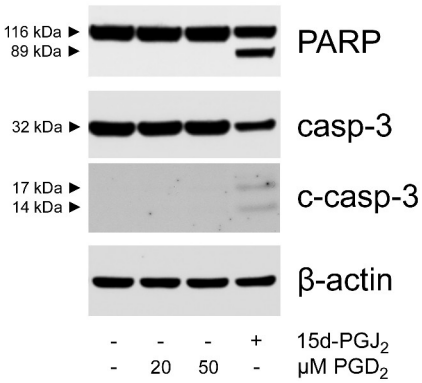

Figure 24: 15d-PGJ$_2$-induced apoptosis is not mimicked by PGD$_2$.

MG-63 cells were treated with 20 µM 15d-PGJ$_2$ or at indicated concentrations of PGD$_2$ for 24 h. Cells lysates were subjected to Western blot analysis using antibodies against PARP and caspase-3. The proform of caspase-3 (casp-3; 32 kDa) is cleaved upon activation to a 14 kDa and a 17 kDa fragment (c-casp-3). For normalization, membranes were stripped and reprobed with an anti-β-actin antibody. One representative experiment out of two is shown.

4.2.5 15d-PGJ_2-induced Apoptosis is regulated by the intracellular Redox Balance

An imbalanced redox status has been identified as a critical trigger for the induction of programmed cell death in response to 15d-PGJ_2. Alterations in the intracellular redox balance provoked by the reactive carbon centre of 15d-PGJ_2 seem to be involved in the induction of apoptosis in MG-63 cells, too. Similarly as shown for 15d-PGJ_2-induced Cox-2 expression, the non-electrophilic 15d-PGJ_2 analogue 9,10-dihydro-15d-PGJ_2 of did not induce caspase-3 activation and PARP cleavage (Figure 25). Furthermore, the antioxidants and GSH precursors MPG and GSH ethyl ester had a reversible effect on 15d-PGJ_2-mediated caspase-3 activation and PARP cleavage (Figure 26 B). Unlike GSH ethyl ester, MPG did not reverse the impaired cell viability; in contrast, MG-63 exhibited decreased proliferation in the presence of this compound (Figure 26 A). It might be speculated that MPG elicits on the one hand anti-apoptotic effects in the presence of cell death-inducing agents and on the other hand anti-proliferative effects which are not connected to apoptosis.

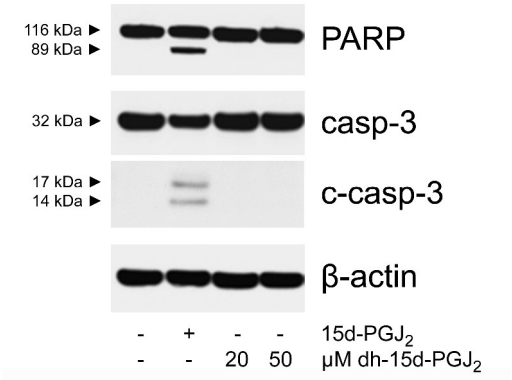

Figure 25: 15d-PGJ_2-induced apoptosis is related to its electrophilic carbon.
MG-63 cells were treated with 20 µM 15d-PGJ_2 or at indicated concentrations of 9,10-dihydro-15d-PGJ_2 (dh-15d-PGJ_2) for 24 h. Cells lysates were subjected to Western blot analysis using specific antibodies against PARP and caspase-3. The proform of caspase-3 (casp-3; 32 kDa) is cleaved upon activation to a 14 kDa and a 17 kDa fragment (c-casp-3). For normalization, membranes were stripped and reprobed with an anti-β-actin antibody. One representative experiment out of two is shown.

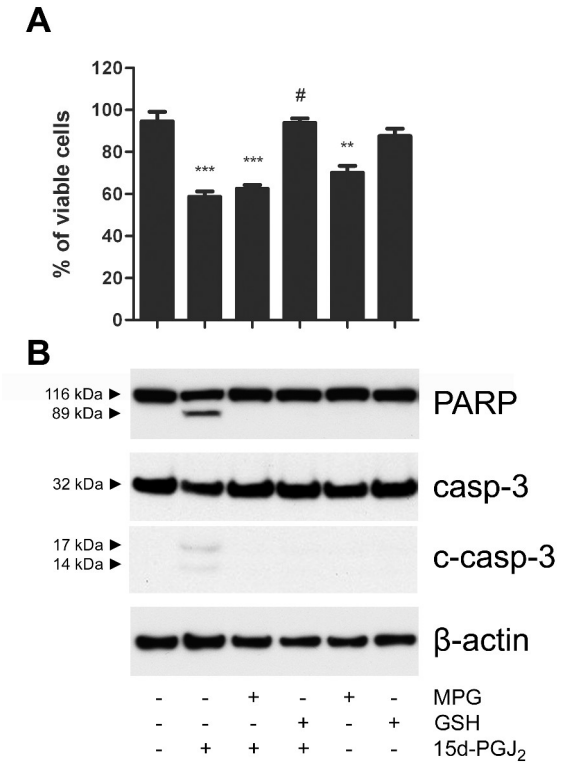

Figure 26: 15d-PGJ$_2$-mediated effects on cell viability and apoptosis in the presence of antioxidants

MG-63 cells were pretreated for 60 min with 5 mM MPG or 10 mM GSH ethyl ester (GSH). Then, the cells were treated with 20 µM 15d-PGJ$_2$ for 24 h to follow cell viability (A) and induction of apoptotic markers (B). As a control, cells were treated with GSH and MPG alone. (A) Cell viability was determined by MTT assay. The bar chart displays the amount of viable cells after treatment (% of vehicle-treated cells). Data are expressed as mean ± SD. $^{**}P<0.01$, $^{***}P<0.001$ versus vehicle-treated cells, $^{\#}P<0.001$ versus 15d-PGJ$_2$-treated cells. (B) Cells lysates were subjected to Western blot analysis using specific antibodies against PARP and caspase-3. The proform of caspase-3 (casp-3; 32 kDa) is cleaved upon activation to a 14 kDa and a 17 kDa fragment (c-casp-3). For normalization, membranes were stripped and reprobed with an anti-β-actin antibody. (A, B) One representative experiment out of three is shown.

4.2.6 Status of early apoptotic Markers in Response to 15d-PGJ$_2$

Caspase-3 activation and PARP cleavage belong to the late apoptotic events. The initial apoptotic cascade that finally converges on the activation of effector caspases may be triggered by death receptor signal transduction or release of pro-apoptotic factors from disrupted mitochondria (see Introduction, section 1.4.2). As a

representative event of the receptor-mediated pathway the activation of caspase-8 was followed. Western blot analysis revealed a cleavage/reduction of the 55 kDa procaspase-8 after 24 and 48 h treatment with 15d-PGJ_2 (Figure 27 A). To cover the mitochondrial pathway, expression levels of pro- and anti-apoptotic members of the Bcl-2 family were recorded. The expression of the pro-apoptotic protein Puma was increased upon 15d-PGJ_2 treatment after 16 and 24 h whereas the expression profile of the pro-apoptotic proteins Bax did not change significantly over the time course (Figure 27 A). The expression level of anti-apoptotic Bcl-x_L protein was constant whereas Bcl-2 expression was decreased after 48 h (Figure 27 B), a time point where cell viability was decreased by approx. 75% (Figure 20 A).

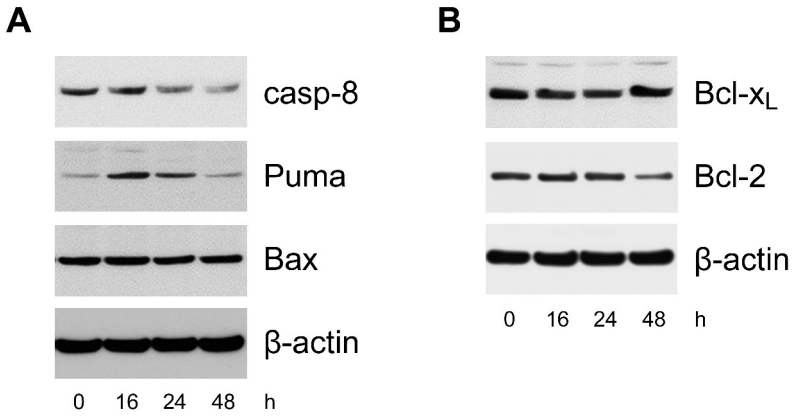

Figure 27: Status of early apoptotic markers in response to 15d-PGJ_2.
MG-63 cells were treated for indicated time periods with 20 µM 15d-PGJ_2. Cell lysates were subjected to Western blot analysis using specific antibodies against (A) pro-apoptotic markers procaspase-8 (casp-8), Puma, and Bax, and (B) anti-apoptotic markers Bcl-x_L and Bcl-2. For normalization membranes were stripped and reprobed with an anti-β-actin antibody. One representative experiment out of two is shown.

4.2.7 15d-PGJ_2-induced Apoptosis is Caspase-dependent

The activation of the caspase-cascade is an important event that differentiates apoptotic cell death from necrosis. In MG-63 cells, the pan-caspase inhibitor z-VAD-FMK reversed 15d-PGJ_2-mediated caspase-3 activation and PARP cleavage (Figure 28 B), however, decreased cell viability was just slightly improved (Figure 28 A). To

clarify which caspases are involved in 15d-PGJ_2-induced apoptosis, specific inhibitors of caspase-8, caspase-9 or caspase-3 could be used. This may also facilitate to interpret if 15d-PGJ_2-induced apoptosis occurs in a receptor- or mitochondria-dependent way or if both pathways are involved.

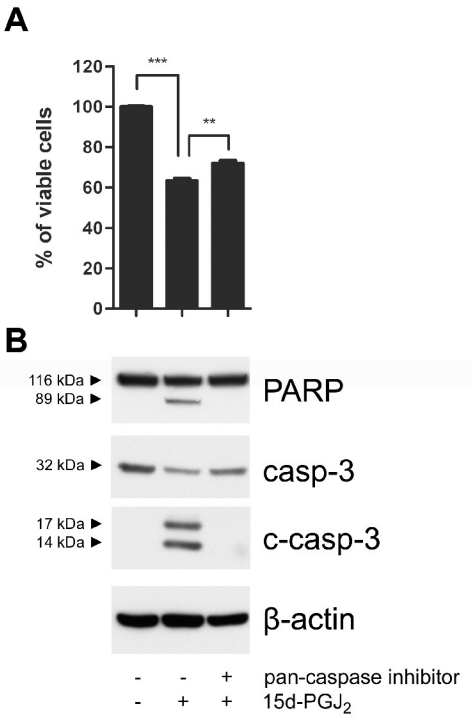

Figure 28: 15d-PGJ_2-mediated apoptotic effects are caspase-dependent

MG-63 cells were pretreated for 30 min with 1 µM of the pan-caspase inhibitor z-VAD-FMK prior to stimulation of cells with 20 µM 15d-PGJ_2 for 24 h to follow cell viability (A) and induction of apoptotic markers (B). (A) Cell viability was determined by MTT assay. The bar chart displays the amount of viable cells after treatment (% of vehicle-treated cells). Data are expressed as mean ± SD. ***P<0.001 versus vehicle-treated cells, **P<0.01 versus 15d-PGJ_2-treated cells. (B) Cells lysates were subjected to Western blot analysis using antibodies against PARP and caspase-3. The proform of caspase-3 (casp-3; 32 kDa) is cleaved upon activation to a 14 kDa and a 17 kDa fragment (c-casp-3). For normalization, membranes were stripped and reprobed with an anti-β-actin antibody. One experiment out of three is shown.

4.2.8 15d-PGJ_2-induced apoptotic Markers are not influenced upon Cox-2 Inhibition

Cox-2 has been implicated as an anti-apoptotic factor in various studies, most likely related to PGE_2 production (see Discussion, section 5.5.1). To elucidate if Cox-2 activity might be involved in 15d-PGJ_2-induced programmed cell death, MG-63 cells were preincubated with the selective Cox-2 inhibitor NS-398 prior to stimulation with 15d-PGJ_2. As the induction of PARP and procaspase-3 cleavage in response to 20 µM 15d-PGJ_2 – a concentration highly inducing Cox-2 protein expression (Figure 1 B) – is similar in the absence (Figure 21 B) and presence (Figure 29) of the Cox-2 inhibitor, it is assumed that 15d-PGJ_2-induced apoptosis is Cox-2-independent under the respective conditions.

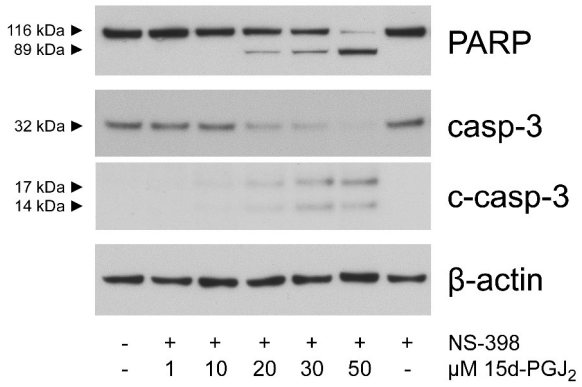

Figure 29: Cox-2 inhibition does not influence 15d-PGJ_2-mediated apoptotic events
MG-63 cells were pretreated for 30 min with 250 nM of the Cox-2 inhibitor NS-398 prior to stimulation of cells with 20 µM 15d-PGJ_2 for 24 h. As a control, cells were incubated with the inhibitor alone. Cells lysates were subjected to Western blot analysis using specific antibodies against PARP and caspase-3. The proform of caspase-3 (casp-3; 32 kDa) is cleaved upon activation to a 14 kDa and a 17 kDa fragment (c-casp-3). For normalization, membranes were stripped and reprobed with an anti-β-actin antibody. One experiment out of two is shown.

4.3 Cytoprotective Responses induced by 15d-PGJ_2

4.3.1 15d-PGJ_2-mediated Induction of GSH Synthesis

Alterations in the intracellular redox balance may induce apoptotic and/or cytotoxic effects but also cytoprotective responses such as induction of stress and detoxification enzymes (see Introduction, section 1.3.1.4). As described in the first part of the thesis, 15d-PGJ_2 mediates a rapid decrease of total intracellular GSH concentrations. Figure 30 A displays that GSH levels adjusted to initial levels after 6 h treatment with 15d-PGJ_2, increased by two-fold after 16 h and remained elevated up to 48 h.

The next series of experiments was aimed to explore if elevated GSH levels play a protective role in events induced after long-termed administration of 15d-PGJ_2. Therefore, GSH pools were depleted by the GSH synthesis inhibitor BSO (Figure 30 B). Indeed, over night treatment of MG-63 cells with BSO potentiated 15d-PGJ_2-mediated decreased cell viability (Figure 31 A), activation of caspase-3, and cleavage of PARP (Figure 31 B).

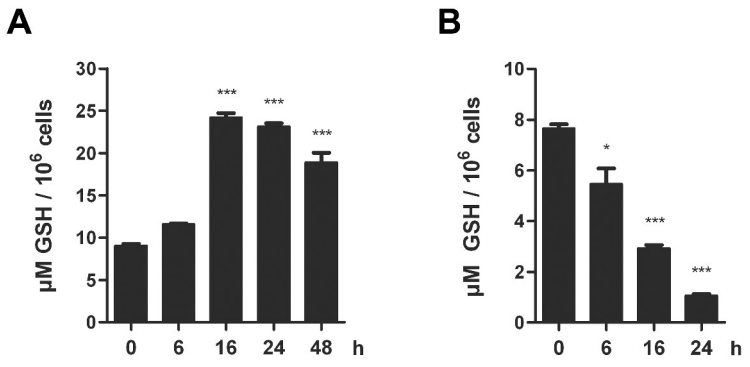

Figure 30: 15d-PGJ_2 triggers an increase in GSH levels after long-termed incubations. MG-63 cells were treated for indicated time periods with 20 µM 15d-PGJ_2 (A) and with 10 µM BSO (B). Intracellular GSH contents were determined with a Glutathione Assay Kit (Cayman Chemical) according to the supplier's manual. The results are reported as µM total GSH normalized to 10^6 cells. Data are expressed as mean ± SD. *P<0.001 versus vehicle-treated cells. One representative experiment out of two is shown.

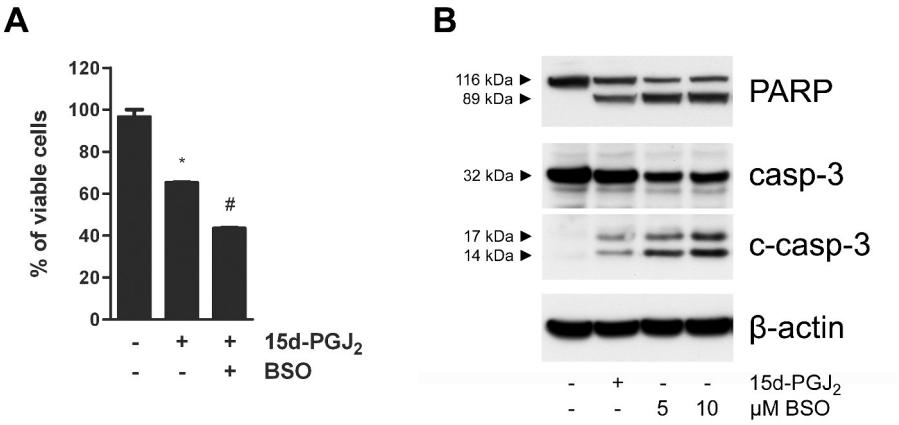

Figure 31: Depletion of GSH pools potentiates 15d-PGJ$_2$-mediated effects.
MG-63 cells were pretreated for 20 h with BSO prior to stimulation with 20 µM 15d-PGJ$_2$ for 24 h to follow cell viability (A) and induction of apoptotic markers (B). (A) Cell viability was determined by MTT assay. The bar chars displays the amount of viable cells after treatment (% of vehicle-treated cells). Data are expressed as mean ± SD. *P<0.001 versus vehicle-treated cells, $^{\#}P$<0.001 versus 15d-PGJ$_2$-treated cells. (B) Cells lysates were subjected to Western blot analysis using specific antibodies against PARP and caspase-3. The proform of caspase-3 (casp-3; 32 kDa) is cleaved upon activation to a 14 kDa and a 17 kDa fragment (c-casp-3). For normalization, membranes were stripped and reprobed with an anti-β-actin antibody. (A, B) One representative experiment out of two is shown.

4.3.2 15d-PGJ$_2$ upregulates HO-1 Expression

HO-1 belongs to the group of phase II detoxification enzymes that are upregulated under various stress conditions, including electrophilic stress. Through its metabolites bilirubin and CO, HO-1 might exert cytoprotective or anti-apoptotic effects (see Introduction, section 1.3.1.6). 15d-PGJ$_2$ treatment induced HO-1 expression on mRNA and protein level in MG-63 cells (Figure 32). HO-1 protein expression is most pronounced at concentrations of 10 and 20 µM 15d-PGJ$_2$ and decreased with higher amounts of the cyclopentenone (Figure 32 B) whereas HO-1 mRNA was still highly induced (Figure 32 A). In time-course experiments, elevated HO-1 mRNA expression was detected between 2 and 48 h (Figure 32 C). HO-1 protein expression started after 4 h and declined after 24 h (Figure 32 D).

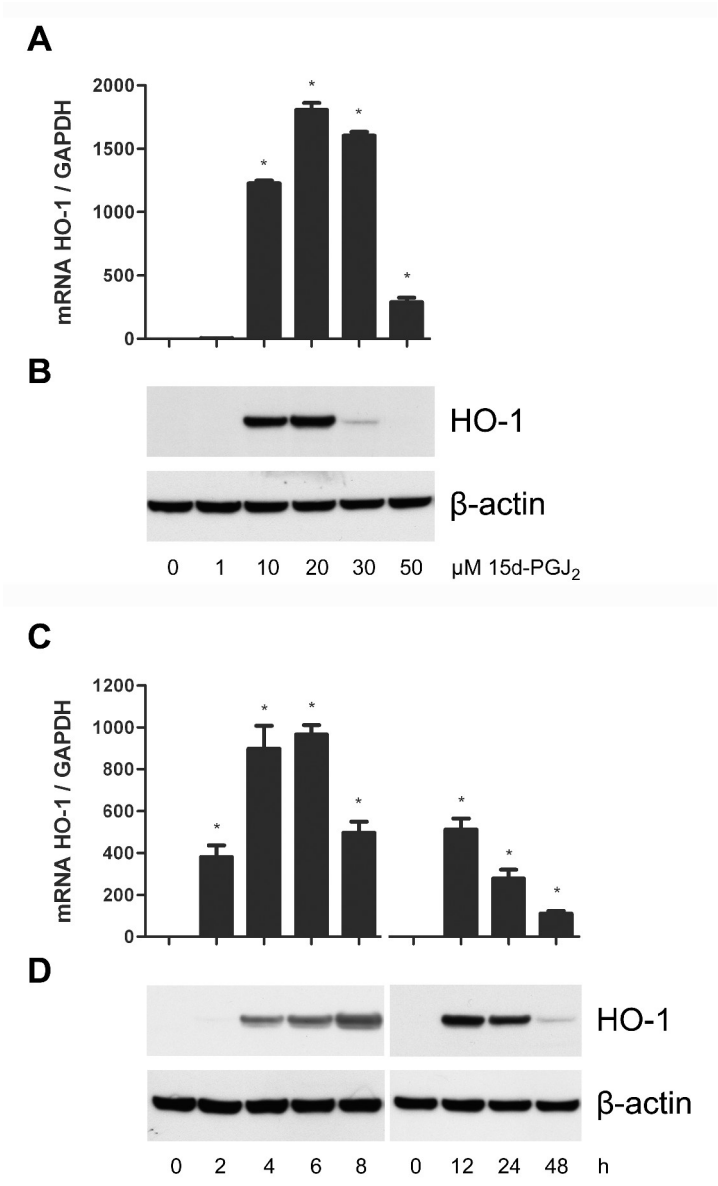

Figure 32: Elevated HO-1 expression in response to 15d-PGJ$_2$.

(A, B) MG-63 cells were treated with indicated concentrations of 15d-PGJ$_2$ for 6 h to follow HO-1 mRNA expression (A) and for 8 h to follow HO-1 protein expression (B). (C, D) MG-63 cells were treated with 20 µM 15d-PGJ$_2$ at indicated time periods to follow HO-1 mRNA and protein expression. (A, C) For determination of HO-1 mRNA expression, cDNA was generated and subjected to qPCR using specific primers for HO-1. HO-1 expression was normalized to GAPDH and values are expressed as mean ± SD. **P*<0.001 versus vehicle-treated cells. One representative experiment out of two is shown. (B, D) Cell lysates were subjected to Western blot analysis using a specific anti-HO-1 antibody. For normalization, membranes were stripped and reprobed with an anti-β-actin antibody. One representative experiment out of three is shown.

4.3.3 15d-PGJ_2-mediated Induction of Stress-responsive Transcription Factors

In response to oxidative or electrophilic stress, HO-1 expression is regulated by activation of the transcription factor Nrf-2, binding to ARE/EpREs in the promoter region of HO-1. Another transcription factor that has been related to elevated HO-1 expression is Egr-1 (see Introduction, section 1.3.1.6). Figure 33 displays that Nrf-2 and Egr-1 expression levels are highly elevated in 15d-PGJ_2-treated MG-63 cells, starting 2 h after treatment. As HO-1 mRNA expression is induced in a similar sequence (Figure 32 B), it is plausible that one of these transcription factors may regulate the transcription. The pronounced nuclear localization of Nrf-2 and Egr-1 (Figure 34) support the assumption that these transcription factors are activated under our experimental conditions and might be involved in the expression of cytoprotective genes like HO-1 and GCL.

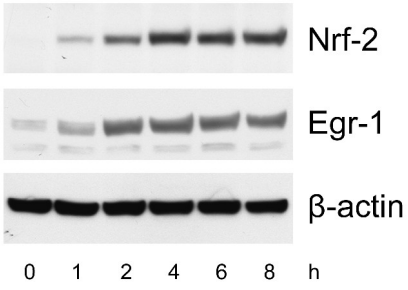

Figure 33: 15d-PGJ_2 induces expression levels of Nrf-2 and Egr-1.
MG-63 cells were treated with 20 µM 15d-PGJ_2 at indicated time periods. Cell lysates were subjected to Western blot analysis using specific antibodies against Nrf-2 and Egr-1. For normalization, membranes were stripped and reprobed with an anti-β-actin antibody. One representative experiment out of three is shown.

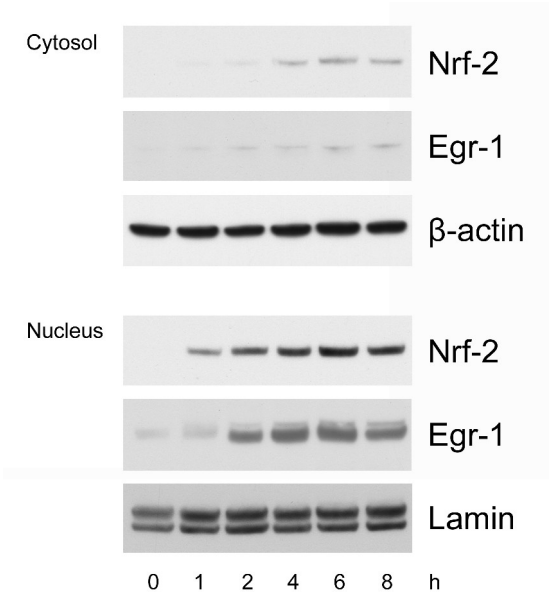

Figure 34: Nuclear translocation of Nrf-2 and Egr-1 in response to 15d-PGJ_2.
MG-63 cells were treated for indicated time periods with 20 µM 15d-PGJ_2 followed by isolation of nuclear and cytosolic proteins. Equal amounts of proteins were subjected to Western blot analysis using specific antibodies for Nrf-2 and Egr-1. For normalization of the cytosolic fraction β-actin was used. For normalization of the nuclear fraction lamin A/C was used. One representative experiment out of two is shown.

5 DISCUSSION

PGs play an important role in oncogenesis, as eicosanoids are local mediators of tumor progression. The most abundant eicosanoid in bone, PGE_2, is a potent modulator of tumor cell proliferation, angiogenesis, invasion and immunosuppression [Wang and Dubois, 2006]. Biosynthesis of PGs is mediated by rate limiting bifunctional enzymes, Cox-1 and/or Cox-2. There are specific differences in PG production by both enzymes with Cox-2 being more efficient than Cox-1 under many circumstances [Blackwell et al., 2010]. In addition to the constitutively expressed isoform Cox-1, most tissues express the inducible isoform Cox-2 in the presence of a variety of agonists and stimuli. Several lines of evidence indicate that Cox-2 (over)expression can be a causal factor for tumor growth and metastasis by its ability to lead to a burst in PG biosynthesis [Surh and Kundu, 2005]. However, the role of Cox-2 in human osteosarcoma is not clearly defined. Selective Cox-2 inhibitors exhibited beneficial effects in human osteosarcoma cell lines [Liu et al., 2008; Masi et al., 2007; Naruse et al., 2006], however, observations from clinical studies and *in vitro* experiments regarding Cox-2 (over)expression are controversial (see Introduction, section 1.2.4.1). Furthermore, vector-based overexpression of Cox-2 in human osteosarcoma cells led to contrasting findings. While overexpression of murine Cox-2 decreased cell proliferation of SaOS-2 cells [Xu et al., 2006], overexpression of human Cox-2 promoted cell growth, migration and invasion of U2OS cells [Lee et al., 2007], apparently the consequence of enhanced PGE_2 production.

In the present study, the induction and regulation of endogenous Cox-2 in human MG-63 osteosarcoma cells was investigated. The findings that these cells obviously lack Cox-1 protein expression (Figure 18 B) [Laulederkind et al., 2000] and Cox-1-mediated PG synthesis (Figure 18 C), define MG-63 cells as a candidate cellular model to investigate the role of Cox-2 in osteosarcoma. Although various stimuli may cause an induction of Cox-2 in MG-63 cells, the electrophilic cyclopentenone 15d-PGJ_2 was used. 15d-PGJ_2 was initially identified *in vitro* as a dehydration product of PGD_2 [Fitzpatrick and Wynalda, 1983]. As PGD_2 is generated by normal human osteoblasts [Gallant et al., 2005], 15d-PGJ_2 is likely occurring in the local environment of osteosarcoma.

5.1 The physiological Role of 15d-PGJ_2

A critical point regarding cyclopentenone PGs is whether they play a role in normal physiology. The conversion of precursor PGs to cyclopentenones was mostly described by *in vitro* studies. Nevertheless, there is abundant evidence that these bioactive compounds do exist *in vivo*. Endogenously produced 15d-PGJ_2 was detected by a monoclonal antibody in human atherosclerotic aorta [Shibata et al., 2002] and murine pleural macrophages [Itoh et al., 2004]. Extracellular production of 15d-PGJ_2 was determined by enzyme immunoassays in cell culture supernatants of RAW 264.7 murine macrophages [Shibata et al., 2002], human aortic endothelial cells [Hosoya et al., 2005], in rat [Gilroy et al., 1999] and murine [Rajakariar et al., 2007] inflammatory fluids, and in plasma of ischemic stroke patients [Blanco et al., 2005]. These immunochemical studies reveal that intracellular and extracellular 15d-PGJ_2 could function as both, autocrine and paracrine factor.

According to findings in inflammatory animal models, it is proposed that the late-phase induction of Cox-2 may contribute to the resolution of inflammation by producing the cyclopentenone 15d-PGJ_2 [Gilroy et al., 1999]. Endogenous Cox-2-derived 15d-PGJ_2 accumulation and exogenous administration of 15d-PGJ_2 exert beneficial effects in murine models of carrageenin-induced acute lung injury and pleurisy. The redox sensitive transcription factor Nrf-2 turned out to be an important mediator in the resolution process as the duration and magnitude of acute inflammation was markedly enhanced in Nrf-2 knock-out mice compared to wildtype mice and Nrf-2 knock-out mice did not respond to 15d-PGJ_2 administration [Itoh et al., 2004; Mochizuki et al., 2005]. Although 15d-PGJ_2 is detected at low nanomolar concentrations, the plasma levels of 15d-PGJ_2 may not reflect the compound concentration present at the site of inflammation. PGs are physiologically present in body fluids in picomolar to nanomolar concentrations, however, local PG concentrations at sites of acute inflammation have been detected in the micromolar range [Uchida and Shibata, 2008]

In the present study, cells have been treated with 20 µM 15d-PGJ_2, which is in the range what is widely used in *in vitro* experiments to exert its pharmacological effects. It is difficult to compare the concentrations used in different studies, because 15d-PGJ_2 is unstable and different serum concentrations of the growth media have

an impact on the efficacy of 15d-PGJ_2 [Levonen et al., 2001; Oh et al., 2008]. Under the present experimental conditions, a pronounced proportion of 15d-PGJ_2 may be metabolized by a serum component as it became apparent that notably lower concentrations of 15d-PGJ_2 (around 5 µM) were sufficient to induce p38 MAPK phosphorylation after short time incubation performed in medium without FCS or in buffer (Figure 3). A critical serum constituent might be albumin as it was reported that 15d-PGJ_2, when associated with serum albumin, failed to induce apoptosis in WISH epithelial cells [Berry et al., 2004] and activation of PPARγ in choriocarcinoma cells [Person et al., 2001].

5.2 15d-PGJ_2 and Cellular Redox Regulation

5.2.1 Intracellular ROS Accumulation

15d-PGJ_2 is a highly bioactive compound, exerting a variety of cellular responses via different regulatory mechanisms (see Introduction, Scheme 3). Striking evidence exists that many cellular events are related to the electrophilic character of 15d-PGJ_2. Using biotinylated 15d-PGJ_2, a number of protein targets participating in redox cell signalling have been identified [Landar et al., 2006]. Oxidation and reduction of thiol proteins are thought to be the major mechanisms by which reactive oxidants integrate into cellular signal transduction pathways [Winterbourn and Hampton, 2008]. The cyclopentenone may modulate the intracellular redox status and/or protein functions through direct interaction with critical cysteine residues [Straus and Glass, 2001]. Brunoldi and coworkers [Brunoldi et al., 2007] have shown that 15d-PGJ_2 can be metabolized by HepG2 cells via conjugation with GSH, a reaction that is accelerated by glutathione *S*-transferase [Paumi et al., 2004], an enzyme involved in metabolic elimination of a variety of xenobiotic electrophilic substances [Straus and Glass, 2001]. Once formed, GSH-conjugates are eliminated from cells via MRP1 and MRP2 [Paumi et al., 2003].

The present study demonstrates that treatment of MG-63 osteosarcoma cells with 15d-PGJ_2 results in a fast and progressive reduction of total intracellular GSH

levels, without changes in the GSH/GSSG ratios (Figure 14 B). This process is tightly coupled to an imbalance of the oxidation/reduction status of the cell (Figure 14 A). Radicals produced as a consequence of mitochondrial dysfunction or increased NADPH oxidase activity seem not to be involved in 15d-PGJ_2-induced ROS levels in MG-63 cells as neither the mitochondrial complex I inhibitor rotenone nor the NADPH oxidase inhibitor apocynin reduced ROS-dependent DCF fluorescence (Figure 14 D). These findings led to the assumption that the rapid decrease of intracellular GSH and parallel increase in ROS levels might occur due to an export of 15d-PGJ_2-GSH conjugates [Brunoldi et al., 2007] rather than due to oxidation of GSH to GSSG by *de novo* synthesized oxygen radicals.

In the present study, increased intracellular ROS levels have further been identified as an initiating event in activating signalling cascades as MAPK/EGFR blockers did not inhibit 15d-PGJ_2-induced DCF fluorescence (Figure 14 C). The electrophilic carbon centre is essential for 15d-PGJ_2-generated effects in MG-63 cells as the non-polar compound 9,10-dihydro-15d-PGJ_2 did not influence intracellular ROS levels and failed to induce MAPK and EGFR activation, Cox-2 expression (Figure 15) as well as activation of apoptosis markers (Figure 25).

5.3 15d-PGJ_2-induced Signal Transduction Pathways

5.3.1 MAPK signalling

It has been shown that MAPKs are important regulators in signalling pathways supporting oncogene expression. In various cellular systems, Cox-2 expression is regulated by various MAPK family members. The MAPK signalling pathway consists of three distinct groups of well characterized serine-threonine protein kinases that include p42/44 MAPK (also designed as ERK1/2), JNKs (JNK1, JNK2, and JNK3), and the four p38 enzymes (p38α, p38β, p38γ and p38δ). The activated form of each MAPKs mentioned above amplifies signal cascades through phosphorylation of down-stream molecules like other protein kinases, phospholipases, transcription factors, and cytoskeletal proteins [Chun and Surh, 2004; Surh and Kundu, 2005].

The activation of MAPKs in response to redox changes is established in various cell systems; for example, H_2O_2, hypoxia, ionizing radiation, UV radiation, and heat shock have been used to mimic oxidative stress conditions (reviewed in [Allen and Tresini, 2000]). Activation of p38 MAPK and JNK is found to be redox-sensitive, whereas the sensitivity of p42/44 MAPK to oxidative stress is uncertain [Aslan and Ozben, 2003]. In MG-63 cells, ROS accumulation is paralleled by a rapid activation of p38 MAPK and JNK1/2 (approx. 10 min) whereas delayed activation of p42/44 MAPK (> 1 h) (Figure 2 A) occurred through intermediate oxidative stress-dependent activation of the EGFR. By inhibition of these pathways with specific pharmacological blockers, it was detected that p38 MAPK and p42/44 MAPK are involved in Cox-2 expression (Figure 4 A, B). It is assumed that these pathways regulate 15d-PGJ_2-induced Cox-2 expression by independent mechanisms as phosphorylation of p42/44 MAPK, but not p38 MAPK, was identified as a downstream event of EGFR activation (Figure 11 A). The observation that inhibition of p38 MAPK did not influence EGFR tyrosine phosphorylation (Figure 12 A) and p42/44 MAPK activation (Figure 12 B) strengthens the assumption that 15d-PGJ_2 induces independent signalling pathways in a ROS-dependent manner, both upregulating Cox-2 expression (Scheme 7). H_2O_2 mimicked 15d-PGJ_2-mediated activation of signalling events and Cox-2 expression (Figure 17) suggesting that increasing H_2O_2 concentrations may contribute to increased DCF fluorescence.

At the molecular level, the mechanisms of redox regulation of signal transduction and alterations in gene expression are not fully understood. However, in many cases, the stress response seems to be mediated through oxidation and reduction of protein sulfhydryls leading to conformational and functional changes [Allen and Tresini, 2000]. Prolonged phosphorylation of p42/44 MAPK and JNK1/2 up to 48 h (Figure 2 A) might be explained by the inhibition of phosphatases, mediating dephosphorylation of MAPKs [Wu et al., 2008]. Both, serine/threonine phosphatases and phospho-tyrosine phosphatases are known to be redox sensitive and can be inactivated by oxidation of catalytic cysteine residues [Allen and Tresini, 2000]. Next to GSH, thioredoxin (Trx) is a redox-sensitive molecule that can be oxidized at two redox-active cysteine residues, a reaction that can be reversed by Trx reductase activity [Holmgren, 1995]. Under normal conditions, Trx has been shown to bind to and inhibit the activity of Ask-1, a MAPK kinase kinase involved in both, JNK1/2 and p38 MAPK activation [Saitoh et al., 1998]. Interestingly, Trx has been identified as a

target of the cyclopentenones 15d-PGJ_2 [Shibata et al., 2003] and PGA_1 [Moos et al., 2003] which form covalent adducts with Trx cysteine residues and thereby inactivate its antioxidant capacity. 15d-PGJ_2 caused transient activation of Ask-1 and MAPKs, which was prevented by N-acetyl-L-cysteine (NAC) pretreatment in cultured primary astrocytes [Lennon et al., 2002]. Thus, the activity of Trx and Ask-1 might be influenced under 15-PGJ_2-induced oxidative stress conditions leading to induction of MAPKs in MG-63 cells which has to be proven in further studies.

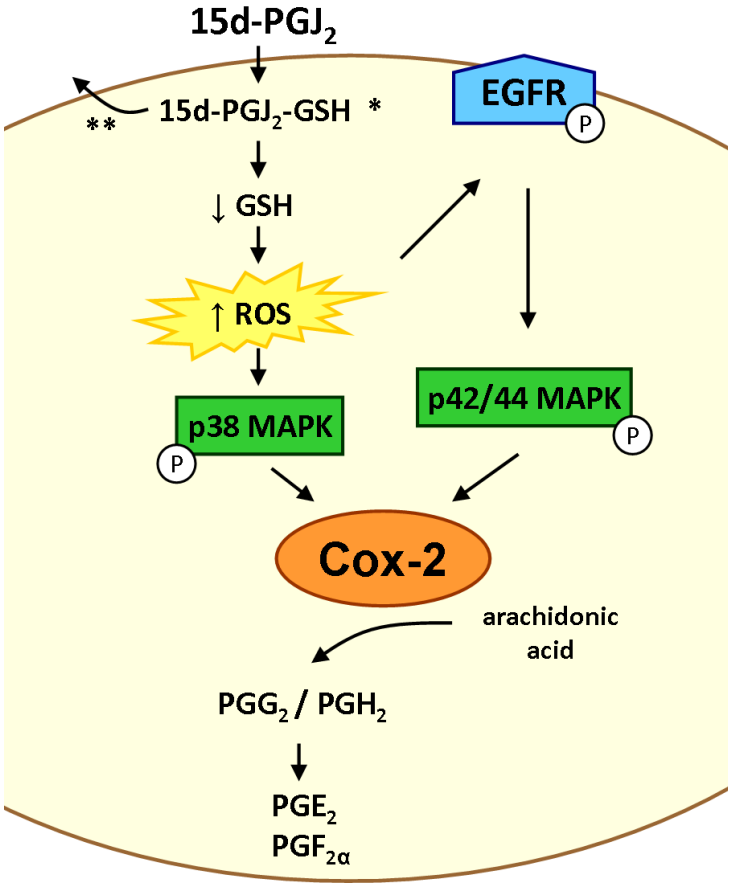

Scheme 7: Overview of 15d-PGJ_2-induced Cox-2 expression via MAPK and EGFR activation in the human osteosarcoma cell line MG-63.

The mechanisms involve generation of ROS through modification of reduced GSH *[Brunoldi et al., 2007]. 15d-PGJ_2-GSH conjugates might be exported from cells **[Paumi et al., 2003]. Elevated oxidative stress leads to activation of p38 MAPK signalling and EGFR activation which induces p42/44 MAPK phosphorylation. Both events contribute to Cox-2 expression. The enzymatic functionality of Cox-2 was proven by detection of PGE_2 and $PGF_{2\alpha}$ production.

5.3.2 EGFR signalling

ROS such as superoxide anion and H_2O_2 function also as activators of growth factor receptor signalling [Aslan and Ozben, 2003]. The production of oxygen radicals can be induced by several growth factors and ROS can activate tyrosine kinase activation. The EGF/EGFR signalling system comprises of four different receptors, ErbB1, ErbB2, ErbB3, and ErbB4, which form dimers or oligomers upon ligand binding. Activated receptors recruit adaptor proteins such as receptor-bound protein 2 (Grb2) and son of sevenless nucleotide exchange factor (Sos), promoting Ras activation and MAPK signalling. The vasoactive hormone angiotensin II stimulates EGFR transactivation through superoxide anion formation by the NAPDH oxidase system [Aslan and Ozben, 2003]. Furthermore, H_2O_2 induces EGFR tyrosine phosphorylation and subsequent association of adapter proteins. It is thought that ROS-mediated transactivation of the EGFR is regulated by several mechanisms: (i) inhibition of tyrosine phosphatases, (ii) metalloprotease-dependent shedding of membrane-bound heparin-binding EGF (HB-EGF), (iii) elevation of intracellular Ca^{2+}, and (iv) activation of tyrosine kinases such as c-Src, JAK2, PKC-δ, and PYK2. Ca^{2+} and c-Src have been identified as upstream regulators of HB-EGF release and the c-Src inhibitor PP2 blocks angiotensin II- and H_2O_2-induced EGFR activation and signalling cascades [Frank and Eguchi, 2003].

5.3.3 PGD_2 Receptor-independent Activities

15d-PGJ_2 has been identified as an agonist for the PGD_2 receptor subtypes DP and CRTH2. The binding affinity of 15d-PGJ_2 to PGD_2 receptors, particularly to CRTH2 [Monneret et al., 2002; Sawyer et al., 2002], is several orders of magnitude greater than that observed for PPARγ, which is in the low micromolar range [Kliewer et al., 1995]. In the present study, the rapid activation of p38 MAPK raised the question if 15d-PGJ_2 might activate intracellular signalling cascades through the activation of candidate GPCRs which are likely involved in fast signal transduction from extracellular stimuli. However, a contribution of PGD_2 receptor subtypes in 15d-PGJ_2-induced MAPK/JNK activation and Cox-2 expression can be excluded as treatment of MG-63 cells with PGD_2 (Figure 7) as well as synthetic agonists of DP and CRTH2 (Figure 8 A) did not mimic 15d-PGJ_2-mediated effects. Furthermore, antagonists of DP and CRTH2 did not impair 15d-PGJ_2-mediated cellular responses

(Figure 8 B). High concentrations (50 µM) of PGD_2 slightly increased Cox-2 expression (Figure 7 B) which rather argues for receptor-independent effects – probably by its dehydration product 15d-PGJ_2 – as DP and CRTH2 are stimulated by low nanomolar PGD_2 concentrations [Sawyer et al., 2002].

5.4 Regulation of Cox-2 expression

5.4.1 Signalling Cascades and Cox-2 mRNA Stability

Cox-2 belongs to early response genes which are usually transiently expressed during stress periods. Cox-2 expression can be regulated by transcriptional and post-transcriptional mechanisms [Harper and Tyson-Capper, 2008]. In MG-63 cells, Cox-2 expression is induced by 15d-PGJ_2 by both stimulating transcription and stabilizing mRNA. This conclusion is supported by several findings. First, inhibition of the phosphorylation status of p38 MAPK, p42/44 MAPK (Figure 4 A, B) and the EGFR (Figure 11 A) highly reduced Cox-2 expression. Second, addition of the transcriptional inhibitor ActD after induction of Cox-2 mRNA expression identified a sustained level of Cox-2 mRNA in 15d-PGJ_2-treated cells compared to vehicle-treated cells (Figure 10 A). Third, the impaired degradation of Cox-2 mRNA was reversed by addition of the p38 MAPK blocker PD169316 but was not affected by an inhibitor of p42/44 MAPK (Figure 10 B). This findings led to the conclusion that the EGFR/p42/44 MAPK route is rather involved in transcriptional regulation whereas the p38 MAPK signalling pathway regulates (also) Cox-2 mRNA stability.

In concordance with the present results, Subbamariah and coworkers [Subbaramaiah et al., 2003] reported that different pathways are responsible for Cox-2 expression induced by taxanes in mammary cancer cells. P42/44 MAPK, p38 MAPK, JNK, and PKC were involved in Cox-2 upregulation whereas just p38 MAPK and PKC could be identified as mRNA stabilizing pathways. MAPKAPK-2 was identified as a p38 MAPK downstream target under these conditions. PKC and MAPKAPK-2 were not considered in the present study but might be included in future

experiments to identify more detailed regulatory mechanisms of Cox-2 transcription and/or mRNA stabilization.

The major signalling molecule mediating Cox-2 mRNA stability appears to be p38 MAPK [Tsatsanis et al., 2006] mediating the nuclear translocation and binding of the mRNA stabilizing factor HuR to AREs in the 3'UTR of Cox-2 mRNA in various cellular systems [Cok et al., 2003; Sengupta et al., 2003; Subbaramaiah et al., 2003]. 15d-PGJ_2 upregulates the expression of IL-8 [Jozkowicz et al., 2008] and HO-1 [Li et al., 2004] via p38 MAPK-dependent increased mRNA stability. However, it was not clarified if HuR was involved in these studies.

In rat intestinal epithelial cells, Cox-2 mRNA stability is related to activation of the PI3K/Akt route by mutated k-Ras [Sheng et al., 2001]. This pathway might also be involved in MG-63 cells as inhibition of PI3K by LY294002 and inhibition of Ras by manumcyin A reduced Cox-2 protein expression (Figure 4 C). Interestingly, inhibition of Akt, a well-described downstream target of PI3K, was ineffective in blocking Cox-2 expression which accounts for an Akt-independent mechanism. Alternatively, PI3K induces signalling pathways others than Akt including the small GTPases Rac and Rho which are also involved in the regulation of p38 MAPK and JNK [Cantrell, 2001].

5.4.2 ROS-dependent Cox-2 Expression

Oxidative signalling has been implicated in the upregulation of diverse inflammatory genes, including Cox-2. Federico et al. even suggest that free radicals might link inflammation processes and tumorgenesis. Cytokines such as TNF-α, IL-1β, and IFN-γ are involved in ROS and reactive nitrogen species production by inflammatory cells [Federico et al., 2007] and induce Cox-2 expression in rat mesangial cells [Feng et al., 1995]. Cytokine-induced Cox-2 expression and PG synthesis is blocked by ROS scavengers [Feng et al., 1995; Harris et al., 2006]. Oxidative stress regulates Cox-2 upregulation in neuronal cells through various signal transduction routes including PI3K/Akt and MAPKs [Rockwell et al., 2004; Song et al., 2007]. Furthermore, redox sensitive transcription factors such as AP-1, CREB, and NF-κB are involved [Lu and Wahl, 2005; Song et al., 2007].

The upregulation of Cox-2 expression might be related to various sources as ROS. The depletion of NAPDH oxidase-derived radicals blocked Cox-2 induction in rat mesangial cells [Feng et al., 1995] whereas increased Ca^{2+}-dependent

mitochondrial ROS production was linked to downstream Cox-2 and PG production in human chondrocytes [Cillero-Pastor et al., 2008]. As ROS-mediated Cox-2/PGE_2 upregulation is reversed in several studies by the thiol antioxidant NAC [Cillero-Pastor et al., 2008; Song et al., 2007; Syeda et al., 2008], it is suggested that thiol-sensitive molecules such as GSH might also be involved in regulation of Cox-2 expression. Reyes-Martin and coworkers [Reyes-Martin et al., 2008] reported on a thiol-dependent Cox-2 induction in response to 15d-PGJ_2. ROS-dependent Cox-2 expression was diminished in the presence of NAC and potentiated after preincubation with BSO suggesting that GSH-sensitive mechanisms are involved. Of note, 15d-PGJ_2 inhibited PGE_2 production independently of its effect on Cox-2 expression. A similar mechanism is involved in 15d-PGJ_2-induced Cox-2 expression in MCF-7 breast cancer cells; Kim et al. demonstrated that 15d-PGJ_2 increased intracellular ROS levels that favor phosphorylation of Akt, and subsequent binding of AP-1 to CRE sequences [Kim et al., 2008a]. 15d-PGJ_2-mediated Cox-2 expression in MG-63 cells is proposed to be related to the intracellular redox balance as the thiol antioxidants MPG and GSH ethyl ester block 15d-PGJ_2-induced ROS accumulation, signalling cascades and downstream Cox-2 expression (Figure 16). However, the Akt/AP-1 pathway may not contribute to 15d-PGJ_2-induced Cox-2 expression in MG-63 cells as inhibition of Akt did not block Cox-2 expression (Figure 4 C) and the JNK pathway – a well-described activation route of the AP-1 subunit c-jun – is not involved in elevated Cox-2 expression (Figure 4 A, B).

An interesting aspect of the present study is that ROS-mediated expression of Cox-2 is not paralleled by elevation of PGs derived from endogenous AA. This indicates that the 15d-PGJ_2/ROS axis does not induce endogenous PLA_2 activity per se. However, functional activity of Cox-2 expression under the control of 15d-PGJ_2 was verified by stimulating PLA_2-mediated liberation of AA via bradykinin [Brechter and Lerner, 2007] or by addition of exogenous AA (Figure 10). As already reported for various tumor tissues, the most abundant PG formed under these experimental conditions is PGE_2 followed by lower $PGF_{2\alpha}$ levels. In osteoblastic cells, an autoamplification of Cox-2 by PGE_2 that involves multiple pathways including alterations on the transcriptional level has been reported [Huang et al., 2010; Pilbeam et al., 1995]. This mechanism is not likely in MG-63 cells as 15d-PGJ_2 (although inducing Cox-2 expression) did not lead to an increase of PGE_2 up to 24 h from endogenous AA (data not shown; measurements by Prof. Manfred Kollroser,

Institute of Forensic Medicine, Medical University of Graz, Austria). Furthermore, we can exclude an autocrine feedback mechanism for PGD_2, the precursor of 15d-PGJ_2, as no PGD_2 was measured in the cellular supernatant of MG-63 cells (data not shown). Nevertheless, cultured osteoblasts can synthesize PGD_2 [Gallant et al., 2005]; as osteoblasts are present in bone tumor surrounding areas, PGD_2 could exert paracrine effects on osteosarcoma.

5.4.3 PPARγ-dependent and PPARγ-independent Cox-2 Expression

Another plausible mechanism for modulating Cox-2 expression involves PPARγ activation. In general, PPARγ heterodimerizes with RXR to a functional transcriptional complex that binds to PPREs located in regulatory regions of target genes [Chun and Surh, 2004]. PPARγ is of particular interest in mediating part of PG action because of the high potency of 15d-PGJ_2 as an endogenous ligand for this receptor [Forman et al., 1995; Kliewer et al., 1995]. However, there has been recent controversy over the link between the action of PPARγ and Cox-2 expression. The regulation of Cox-2 expression by PPARγ is complex and appears to be cell-specific.

One hypothesis is that activation of PPARγ causes an inhibition of cytokine-induced Cox-2 expression. In concordance, overexpression of PPARγ suppressed Cox-2 expression in non-small-cell lung cancer cells [Bren-Mattison et al., 2008]. 15d-PGJ_2 reduces elevated Cox-2 expression through a PPARγ-dependent inhibition of AP-1 activity in breast cancer cells [Subbaramaiah et al., 2001], and cervical cancer cells [Han et al., 2003]. In human leukemic monocytes, 15d-PGJ_2-mediated activation of PPARγ inhibited upregulated Cox-2 expression by interference with the NF-κB pathway [Inoue et al., 2000]. It was further shown that PPARγ diminished AP-1-dependent transcription by a competition for the general transcription factor CBP/p300 [Subbaramaiah et al., 2001] (Scheme 8), a mechanism that is thoroughly conceivable for PPARγ-dependent inhibition of NF-κB signalling.

There is also evidence that PPARγ positively regulates Cox-2 expression in certain cell types. The human Cox-2 gene contains a PPRE located approx. 3900 bp upstream of the transcriptional start site, that is transcriptionally activated by ligand-bound PPARγ [Meade et al., 1999; Pontsler et al., 2002] (Scheme 8).

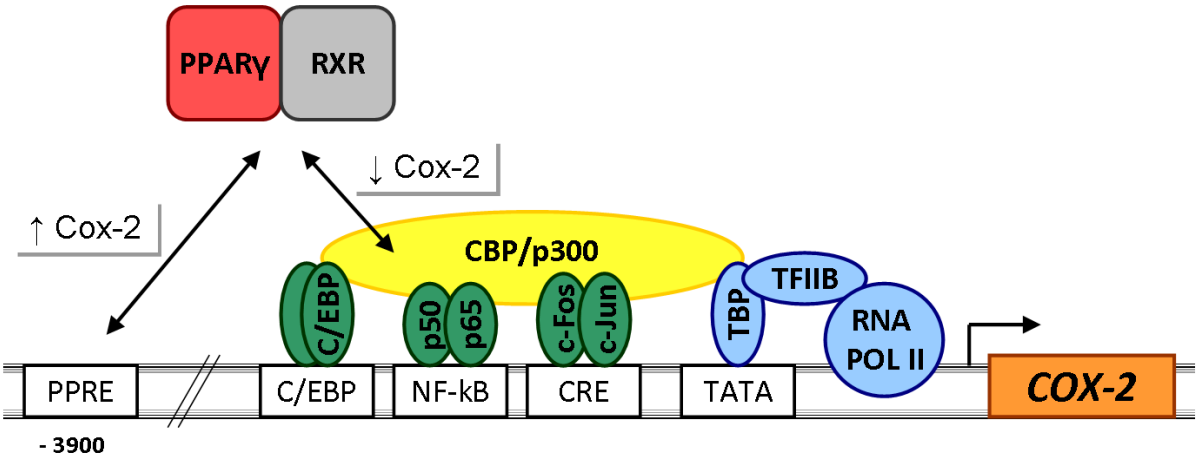

Scheme 8: How PPARγ activation may regulate Cox-2 expression.
Active PPARγ may regulate Cox-2 expression in a positive or negative way, depending on different mechanisms. (i) PPARγ diminished AP-1-dependent transcription by a competition for the general transcription factor CBP/p300 [Subbaramaiah et al., 2001]. (ii) PPARγ upregulates Cox-2 expression by binding to a PPRE located approx. 3900 bp upstream of the transcriptional start site [Meade et al., 1999; Pontsler et al., 2002].

PPARγ ligands may regulate Cox-2 expression also without activation of PPARγ. As described above, 15d-PGJ_2 induced Cox-2 upregulation in a ROS-dependent manner [Kim et al., 2008a; Reyes-Martin et al., 2008]. MG-63 cells express PPARγ on mRNA (Figure 5) and protein level [Haydon et al., 2002; Lucarelli et al., 2002]. However, the present study reveals that pharmacological inhibition of PPARγ and silencing of PPARγ expression did not alter 15d-PGJ_2-induced MAPK activation and Cox-2 expression (Figure 6). 15d-PGJ_2 provokes not only Cox-2 upregulation but also Cox-2 repression in a PPARγ-independent manner. It was also shown that 15d-PGJ_2 still exerts its anti-inflammatory actions – including suppression of Cox-2 expression – in PPARγ-deficient mice [Chawla et al., 2001]. In line with the present study, 15d-PGJ_2 reduced cytokine-induced Cox-2 expression in a PPARγ-independent manner by interference with AP-1 [Sawano et al., 2002] or NF-κB signalling [Ackerman et al., 2005; Bianchi et al., 2005]. The impaired AP-1 activity in mesangial cells was most likely regulated through 15d-PGJ_2-mediated inhibition of MAPK signalling [Sawano et al., 2002]. Alternatively, 15d-PGJ_2 may directly modify the AP-1 subunit c-jun and thereby inhibit its DNA-binding capacity [Perez-Sala et al., 2003]. 15d-PGJ_2 may also block NF-κB signalling by modifications of critical cysteine

residues of IKK or Rel proteins [Cernuda-Morollon et al., 2001; Rossi et al., 2000; Straus et al., 2000] (see Introduction, section 1.3.1.3). In contrast, NF-κB has been shown to be a positive regulator of Cox-2 expression [Chun and Surh, 2004] and oxidative stress has been identified as an inducer of NF-κB activity [Lu and Wahl, 2005]. In the present study, transcriptional regulation of prolonged Cox-2 expression by NF-κB can be excluded as inhibitors of NF-κB (Figure 9 A) and IKK (Figure 9 B) failed to alter 15d-PGJ_2-mediated Cox-2 expression in MG-63 cells. Furthermore, 15d-PGJ_2 did not favor nuclear translocation of the NF-κB subunit p65 (Figure 9 C).

5.4.4 Activities of Retinoids

Retinoids are a group of naturally occurring and synthetic analogues of vitamin A, such as all-*trans*-RA, 13-*cis*-RA, 9-*cis*-RA, and retinyl acetate [Mestre et al., 1997a]. RA isomers have been shown to regulate the transcription of many genes via binding to nuclear receptors such as the RA receptor (RAR) and/or the RXR. Both RAR and RXR belong to a nuclear receptor superfamily and each has at least three isoforms (α, β, γ). All-*trans*-RA and 9-*cis*-RA bind to RAR, whereas only 9-*cis*-RA binds to RXR. After ligand binding, these receptors form a homodimer (RAR/RAR) or a heterodimer (RAR/RXR) and regulate the transcription of target genes regulated by RA-response elements [Jiang et al., 2003]. RXR isoforms may also heterodimerize with other nuclear receptors such as PPARs, liver X receptors, and farnesoid X receptors [Wolf, 2006].

Since RXR forms a transcriptional complex with PPARγ, effects of PPARγ agonists might be potentiated by RXR ligands. Indeed, the simultaneous administration of PPARγ and RXR ligands resulted in additive effects on B cell proliferation and differentiation [Garcia-Bates et al., 2009]. In colon cancer cells, the combination of the selective RXR agonist bexarotene and the PPARγ agonist rosiglitazone has a greater efficacy in inhibiting cell growth, suppressing Cox-2 expression, and inducing terminal differentiation than the single agents [Cesario et al., 2006]. Thus, it is likely that PPARγ is participating in these processes. The finding that the preincubation with 9-*cis*-RA did not potentiate 15d-PGJ_2-induced Cox-2 expression supports the suggestion that the observed 15d-PGJ_2-mediated effects in MG-63 cells are unrelated to PPARγ activation. In contrast, 9-*cis*-RA blocked 15d-

PGJ_2- as well as LPA-mediated Cox-2 expression in MG-63 cells by a ROS-independent mechanism (Figure 19). Both substances have been identified as PPARγ ligands [Forman et al., 1995; Kliewer et al., 1995; McIntyre et al., 2003]. At least 15d-PGJ_2-induced Cox-2 expression is PPARγ-independent, however, according to the present data it can not be excluded that this receptor is involved in the 9-*cis*-RA-mediated downregulation of Cox-2 expression.

It is also reported in other studies, that retinoids repressed Cox-2 expression – induced by EGF, phorbol ester, or serum – in the absence of PPARγ agonists [Kanekura et al., 2000; Mestre et al., 1997a; Mestre et al., 1997b]. It is speculated that retinoids may regulate Cox-2 expression by blocking AP-1 mediated gene expression as 9-*cis*-RA inhibits AP-1 promoter activity and c-jun expression [Yamazaki et al., 2007]. However, a direct link between AP-1 activity/expression and Cox-2 levels in the presence of retinoids and if PPARγ is involved has not been shown so far. Another critical point for the efficiency of retinoids is the phosphorylation status of RXRα as p42/44-dependent phosphorylation of RXRα influenced its transactivational activity in a negative way [Yamazaki et al., 2007].

5.5 15d-PGJ_2-induced Apoptosis

15d-PGJ_2 induces apoptosis in a number of cell lines confirmed by various criteria such as cellular shrinkage, membrane blebbing [Bishop-Bailey and Hla, 1999], DNA condensation and fragmentation, caspase activation, PARP cleavage [Keelan et al., 2001] and expression of genes which are critical mediators of cell cycle arrest and programmed cell death [Kim et al., 2003; Kondo et al., 2002].

In MG-63 cells, administration of 15d-PGJ_2 decreased cell viability in a time- and concentration-dependent manner (Figure 20). The cytotoxicity was paralleled with activation of caspase-3 and cleavage of PARP (Figure 21), indicating that MG-63 cells undergo programmed cell death. Anti-proliferative and growth inhibitory effects of PPARγ ligands can be achieved through either PPARγ-dependent [Bishop-Bailey and Hla, 1999; Kim et al., 2003] or PPARγ-independent [Clay et al., 2001; Qiao et al., 2008] mechanisms. The PPARγ ligands troglitazone and ciglitazone

decreased survival of several human osteosarcoma cell lines, including MG-63 cells [Haydon et al., 2002]. This effect was potentiated by co-treatment with the RXR ligand 9-*cis*-RA, however, the underlying mechanisms – particularly if PPARγ is involved – were not elucidated. 15d-PGJ_2-induced apoptosis of human myofibroblasts is unrelated to PPARγ, because PPARγ is not expressed in these cells [Li et al., 2001a]. Similarly, 15d-PGJ_2-induced caspase-3 activation and PARP cleavage in MG-63 cells occur independently of PPARγ as these events were not blocked by siRNAs and pharmacological inhibitors directed against PPARγ (Figure 23). Furthermore, these apoptotic effects are likely unrelated to PGD_2 receptors as PGD_2 failed to mimic the events induced by its metabolite 15d-PGJ_2 (Figure 24).

Previous studies have shown that PPARγ agonists activate different MAPK subfamilies and these kinases may contribute to cell death [Jung et al., 2007; Kim et al., 2006b; Lee et al., 2008]. For example, in mouse MC3T3-E1 osteoblastic cells, 15d-PGJ_2 induces apoptosis in a JNK-dependent manner [Lee et al., 2008]. In the present study, similarly as in 15d-PGJ_2-treated renal epithelial cells [Kang et al., 2006], a MAPK-independent induction of apoptosis occurs in MG-63 cells.

It is proposed that oxidative stress caused by cyclopentenone PGs is related to their cytotoxicity [Keelan et al., 2001; Kondo et al., 2001; Li et al., 2001a; Pignatelli et al., 2005]. The finding that the non-electrophilic compound 9,10-dihydro-15d-PGJ_2 did not exert apoptotic features (Figure 25) and the thiol antioxidants MPG and GSH ethyl ester prevented 15d-PGJ_2-induced caspase-3 activation and PARP cleavage (Figure 26) led to the assumption that oxidative stress is involved in 15d-PGJ_2-induced apoptosis in MG-63 cells. In line with these results, 15d-PGJ_2 caused a rapid ROS elevation while inducing apoptosis in hepatic myofibroblasts and neuroblastoma cells, effects that were reproduced by H_2O_2 and blocked by antioxidants, such as NAC, MPG and pyrrolidine dithiocarbamate [Kondo et al., 2001; Li et al., 2001a]. 15d-PGJ_2-induced ROS are also involved in the dissipation of the mitochondrial transmembrane potential and cytochrome C release [Liu et al., 2007; Nencioni et al., 2003].

15d-PGJ_2-induced apoptosis is accompanied by caspase activation in MG-63 (Figure 21, Figure 27) and other cells [Chen et al., 2005; Hashimoto et al., 2002; Kim et al., 2003; Nencioni et al., 2003; Okano et al., 2003]. 15d-PGJ_2-induced caspase-3 activation and PARP cleavage were reversed by the pan-caspase inhibitor z-VAD-FMK suggesting that the caspase cascade is important for triggering apoptosis under

the respective conditions, supporting previous findings in other cell types including human pancreatic cancer, MDA-MB-231 human mammary cancer, HT-29 colon cancer, JEG-3 choriocarcinoma, and neuroblastoma SH-SY5Y cells [Na and Surh, 2003]. To clarify if the activation of caspase-3 and caspase-8 is critical for the induction of 15d-PGJ_2-mediated MG-63 programmed cell death, selective caspase inhibitors might be used to address this question. Caspase inhibitors might also give information if 15d-PGJ_2-mediated apoptosis is related to DR- or mitochondria-dependent mechanisms; for example, caspase-9 is generally activated in course of mitochondrial disruption and subsequent cytochrome C release [Li et al., 1997].

Within the regulation of mitochondria-mediated apoptosis, the expression status and localization of Bcl-2 family members are critical events. 15d-PGJ_2 decreased the expression of anti-apoptotic Bcl-x_L, Bcl-2, and Mcl-1 [Kim et al., 2003; Liu et al., 2007]. In concordance, overexpression of Bcl-2 and Bcl-x_L completely inhibited the initiation of apoptosis in Jurkat T cells [Nencioni et al., 2003]. Downregulation of XIAP, an inhibitor of caspase-3 and caspase-9, was detected in 15d-PGJ_2-induced apoptosis in SK-Hep1 cells [Okano et al., 2003] and HL-60 cells [Han et al., 2007]. Likewise, loss of XIAP sensitizes in colon cancer cells to 15d-PGJ_2 and troglitazone-dependent apoptosis [Qiao et al., 2008]. Furthermore, an increased expression of pro-apoptotic Bax has been connected to 15d-PGJ_2-induced apoptosis in several cell lines, including MC3T3-E1 cells [Kim et al., 2008a; Kim et al., 2003; Kondo et al., 2002; Lee et al., 2008; Liu et al., 2007]. In MG-63 cells, Bax is constitutively expressed upon 15d-PGJ_2 treatment (Figure 27), however, next to the expression levels, the location as well as homo- and heterodimerization with other Bcl-2 family members determine the functionality of Bcl-2 family members [Hengartner, 2000; Zimmermann et al., 2001]. In future studies, the translocation of Bax from the cytosol to the mitochondria, where it is most likely involved in the permeabilization process [Cory and Adams, 2002], as well as the release of apoptogenic factors such as cytochrome C, AIF, and Smac/DIABLO [Han et al., 2007] from the mitochondrial innermembrane space should be followed.

p53, an important regulator of cell cycle progression as well as apoptosis, has also been implicated in 15d-PGJ_2-modulated cell viability [Ho et al., 2008; Kobayashi et al., 2006; Kondo et al., 2002]. 15d-PGJ_2 stimulated p53 activation and accumulation through ataxia-telangiectasia mutated protein-dependent [Kobayashi et al., 2006] or ROS-dependent [Ho et al., 2008] mechanisms. 15d-PGJ_2-mediated

induction of p53 is accompanied by expression of p53-responsive genes such as GADD45, p21, and MDM2, which are cell cycle arrest regulators [Kondo et al., 2002]. Furthermore, 15d-PGJ_2-induced cell cycle arrest was detected in the presence of increased levels of the G2/M phase regulatory protein cyclin B1 but decreased levels of cdk2, cdk4, cyclin A, cyclin D1, cyclin E, and cdc25C [Kim et al., 2003]. p53 has also been comprised in one of the few studies reporting on DR-related apoptosis caused by 15d-PGJ_2 involving activation of the Fas/FasL system [Kondo et al., 2002]. The presence of p53 in Fas/FasL-mediated apoptosis seems to be a critical factor as blocking of this DR pathway in FADD knock-out and caspase-8 knock-out Jurkat T cells – which lack functional p53 [Pan and Haines, 1999] – had no influence on 15d-PGJ_2-induced apoptosis [Nencioni et al., 2003]. p53-mediated responses of 15d-PGJ_2 in MG-63 cells can also be ruled out as these cells do not express p53 [Diller et al., 1990]. However, 15d-PGJ_2 may target another extrinsic pathway as the cyclopentenone potentiates TRAIL-induced apoptosis in human malignant tumor cells by upregulation of DR5 expression [Nakata et al., 2006]. Thus, 15d-PGJ_2 might be useful for the sensitization of osteosarcoma cell lines which are widely resistant to TRAIL as a single agent [Wachtel and Schafer, 2010].

5.5.1 Cox-2 and Apoptosis

In cancerous tissues, high levels of Cox-2 are generally believed to be a critical tumorigenic factor involved in anti-apoptotic events. Cox-2 may prevent apoptosis by several mechanisms, including (i) production of PGs that act as anti-apoptotic or survival factors; (ii) metabolization of AA, a pro-apoptotic substrate that activates caspase-3 and modulates mitochondrial permeability; (iii) increased expression of the anti-apoptotic protein Bcl-2 and (iv) activation of the pro-survival PI3K/Akt pathway [de Moraes et al., 2007]. The inductions of the PI3K/Akt pathway and Bcl-2 expression have been related to PGE_2 signalling. Furthermore, PGE_2 enhances the expression of the anti-apoptotic protein Mcl-1 and downregulates expression levels of pro-apoptotic factors such as Bad and caspases [Telliez et al., 2006].

Recent studies report that Cox-2 might also be involved in pro-apoptotic processes under certain circumstances. Cox-2 induction in response to moderate oxidative stress in rat PC12 cells had protective effects on high dose H_2O_2-induced

apoptosis. This effect is suggested to be regulated by PGs as inhibition of Cox-2 by NS-398 reversed the protective effect [Tang et al., 2006]. In cervical carcinoma cells [Eichele et al., 2008] and human leukemia cells [Chen et al., 2005], Cox-2-mediated apoptosis was related to PGD_2 and 15d-PGJ_2 synthesis. In addition to Cox-2-derived anti-apoptotic PGs, Cox-2-generated ROS, which are side products of the peroxidase reaction, were linked to decreased proliferation and increased apoptosis in the human osteosarcoma cell line SaOS-2 [Xu et al., 2006]. Considering these results, Cox-2 inhibition during cancer therapy might diminish its efficacy.

15d-PGJ_2-induced ROS levels in MG-63 cells are suggested to be related to an imbalanced GSH metabolism. If Cox-2-related radicals are present after longer incubation periods in MG-63 cells has not been followed yet. Interestingly, Cox-2 protein expression was abolished at high 15d-PGJ_2 concentrations (> 20 µM) (Figure 1 B) that impair cell viability after 24 h incubation by more than 50% (Figure 20 B). Similar effects have also been observed for HO-1 expression, suggesting that under these cytotoxic conditions, the expression of Cox-2 and other anti-apoptotic factors might be diminished in favor of expression of late-apoptotic and/or necrotic factors. As the anti-apoptotic response in case of Cox-2 overexpression is most likely linked to high levels of PGE_2, it would be interesting to explore if Cox-2-derived PGE_2 might counteract apoptosis in MG-63 cells. This could be addressed by administration of free AA at time points when Cox-2 expression is assessed and further monitoring of apoptotic markers. Alternatively, addition of exogenous PGE_2 directly into the medium of 15d-PGJ_2-stimulated cells might be helpful to elucidate this hypothesis.

5.6 Cytoprotective/Anti-Apoptotic Responses

5.6.1 Glutathione

The role of GSH in the protection of cells against oxidative stress and other xenobiotic compounds has been well established. The intracellular GSH content is regulated by GCL activity, cysteine availability, and GSH feedback inhibition together.

GCL is the rate-limiting enzyme in GSH *de novo* synthesis, consisting of a catalytic subunit and a modulatory subunit [Chen et al., 2006].

15d-PGJ_2 causes a fast decrease of intracellular GSH levels in MG-63 cells (Fig. 14 B), however, GSH concentrations were doubled at longer stimulation periods starting after 16 h (Fig. 30). Similar mechanisms were reported in rat neuronal PC12 cells [Chen et al., 2006] and HUVECs [Levonen et al., 2001]. The elevation of 15d-PGJ_2-induced GSH synthesis was explained by an Nrf-2-dependent increased gene expression of both GCL subunits [Chen et al., 2006; Levonen et al., 2001]. In human retinal pigment epithelial cells, p38 MAPK and JNK pathways contribute to 15d-PGJ_2-dependent induction of GCL expression [Qin et al., 2006]. To elucidate the mechanisms of elevated GSH concentration, it is of further interest to follow the expression levels of GCL subunits on mRNA and protein level in MG-63 cells treated with 15d-PGJ_2. If Nrf-2 is involved in the potential upregulation of these enzymes could be established by Nrf-2 knock-down experiments.

The intracellular glutathione status seems to be crucial for the regulation of the cellular fate as overexpression of GCL protects against apoptosis whereas GCL knock-down induces time-dependent cell death in various cell types [Franco and Cidlowski, 2009]. 15d-PGJ_2 protected primary cortical neurons from glutamate-induced GSH depletion and subsequent cell death [Saito et al., 2007]. Depletion of GSH pools by the GCL inhibitor BSO significantly potentiated the apoptotic events induced by 15d-PGJ_2 in MG-63 cells (Figure 31) and decreased cell viability in PC12 cells [Chen et al., 2006] and human retinal pigment epithelial cells [Qin et al., 2006].

It is proposed that the cellular response depends on the doses of 15d-PGJ_2 and the levels of intracellular ROS; low micromolar concentrations (< 5 µM) of 15d-PGJ_2 caused an increase in cellular GSH and resistance against oxidative stress in human epithelial [Levonen et al., 2001] and rat PC12 cells [Na and Surh, 2003]; higher doses (> 10 µM) of 15d-PGJ_2 induced endothelial cell apoptosis, which was potentiated by inhibition of GSH synthesis [Levonen et al., 2001].

5.6.2 Heme Oxygenase-1

HO-1 is a key enzyme in heme metabolism which is inducible by various stress stimuli. 15d-PGJ_2 and other cyclopentenones including PGA_1, and PGJ_2 induce HO-1 expression in various cell systems [Alvarez-Maqueda et al., 2004; Gong

et al., 2002; Lee et al., 2003; Lim et al., 2007]. Regarding the mechanism of HO-1 induction, several studies have suggested an involvement of MAPK, JNK, and PI3K/Akt pathways [Alvarez-Maqueda et al., 2004; Kim et al., 2008b; Lim et al., 2007; Lin et al., 2010]. Conversely, 15d-PGJ_2-induced HO-1 expression in HepG2 hepatoma cells occurs independently of MAPK activation and is rather related to the electrophilic character of 15d-PGJ_2 as NAC and dithiothreitol reversed this effect [Liu et al., 2004]. Similarly, 15d-PGJ_2 upregulates HO-1 expression in human lymphocytes in a ROS-dependent manner; the intracellular GSH content might also be involved as 15d-PGJ_2-induced HO-1 expression was blocked by NAC and potentiated by BSO [Alvarez-Maqueda et al., 2004]. MAPK-independent upregulation of HO-1 expression is most likely regulated by covalent modifications of critical thiol residues of Keap1 and subsequent release and translocation of Nrf-2 to the nucleus where it increases the expression of genes under the control of the ARE/EpRE [Oh et al., 2008].

In MG-63 cells, HO-1 expression is highly induced on mRNA and protein level up to 24 h (Figure 32). Elevated expression and nuclear translocation of Nrf-2 and of Egr-1 (Figure 34), another candidate transcription factor regulating HO-1 expression, could be demonstrated. Molecular silencing of Nrf-2 and Egr-1 will clarify which molecule is directly contributing to HO-1 transcription. As HO-1 expression is also regulated in a PPARγ-dependent manner under certain conditions (see Introduction, section 1.3.1.6), it should be clarified if PPRE-mediated transcription is involved in 15d-PGJ_2-induced HO-1 levels in MG-63 cells. The regulation of Egr-1 by 15d-PGJ_2 is an interesting aspect in this study per se as, to the best of our knowledge, 15d-PGJ_2-induced Egr-1 expression and nuclear translocation has not been described before. In contrast, Okada and coworkers [Okada et al., 2002] reported that 15d-PGJ_2 and troglitazone decreased hypoxia-induced Egr-1 expression and DNA binding activity. Furthermore, troglitazone has been identified as an inducer of Egr-1-dependent expression of the transforming growth factor-β superfamily member NAG-1, however, a similar mechanism could not be determined for 15d-PGJ_2 [Baek et al., 2004]. RNA microarray analysis and 2D gel analysis might be a useful screening tool to elucidate candidate targets that are regulated by Egr-1 in response to 15d-PGJ_2.

Ricart and coworkers [Ricart et al., 2009] demonstrated that the mitochondrial localization of 15d-PGJ_2 might be critical for the induction of the Keap1/Nrf-2 signal transduction leading to HO-1 expression. Moreover, mitochondrial targeting of 15d-

PGJ_2 causes an increased mitochondrial membrane polarization and apoptotic cell death but is less potent in inducing HO-1 [Diers et al., 2009] suggesting that there might be a direct link between HO-1 expression/activity and the stage of apoptosis. Indeed, 15d-PGJ_2-induced HO-1 expression exerts beneficial effects regarding H_2O_2-induced apoptosis in PC12 cells [Kim et al., 2008b] and oxidative stress in megakaryocytes [O'Brien et al., 2009]. HO-1 exerts cytoprotective effects through its metabolite CO which suppressed apoptosis in endothelial cells [Brouard et al., 2000; Soares et al., 2002; Wang et al., 2007]. Conversely, Qin and coworkers [Qin et al., 2006] reported that 15d-PGJ_2-induced cytoprotective effects in H_2O_2-treated cells could not be related to elevated HO-1 expression suggesting that other enzymes are involved as well.

In future experiments, it should be clarified if there is a link between HO-1 expression and apoptosis in MG-63 cells. If HO-1 activity functions cytoprotective in apoptotic MG-63 cells, a reduction of HO-1 activity should potentiate 15d-PGJ_2-induced cell death. This question could be addressed by using siRNAs or pharmacological blockers (e.g. zinc protophorphyrin) directed against HO-1 or the CO scavenger hemoglobin. Furthermore, HO-1 inducers such as hemin and CoPP as well as the CO releasing molecule tricarbonyldichlororuthenium II should have beneficial effects on 15d-PGJ_2-induced programmed cell death. A putative connection between HO-1 expression and apoptosis is given by the finding that HO-1 expression in MG-63 cells is diminished at time points (48 h) and at concentrations (30 – 50 µM) (Figure 32) at which 15d-PGJ_2 highly induces apoptotic features (Figure 21). HO-1 expression is negatively regulated by HSF-1 which binds to a *cis*-acting regulatory sequence located on the HO-1 promoter [Chou et al., 2005]. Various extracellular stresses, including administration of 15d-PGJ_2, activate heat shock proteins/factors like Hsp-70 or HSF-1 [Chou et al., 2005]. It is of further interest if a reduction of HO-1 expression conditions might be connected to an increased expression of HSF-1 or other heat shock proteins.

6 CONCLUDING REMARKS

An aberrant PG metabolism has been connected to tumorigenesis in many cases. It became apparent that the cellular response varies dramatically depending on the present PG type. PGE_2 is connected to pro-inflammatory and anti-apoptotic effects supporting cancer initiation. In contrast, PGD_2 is related to mechanisms supporting the resolution of inflammatory processes. The present study highlights new insights of the cyclopentenone 15d-PGJ_2, a metabolite of PGD_2, regarding signal transduction, Cox-2 expression, and apoptosis.

15d-PGJ_2-induced ROS accumulation was identified as an initiating event for the activation of signal transduction pathways that were connected to Cox-2-derived PG biosynthesis. It was shown that the activation of p38 MAPK and EGFR/p42/44 MAPK routes were dependent on the reactive α,β-unsaturated carbonyl group of the cyclopentenone PG as 9,10-dihydro-15d-PGJ_2 failed to induce these signalling cascades. Both signalling pathways contribute independently to an elevated expression of a functional Cox-2 enzyme.

The intracellular redox status was also related to the induction of 15d-PGJ_2-mediated programmed cell death. Several apoptotic markers were induced upon 15d-PGJ_2 treatment which might be involved in death receptor- and/or mitochondria-dependent pathways. Furthermore, 15d-PGJ_2 triggered antioxidative responses shown by the elevation of the intracellular GSH content and overexpression of HO-1. It is of further interest to elucidate the interaction of pro-apopotic and cytoprotective events as it is likely that an increased expression of cytoprotective enzymes support cells to acquire resistance to oxidative stress and cytotoxicity in further consequence.

These *in vitro* data provide an interesting mechanism of PG feedback regulation and may contribute to a better understanding of Cox-2-mediated (patho)physiology of bone and bone tumor cells. As chronic inflammation and an imbalanced redox homeostasis are well-known risk factors in cancer development, insights in relationships between ROS and PG metabolism and their mode of action might be helpful in finding new strategies for osteosarcoma treatment.

7 REFERENCES

Abed R, Grimer R. 2010. Surgical modalities in the treatment of bone sarcoma in children. Cancer Treat Rev 36:342-7.

Ackerman WEt, Zhang XL, Rovin BH, Kniss DA. 2005. Modulation of cytokine-induced cyclooxygenase 2 expression by PPARG ligands through NFkappaB signal disruption in human WISH and amnion cells. Biol Reprod 73:527-35.

Ahmad M, Srinivasula SM, Wang L, Talanian RV, Litwack G, Fernandes-Alnemri T, Alnemri ES. 1997. CRADD, a novel human apoptotic adaptor molecule for caspase-2, and FasL/tumor necrosis factor receptor-interacting protein RIP. Cancer Res 57:615-9.

Aina V, Perardi A, Bergandi L, Malavasi G, Menabue L, Morterra C, Ghigo D. 2007. Cytotoxicity of zinc-containing bioactive glasses in contact with human osteoblasts. Chem Biol Interact 167:207-18.

Allen RG, Tresini M. 2000. Oxidative stress and gene regulation. Free Radic Biol Med 28:463-99.

Almishri W, Cossette C, Rokach J, Martin JG, Hamid Q, Powell WS. 2005. Effects of prostaglandin D2, 15-deoxy-Delta12,14-prostaglandin J2, and selective DP1 and DP2 receptor agonists on pulmonary infiltration of eosinophils in Brown Norway rats. J Pharmacol Exp Ther 313:64-9.

Alvarez-Maqueda M, El Bekay R, Alba G, Monteseirin J, Chacon P, Vega A, Martin-Nieto J, Bedoya FJ, Pintado E, Sobrino F. 2004. 15-deoxy-delta 12,14-prostaglandin J2 induces heme oxygenase-1 gene expression in a reactive oxygen species-dependent manner in human lymphocytes. J Biol Chem 279:21929-37.

Antignani A, Youle RJ. 2006. How do Bax and Bak lead to permeabilization of the outer mitochondrial membrane? Curr Opin Cell Biol 18:685-9.

Aslan M, Ozben T. 2003. Oxidants in receptor tyrosine kinase signal transduction pathways. Antioxid Redox Signal 5:781-8.

Baek SJ, Kim JS, Nixon JB, DiAugustine RP, Eling TE. 2004. Expression of NAG-1, a transforming growth factor-beta superfamily member, by troglitazone requires the early growth response gene EGR-1. J Biol Chem 279:6883-92.

Bai XC, Lu D, Liu AL, Zhang ZM, Li XM, Zou ZP, Zeng WS, Cheng BL, Luo SQ. 2005. Reactive oxygen species stimulates receptor activator of NF-kappaB ligand expression in osteoblast. J Biol Chem 280:17497-506.

Bailey SA, Graves DE, Rill R, Marsch G. 1993. Influence of DNA base sequence on the binding energetics of actinomycin D. Biochemistry 32:5881-7.

Berry EB, Sato TA, Mitchell MD, Stewart Gilmour R, Helliwell RJ. 2004. Differential effects of serum constituents on apoptosis induced by the cyclopentenone prostaglandin 15-deoxy-delta12,14-prostaglandin J2 in WISH epithelial cells. Prostaglandins Leukot Essent Fatty Acids 71:191-7.

Bianchi A, Moulin D, Sebillaud S, Koufany M, Galteau MM, Netter P, Terlain B, Jouzeau JY. 2005. Contrasting effects of peroxisome-proliferator-activated receptor (PPAR)gamma

agonists on membrane-associated prostaglandin E2 synthase-1 in IL-1beta-stimulated rat chondrocytes: evidence for PPARgamma-independent inhibition by 15-deoxy-Delta12,14prostaglandin J2. Arthritis Res Ther 7:R1325-37.

Billiau A, Edy VG, Heremans H, Van Damme J, Desmyter J, Georgiades JA, De Somer P. 1977. Human interferon: mass production in a newly established cell line, MG-63. Antimicrob Agents Chemother 12:11-5.

Bishop-Bailey D, Hla T. 1999. Endothelial cell apoptosis induced by the peroxisome proliferator-activated receptor (PPAR) ligand 15-deoxy-Delta12, 14-prostaglandin J2. J Biol Chem 274:17042-8.

Blackwell KA, Raisz LG, Pilbeam CC. 2010. Prostaglandins in bone: bad cop, good cop? Trends Endocrinol Metab 21:294-301.

Blanco M, Moro MA, Davalos A, Leira R, Castellanos M, Serena J, Vivancos J, Rodriguez-Yanez M, Lizasoain I, Castillo J. 2005. Increased plasma levels of 15-deoxyDelta prostaglandin J2 are associated with good outcome in acute atherothrombotic ischemic stroke. Stroke 36:1189-94.

Blobaum AL, Marnett LJ. 2007. Structural and functional basis of cyclooxygenase inhibition. J Med Chem 50:1425-41.

Boie Y, Sawyer N, Slipetz DM, Metters KM, Abramovitz M. 1995. Molecular cloning and characterization of the human prostanoid DP receptor. J Biol Chem 270:18910-6.

Bramwell VH. 2000. Osteosarcomas and other cancers of bone. Curr Opin Oncol 12:330-6.

Brechbuhl HM, Min E, Kariya C, Frederick B, Raben D, Day BJ. 2009. Select cyclopentenone prostaglandins trigger glutathione efflux and the role of ABCG2 transport. Free Radic Biol Med 47:722-30.

Brechter AB, Lerner UH. 2007. Bradykinin potentiates cytokine-induced prostaglandin biosynthesis in osteoblasts by enhanced expression of cyclooxygenase 2, resulting in increased RANKL expression. Arthritis Rheum 56:910-23.

Bren-Mattison Y, Meyer AM, Van Putten V, Li H, Kuhn K, Stearman R, Weiser-Evans M, Winn RA, Heasley LE, Nemenoff RA. 2008. Antitumorigenic effects of peroxisome proliferator-activated receptor-gamma in non-small-cell lung cancer cells are mediated by suppression of cyclooxygenase-2 via inhibition of nuclear factor-kappaB. Mol Pharmacol 73:709-17.

Brouard S, Berberat PO, Tobiasch E, Seldon MP, Bach FH, Soares MP. 2002. Heme oxygenase-1-derived carbon monoxide requires the activation of transcription factor NF-kappa B to protect endothelial cells from tumor necrosis factor-alpha-mediated apoptosis. J Biol Chem 277:17950-61.

Brouard S, Otterbein LE, Anrather J, Tobiasch E, Bach FH, Choi AM, Soares MP. 2000. Carbon monoxide generated by heme oxygenase 1 suppresses endothelial cell apoptosis. J Exp Med 192:1015-26.

Brunoldi EM, Zanoni G, Vidari G, Sasi S, Freeman ML, Milne GL, Morrow JD. 2007. Cyclopentenone prostaglandin, 15-deoxy-Delta12,14-PGJ2, is metabolized by HepG2 cells via conjugation with glutathione. Chem Res Toxicol 20:1528-35.

Cantrell DA. 2001. Phosphoinositide 3-kinase signalling pathways. J Cell Sci 114:1439-45.

Cao Z, Liu LZ, Dixon DA, Zheng JZ, Chandran B, Jiang BH. 2007. Insulin-like growth factor-I induces cyclooxygenase-2 expression via PI3K, MAPK and PKC signaling pathways in human ovarian cancer cells. Cell Signal 19:1542-53.

Cernuda-Morollon E, Pineda-Molina E, Canada FJ, Perez-Sala D. 2001. 15-Deoxy-Delta 12,14-prostaglandin J2 inhibition of NF-kappaB-DNA binding through covalent modification of the p50 subunit. J Biol Chem 276:35530-6.

Cesario RM, Stone J, Yen WC, Bissonnette RP, Lamph WW. 2006. Differentiation and growth inhibition mediated via the RXR:PPARgamma heterodimer in colon cancer. Cancer Lett 240:225-33.

Chakrabarty A, Tranguch S, Daikoku T, Jensen K, Furneaux H, Dey SK. 2007. MicroRNA regulation of cyclooxygenase-2 during embryo implantation. Proc Natl Acad Sci U S A 104:15144-9.

Chawla A, Barak Y, Nagy L, Liao D, Tontonoz P, Evans RM. 2001. PPAR-gamma dependent and independent effects on macrophage-gene expression in lipid metabolism and inflammation. Nat Med 7:48-52.

Chen H, Wang L, Gong T, Yu Y, Zhu C, Li F, Li C. 2010. EGR-1 regulates Ho-1 expression induced by cigarette smoke. Biochem Biophys Res Commun 396:388-93.

Chen YC, Shen SC, Tsai SH. 2005. Prostaglandin D(2) and J(2) induce apoptosis in human leukemia cells via activation of the caspase 3 cascade and production of reactive oxygen species. Biochim Biophys Acta 1743:291-304.

Chen ZH, Yoshida Y, Saito Y, Sekine A, Noguchi N, Niki E. 2006. Induction of adaptive response and enhancement of PC12 cell tolerance by 7-hydroxycholesterol and 15-deoxy-delta(12,14)-prostaglandin J2 through up-regulation of cellular glutathione via different mechanisms. J Biol Chem 281:14440-5.

Chinnaiyan AM, O'Rourke K, Tewari M, Dixit VM. 1995. FADD, a novel death domain-containing protein, interacts with the death domain of Fas and initiates apoptosis. Cell 81:505-12.

Cho WH, Choi CH, Park JY, Kang SK, Kim YK. 2006. 15-deoxy-(Delta12,14)-prostaglandin J2 (15d-PGJ2) induces cell death through caspase-independent mechanism in A172 human glioma cells. Neurochem Res 31:1247-54.

Chou YH, Ho FM, Liu DZ, Lin SY, Tsai LH, Chen CH, Ho YS, Hung LF, Liang YC. 2005. The possible role of heat shock factor-1 in the negative regulation of heme oxygenase-1. Int J Biochem Cell Biol 37:604-15.

Chulada PC, Thompson MB, Mahler JF, Doyle CM, Gaul BW, Lee C, Tiano HF, Morham SG, Smithies O, Langenbach R. 2000. Genetic disruption of Ptgs-1, as well as Ptgs-2, reduces intestinal tumorigenesis in Min mice. Cancer Res 60:4705-8.

Chun KS, Surh YJ. 2004. Signal transduction pathways regulating cyclooxygenase-2 expression: potential molecular targets for chemoprevention. Biochem Pharmacol 68:1089-100.

Cillero-Pastor B, Carames B, Lires-Dean M, Vaamonde-Garcia C, Blanco FJ, Lopez-Armada MJ. 2008. Mitochondrial dysfunction activates cyclooxygenase 2 expression in cultured normal human chondrocytes. Arthritis Rheum 58:2409-19.

Clay CE, Namen AM, Atsumi G, Trimboli AJ, Fonteh AN, High KP, Chilton FH. 2001. Magnitude of peroxisome proliferator-activated receptor-gamma activation is associated with important and seemingly opposite biological responses in breast cancer cells. J Investig Med 49:413-20.

Cok SJ, Acton SJ, Morrison AR. 2003. The proximal region of the 3'-untranslated region of cyclooxygenase-2 is recognized by a multimeric protein complex containing HuR, TIA-1, TIAR, and the heterogeneous nuclear ribonucleoprotein U. J Biol Chem 278:36157-62.

Colby JK, Klein RD, McArthur MJ, Conti CJ, Kiguchi K, Kawamoto T, Riggs PK, Pavone AI, Sawicki J, Fischer SM. 2008. Progressive metaplastic and dysplastic changes in mouse pancreas induced by cyclooxygenase-2 overexpression. Neoplasia 10:782-96.

Cory S, Adams JM. 2002. The Bcl2 family: regulators of the cellular life-or-death switch. Nat Rev Cancer 2:647-56.

Cullinan SB, Gordan JD, Jin J, Harper JW, Diehl JA. 2004. The Keap1-BTB protein is an adaptor that bridges Nrf2 to a Cul3-based E3 ligase: oxidative stress sensing by a Cul3-Keap1 ligase. Mol Cell Biol 24:8477-86.

Cuvillier O, Rosenthal DS, Smulson ME, Spiegel S. 1998. Sphingosine 1-phosphate inhibits activation of caspases that cleave poly(ADP-ribose) polymerase and lamins during Fas- and ceramide-mediated apoptosis in Jurkat T lymphocytes. J Biol Chem 273:2910-6.

Daugas E, Susin SA, Zamzami N, Ferri KF, Irinopoulou T, Larochette N, Prevost MC, Leber B, Andrews D, Penninger J, Kroemer G. 2000. Mitochondrio-nuclear translocation of AIF in apoptosis and necrosis. FASEB J 14:729-39.

de Moraes E, Dar NA, de Moura Gallo CV, Hainaut P. 2007. Cross-talks between cyclooxygenase-2 and tumor suppressor protein p53: Balancing life and death during inflammatory stress and carcinogenesis. Int J Cancer 121:929-37.

Desagher S, Osen-Sand A, Nichols A, Eskes R, Montessuit S, Lauper S, Maundrell K, Antonsson B, Martinou JC. 1999. Bid-induced conformational change of Bax is responsible for mitochondrial cytochrome c release during apoptosis. J Cell Biol 144:891-901.

Di Cello F, Hillion J, Kowalski J, Ronnett BM, Aderinto A, Huso DL, Resar LM. 2008. Cyclooxygenase inhibitors block uterine tumorigenesis in HMGA1a transgenic mice and human xenografts. Mol Cancer Ther 7:2090-5.

Dickens DS, Kozielski R, Khan J, Forus A, Cripe TP. 2002. Cyclooxygenase-2 expression in pediatric sarcomas. Pediatr Dev Pathol 5:356-64.

Dickens DS, Kozielski R, Leavey PJ, Timmons C, Cripe TP. 2003. Cyclooxygenase-2 expression does not correlate with outcome in osteosarcoma or rhabdomyosarcoma. J Pediatr Hematol Oncol 25:282-5.

Diers AR, Higdon AN, Ricart KC, Johnson MS, Agarwal A, Kalyanaraman B, Landar A, Darley-Usmar VM. 2009. Mitochondrial targeting of the electrophilic lipid 15-deoxy-Delta12,14-prostaglandin J2 increases apoptotic efficacy via redox cell signalling mechanisms. Biochem J 426:31-41.

Diller L, Kassel J, Nelson CE, Gryka MA, Litwak G, Gebhardt M, Bressac B, Ozturk M, Baker SJ, Vogelstein B, et al. 1990. p53 functions as a cell cycle control protein in osteosarcomas. Mol Cell Biol 10:5772-81.

Dixon DA, Balch GC, Kedersha N, Anderson P, Zimmerman GA, Beauchamp RD, Prescott SM. 2003. Regulation of cyclooxygenase-2 expression by the translational silencer TIA-1. J Exp Med 198:475-81.

Du C, Fang M, Li Y, Li L, Wang X. 2000. Smac, a mitochondrial protein that promotes cytochrome c-dependent caspase activation by eliminating IAP inhibition. Cell 102:33-42.

Eichele K, Ramer R, Hinz B. 2008. Decisive role of cyclooxygenase-2 and lipocalin-type prostaglandin D synthase in chemotherapeutics-induced apoptosis of human cervical carcinoma cells. Oncogene 27:3032-44.

Ek ET, Dass CR, Choong PF. 2006. Commonly used mouse models of osteosarcoma. Crit Rev Oncol Hematol 60:1-8.

Ellman GL. 1959. Tissue sulfhydryl groups. Arch Biochem Biophys 82:70-7.

Fang J, Sawa T, Akaike T, Akuta T, Sahoo SK, Khaled G, Hamada A, Maeda H. 2003. In vivo antitumor activity of pegylated zinc protoporphyrin: targeted inhibition of heme oxygenase in solid tumor. Cancer Res 63:3567-74.

Federico A, Morgillo F, Tuccillo C, Ciardiello F, Loguercio C. 2007. Chronic inflammation and oxidative stress in human carcinogenesis. Int J Cancer 121:2381-6.

Feng L, Xia Y, Garcia GE, Hwang D, Wilson CB. 1995. Involvement of reactive oxygen intermediates in cyclooxygenase-2 expression induced by interleukin-1, tumor necrosis factor-alpha, and lipopolysaccharide. J Clin Invest 95:1669-75.

Fernandes-Alnemri T, Armstrong RC, Krebs J, Srinivasula SM, Wang L, Bullrich F, Fritz LC, Trapani JA, Tomaselli KJ, Litwack G, Alnemri ES. 1996. In vitro activation of CPP32 and Mch3 by Mch4, a novel human apoptotic cysteine protease containing two FADD-like domains. Proc Natl Acad Sci U S A 93:7464-9.

Fitzpatrick FA, Wynalda MA. 1983. Albumin-catalyzed metabolism of prostaglandin D2. Identification of products formed in vitro. J Biol Chem 258:11713-8.

Fleury C, Petit A, Mwale F, Antoniou J, Zukor DJ, Tabrizian M, Huk OL. 2006. Effect of cobalt and chromium ions on human MG-63 osteoblasts in vitro: morphology, cytotoxicity, and oxidative stress. Biomaterials 27:3351-60.

Forman BM, Tontonoz P, Chen J, Brun RP, Spiegelman BM, Evans RM. 1995. 15-Deoxy-delta 12, 14-prostaglandin J2 is a ligand for the adipocyte determination factor PPAR gamma. Cell 83:803-12.

Forman HJ, Zhang H, Rinna A. 2009. Glutathione: overview of its protective roles, measurement, and biosynthesis. Mol Aspects Med 30:1-12.

Franco R, Cidlowski JA. 2009. Apoptosis and glutathione: beyond an antioxidant. Cell Death Differ 16:1303-14.

Frank GD, Eguchi S. 2003. Activation of tyrosine kinases by reactive oxygen species in vascular smooth muscle cells: significance and involvement of EGF receptor transactivation by angiotensin II. Antioxid Redox Signal 5:771-80.

Gallant MA, Samadfam R, Hackett JA, Antoniou J, Parent JL, de Brum-Fernandes AJ. 2005. Production of prostaglandin D(2) by human osteoblasts and modulation of osteoprotegerin, RANKL, and cellular migration by DP and CRTH2 receptors. J Bone Miner Res 20:672-81.

Gamradt SC, Feeley BT, Liu NQ, Roostaeian J, Lin YQ, Zhu LX, Sharma S, Dubinett SM, Lieberman JR. 2005. The effect of cyclooxygenase-2 (COX-2) inhibition on human prostate cancer induced osteoblastic and osteolytic lesions in bone. Anticancer Res 25:107-15.

Garavito RM, Malkowski MG, DeWitt DL. 2002. The structures of prostaglandin endoperoxide H synthases-1 and -2. Prostaglandins Other Lipid Mediat 68-69:129-52.

Garcia-Bates TM, Baglole CJ, Bernard MP, Murant TI, Simpson-Haidaris PJ, Phipps RP. 2009. Peroxisome proliferator-activated receptor gamma ligands enhance human B cell antibody production and differentiation. J Immunol 183:6903-12.

Ghosh N, Chaki R, Mandal V, Mandal SC. 2010. COX-2 as a target for cancer chemotherapy. Pharmacol Rep 62:233-44.

Gilroy DW, Colville-Nash PR, Willis D, Chivers J, Paul-Clark MJ, Willoughby DA. 1999. Inducible cyclooxygenase may have anti-inflammatory properties. Nat Med 5:698-701.

Goldsby R, Burke C, Nagarajan R, Zhou T, Chen Z, Marina N, Friedman D, Neglia J, Chuba P, Bhatia S. 2008. Second solid malignancies among children, adolescents, and young adults diagnosed with malignant bone tumors after 1976: follow-up of a Children's Oncology Group cohort. Cancer 113:2597-604.

Gong P, Stewart D, Hu B, Li N, Cook J, Nel A, Alam J. 2002. Activation of the mouse heme oxygenase-1 gene by 15-deoxy-Delta(12,14)-prostaglandin J(2) is mediated by the stress response elements and transcription factor Nrf2. Antioxid Redox Signal 4:249-57.

Gorlick R, Anderson P, Andrulis I, Arndt C, Beardsley GP, Bernstein M, Bridge J, Cheung NK, Dome JS, Ebb D, Gardner T, Gebhardt M, Grier H, Hansen M, Healey J, Helman L, Hock J, Houghton J, Houghton P, Huvos A, Khanna C, Kieran M, Kleinerman E, Ladanyi M, Lau C, Malkin D, Marina N, Meltzer P, Meyers P, Schofield D, Schwartz C, Smith MA, Toretsky J, Tsokos M, Wexler L, Wigginton J, Withrow S, Schoenfeldt M, Anderson B. 2003. Biology of childhood osteogenic sarcoma and potential targets for therapeutic development: meeting summary. Clin Cancer Res 9:5442-53.

Han H, Shin SW, Seo CY, Kwon HC, Han JY, Kim IH, Kwak JY, Park JI. 2007. 15-Deoxy-delta 12,14-prostaglandin J2 (15d-PGJ 2) sensitizes human leukemic HL-60 cells to tumor necrosis factor-related apoptosis-inducing ligand (TRAIL)-induced apoptosis through Akt downregulation. Apoptosis 12:2101-14.

Han S, Inoue H, Flowers LC, Sidell N. 2003. Control of COX-2 gene expression through peroxisome proliferator-activated receptor gamma in human cervical cancer cells. Clin Cancer Res 9:4627-35.

Harper KA, Tyson-Capper AJ. 2008. Complexity of COX-2 gene regulation. Biochem Soc Trans 36:543-5.

Harris GK, Qian Y, Leonard SS, Sbarra DC, Shi X. 2006. Luteolin and chrysin differentially inhibit cyclooxygenase-2 expression and scavenge reactive oxygen species but similarly inhibit prostaglandin-E2 formation in RAW 264.7 cells. J Nutr 136:1517-21.

Harris SG, Padilla J, Koumas L, Ray D, Phipps RP. 2002. Prostaglandins as modulators of immunity. Trends Immunol 23:144-50.

Hashimoto K, Ethridge RT, Evers BM. 2002. Peroxisome proliferator-activated receptor gamma ligand inhibits cell growth and invasion of human pancreatic cancer cells. Int J Gastrointest Cancer 32:7-22.

Hata AN, Breyer RM. 2004. Pharmacology and signaling of prostaglandin receptors: multiple roles in inflammation and immune modulation. Pharmacol Ther 103:147-66.

Haydon RC, Zhou L, Feng T, Breyer B, Cheng H, Jiang W, Ishikawa A, Peabody T, Montag A, Simon MA, He TC. 2002. Nuclear receptor agonists as potential differentiation therapy agents for human osteosarcoma. Clin Cancer Res 8:1288-94.

Hengartner MO. 2000. The biochemistry of apoptosis. Nature 407:770-6.

Ho TC, Chen SL, Yang YC, Chen CY, Feng FP, Hsieh JW, Cheng HC, Tsao YP. 2008. 15-deoxy-Delta(12,14)-prostaglandin J2 induces vascular endothelial cell apoptosis through the sequential activation of MAPKS and p53. J Biol Chem 283:30273-88.

Holmgren A. 1995. Thioredoxin structure and mechanism: conformational changes on oxidation of the active-site sulfhydryls to a disulfide. Structure 3:239-43.

Hong HY, Jeon WK, Kim BC. 2008. Up-regulation of heme oxygenase-1 expression through the Rac1/NADPH oxidase/ROS/p38 signaling cascade mediates the anti-inflammatory effect of 15-deoxy-delta 12,14-prostaglandin J2 in murine macrophages. FEBS Lett 582:861-8.

Hong SL, Levine L. 1976. Stimulation of prostaglandin synthesis by bradykinin and thrombin and their mechanisms of action on MC5-5 fibroblasts. J Biol Chem 251:5814-6.

Hosoya T, Maruyama A, Kang MI, Kawatani Y, Shibata T, Uchida K, Warabi E, Noguchi N, Itoh K, Yamamoto M. 2005. Differential responses of the Nrf2-Keap1 system to laminar and oscillatory shear stresses in endothelial cells. J Biol Chem 280:27244-50.

Howe LR, Chang SH, Tolle KC, Dillon R, Young LJ, Cardiff RD, Newman RA, Yang P, Thaler HT, Muller WJ, Hudis C, Brown AM, Hla T, Subbaramaiah K, Dannenberg AJ. 2005. HER2/neu-induced mammary tumorigenesis and angiogenesis are reduced in cyclooxygenase-2 knockout mice. Cancer Res 65:10113-9.

Hsu H, Shu HB, Pan MG, Goeddel DV. 1996. TRADD-TRAF2 and TRADD-FADD interactions define two distinct TNF receptor 1 signal transduction pathways. Cell 84:299-308.

Huang H, Chikazu D, Voznesensky OS, Herschman HR, Kream BE, Drissi H, Pilbeam CC. 2010. Parathyroid hormone induction of cyclooxygenase-2 in murine osteoblasts: role of the calcium-calcineurin-NFAT pathway. J Bone Miner Res 25:819-29.

Huang WC, Chio CC, Chi KH, Wu HM, Lin WW. 2002. Superoxide anion-dependent Raf/MEK/ERK activation by peroxisome proliferator activated receptor gamma agonists 15-deoxy-delta(12,14)-prostaglandin J(2), ciglitazone, and GW1929. Exp Cell Res 277:192-200.

Ianaro A, Ialenti A, Maffia P, Di Meglio P, Di Rosa M, Santoro MG. 2003. Anti-inflammatory activity of 15-deoxy-delta12,14-PGJ2 and 2-cyclopenten-1-one: role of the heat shock response. Mol Pharmacol 64:85-93.

Ichiki T, Tokunou T, Fukuyama K, Iino N, Masuda S, Takeshita A. 2004. 15-Deoxy-Delta12,14-prostaglandin J2 and thiazolidinediones transactivate epidermal growth factor and platelet-derived growth factor receptors in vascular smooth muscle cells. Biochem Biophys Res Commun 323:402-8.

Inoue H, Tanabe T. 1998. Transcriptional role of the nuclear factor kappa B site in the induction by lipopolysaccharide and suppression by dexamethasone of cyclooxygenase-2 in U937 cells. Biochem Biophys Res Commun 244:143-8.

Inoue H, Tanabe T, Umesono K. 2000. Feedback control of cyclooxygenase-2 expression through PPARgamma. J Biol Chem 275:28028-32.

Iochmann S, Reverdiau-Moalic P, Beaujean S, Rideau E, Lebranchu Y, Bardos P, Gruel Y. 1999. Fast detection of tissue factor and tissue factor pathway inhibitor messenger RNA in endothelial cells and monocytes by sensitive reverse transcription-polymerase chain reaction. Thromb Res 94:165-73.

Irmler M, Thome M, Hahne M, Schneider P, Hofmann K, Steiner V, Bodmer JL, Schroter M, Burns K, Mattmann C, Rimoldi D, French LE, Tschopp J. 1997. Inhibition of death receptor signals by cellular FLIP. Nature 388:190-5.

Itoh K, Chiba T, Takahashi S, Ishii T, Igarashi K, Katoh Y, Oyake T, Hayashi N, Satoh K, Hatayama I, Yamamoto M, Nabeshima Y. 1997. An Nrf2/small Maf heterodimer mediates the induction of phase II detoxifying enzyme genes through antioxidant response elements. Biochem Biophys Res Commun 236:313-22.

Itoh K, Mochizuki M, Ishii Y, Ishii T, Shibata T, Kawamoto Y, Kelly V, Sekizawa K, Uchida K, Yamamoto M. 2004. Transcription factor Nrf2 regulates inflammation by mediating the effect of 15-deoxy-Delta(12,14)-prostaglandin j(2). Mol Cell Biol 24:36-45.

Itoh K, Wakabayashi N, Katoh Y, Ishii T, Igarashi K, Engel JD, Yamamoto M. 1999. Keap1 represses nuclear activation of antioxidant responsive elements by Nrf2 through binding to the amino-terminal Neh2 domain. Genes Dev 13:76-86.

Jackson SM, Parhami F, Xi XP, Berliner JA, Hsueh WA, Law RE, Demer LL. 1999. Peroxisome proliferator-activated receptor activators target human endothelial cells to inhibit leukocyte-endothelial cell interaction. Arterioscler Thromb Vasc Biol 19:2094-104.

Jiang YJ, Xu TR, Lu B, Mymin D, Kroeger EA, Dembinski T, Yang X, Hatch GM, Choy PC. 2003. Cyclooxygenase expression is elevated in retinoic acid-differentiated U937 cells. Biochim Biophys Acta 1633:51-60.

Jozkowicz A, Was H, Taha H, Kotlinowski J, Mleczko K, Cisowski J, Weigel G, Dulak J. 2008. 15d-PGJ2 upregulates synthesis of IL-8 in endothelial cells through induction of oxidative stress. Antioxid Redox Signal 10:2035-46.

Jung JY, Yoo CI, Kim HT, Kwon CH, Park JY, Kim YK. 2007. Role of mitogen-activated protein kinase (MAPK) in troglitazone-induced osteoblastic cell death. Toxicology 234:73-82.

Kanekura T, Higashi Y, Kanzaki T. 2000. Inhibitory effects of 9-cis-retinoic acid and pyrrolidinedithiocarbamate on cyclooxygenase (COX)-2 expression and cell growth in human skin squamous carcinoma cells. Cancer Lett 161:177-83.

Kang DS, Kwon CH, Park JY, Kim JH, Woo JS, Jung JS, Kim YK. 2006. 15-deoxy-Delta12,14-prostaglandin J2 induces renal epithelial cell death through NF-kappaB-dependent and MAPK-independent mechanism. Toxicol Appl Pharmacol 216:426-35.

Kansanen E, Kivela AM, Levonen AL. 2009. Regulation of Nrf2-dependent gene expression by 15-deoxy-Delta12,14-prostaglandin J2. Free Radic Biol Med 47:1310-7.

Kansara M, Thomas DM. 2007. Molecular pathogenesis of osteosarcoma. DNA Cell Biol 26:1-18.

Kawamoto Y, Nakamura Y, Naito Y, Torii Y, Kumagai T, Osawa T, Ohigashi H, Satoh K, Imagawa M, Uchida K. 2000. Cyclopentenone prostaglandins as potential inducers of phase

II detoxification enzymes. 15-deoxy-delta(12,14)-prostaglandin j2-induced expression of glutathione S-transferases. J Biol Chem 275:11291-9.

Keelan J, Helliwell R, Nijmeijer B, Berry E, Sato T, Marvin K, Mitchell M, Gilmour R. 2001. 15-deoxy-delta12,14-prostaglandin J2-induced apoptosis in amnion-like WISH cells. Prostaglandins Other Lipid Mediat 66:265-82.

Khachigian LM. 2006. Early growth response-1 in cardiovascular pathobiology. Circ Res 98:186-91.

Kim DH, Kim EH, Na HK, Sun Y, Surh YJ. 2010. 15-Deoxy-Delta(12,14)-prostaglandin J(2) stabilizes, but functionally inactivates p53 by binding to the cysteine 277 residue. Oncogene 29:2560-76.

Kim DH, Kim JH, Kim EH, Na HK, Cha YN, Chung JH, Surh YJ. 2009. 15-Deoxy-Delta12,14-prostaglandin J2 upregulates the expression of heme oxygenase-1 and subsequently matrix metalloproteinase-1 in human breast cancer cells: possible roles of iron and ROS. Carcinogenesis 30:645-54.

Kim EH, Na HK, Kim DH, Park SA, Kim HN, Song NY, Surh YJ. 2008a. 15-Deoxy-Delta12,14-prostaglandin J2 induces COX-2 expression through Akt-driven AP-1 activation in human breast cancer cells: a potential role of ROS. Carcinogenesis 29:688-95.

Kim EH, Na HK, Surh YJ. 2006a. Upregulation of VEGF by 15-deoxy-Delta12,14-prostaglandin J2 via heme oxygenase-1 and ERK1/2 signaling in MCF-7 cells. Ann N Y Acad Sci 1090:375-84.

Kim EH, Surh YJ. 2006. 15-deoxy-Delta12,14-prostaglandin J2 as a potential endogenous regulator of redox-sensitive transcription factors. Biochem Pharmacol 72:1516-28.

Kim EH, Surh YJ. 2008. The role of 15-deoxy-delta(12,14)-prostaglandin J(2), an endogenous ligand of peroxisome proliferator-activated receptor gamma, in tumor angiogenesis. Biochem Pharmacol 76:1544-53.

Kim EJ, Park KS, Chung SY, Sheen YY, Moon DC, Song YS, Kim KS, Song S, Yun YP, Lee MK, Oh KW, Yoon DY, Hong JT. 2003. Peroxisome proliferator-activated receptor-gamma activator 15-deoxy-Delta12,14-prostaglandin J2 inhibits neuroblastoma cell growth through induction of apoptosis: association with extracellular signal-regulated kinase signal pathway. J Pharmacol Exp Ther 307:505-17.

Kim JW, Li MH, Jang JH, Na HK, Song NY, Lee C, Johnson JA, Surh YJ. 2008b. 15-Deoxy-Delta(12,14)-prostaglandin J(2) rescues PC12 cells from H2O2-induced apoptosis through Nrf2-mediated upregulation of heme oxygenase-1: potential roles of Akt and ERK1/2. Biochem Pharmacol 76:1577-89.

Kim SH, Yoo CI, Kim HT, Park JY, Kwon CH, Kim YK. 2006b. Activation of peroxisome proliferator-activated receptor-gamma (PPARgamma) induces cell death through MAPK-dependent mechanism in osteoblastic cells. Toxicol Appl Pharmacol 215:198-207.

Kliewer SA, Lenhard JM, Willson TM, Patel I, Morris DC, Lehmann JM. 1995. A prostaglandin J2 metabolite binds peroxisome proliferator-activated receptor gamma and promotes adipocyte differentiation. Cell 83:813-9.

Kobayashi A, Kang MI, Okawa H, Ohtsuji M, Zenke Y, Chiba T, Igarashi K, Yamamoto M. 2004. Oxidative stress sensor Keap1 functions as an adaptor for Cul3-based E3 ligase to regulate proteasomal degradation of Nrf2. Mol Cell Biol 24:7130-9.

Kobayashi M, Li L, Iwamoto N, Nakajima-Takagi Y, Kaneko H, Nakayama Y, Eguchi M, Wada Y, Kumagai Y, Yamamoto M. 2009. The antioxidant defense system Keap1-Nrf2 comprises a multiple sensing mechanism for responding to a wide range of chemical compounds. Mol Cell Biol 29:493-502.

Kobayashi M, Ono H, Mihara K, Tauchi H, Komatsu K, Shibata T, Shimizu H, Uchida K, Yamamoto K. 2006. ATM activation by a sulfhydryl-reactive inflammatory cyclopentenone prostaglandin. Genes Cells 11:779-89.

Kondo M, Oya-Ito T, Kumagai T, Osawa T, Uchida K. 2001. Cyclopentenone prostaglandins as potential inducers of intracellular oxidative stress. J Biol Chem 276:12076-83.

Kondo M, Shibata T, Kumagai T, Osawa T, Shibata N, Kobayashi M, Sasaki S, Iwata M, Noguchi N, Uchida K. 2002. 15-Deoxy-Delta(12,14)-prostaglandin J(2): the endogenous electrophile that induces neuronal apoptosis. Proc Natl Acad Sci U S A 99:7367-72.

Korsmeyer SJ, Wei MC, Saito M, Weiler S, Oh KJ, Schlesinger PH. 2000. Pro-apoptotic cascade activates BID, which oligomerizes BAK or BAX into pores that result in the release of cytochrome c. Cell Death Differ 7:1166-73.

Koshkina NV, Khanna C, Mendoza A, Guan H, DeLauter L, Kleinerman ES. 2007. Fas-negative osteosarcoma tumor cells are selected during metastasis to the lungs: the role of the Fas pathway in the metastatic process of osteosarcoma. Mol Cancer Res 5:991-9.

Kronke G, Kadl A, Ikonomu E, Bluml S, Furnkranz A, Sarembock IJ, Bochkov VN, Exner M, Binder BR, Leitinger N. 2007. Expression of heme oxygenase-1 in human vascular cells is regulated by peroxisome proliferator-activated receptors. Arterioscler Thromb Vasc Biol 27:1276-82.

Ladanyi M, Cha C, Lewis R, Jhanwar SC, Huvos AG, Healey JH. 1993. MDM2 gene amplification in metastatic osteosarcoma. Cancer Res 53:16-8.

Lamoureux F, Trichet V, Chipoy C, Blanchard F, Gouin F, Redini F. 2007. Recent advances in the management of osteosarcoma and forthcoming therapeutic strategies. Expert Rev Anticancer Ther 7:169-81.

Landar A, Zmijewski JW, Dickinson DA, Le Goffe C, Johnson MS, Milne GL, Zanoni G, Vidari G, Morrow JD, Darley-Usmar VM. 2006. Interaction of electrophilic lipid oxidation products with mitochondria in endothelial cells and formation of reactive oxygen species. Am J Physiol Heart Circ Physiol 290:H1777-87.

Langer C, Hirsh V. 2010. Skeletal morbidity in lung cancer patients with bone metastases: demonstrating the need for early diagnosis and treatment with bisphosphonates. Lung Cancer 67:4-11.

Laulederkind SJ, Kirtikara K, Raghow R, Ballou LR. 2000. The regulation of PGE(2) biosynthesis in MG-63 osteosarcoma cells by IL-1 and FGF is cell density-dependent. Exp Cell Res 258:409-16.

Leach FS, Tokino T, Meltzer P, Burrell M, Oliner JD, Smith S, Hill DE, Sidransky D, Kinzler KW, Vogelstein B. 1993. p53 Mutation and MDM2 amplification in human soft tissue sarcomas. Cancer Res 53:2231-4.

Lee EJ, Choi EM, Kim SR, Park JH, Kim H, Ha KS, Kim YM, Kim SS, Choe M, Kim JI, Han JA. 2007. Cyclooxygenase-2 promotes cell proliferation, migration and invasion in U2OS human osteosarcoma cells. Exp Mol Med 39:469-76.

Lee SJ, Kim MS, Park JY, Woo JS, Kim YK. 2008. 15-Deoxy-delta 12,14-prostaglandin J2 induces apoptosis via JNK-mediated mitochondrial pathway in osteoblastic cells. Toxicology 248:121-9.

Lee TS, Tsai HL, Chau LY. 2003. Induction of heme oxygenase-1 expression in murine macrophages is essential for the anti-inflammatory effect of low dose 15-deoxy-Delta 12,14-prostaglandin J2. J Biol Chem 278:19325-30.

Leis HJ, Hohenester E, Gleispach H, Malle E, Mayer B. 1987. Measurement of prostaglandins, thromboxanes and hydroxy fatty acids by stable isotope dilution gas chromatography/mass spectrometry. Biomed Environ Mass Spectrom 14:617-21.

Leis HJ, Hulla W, Gruber R, Huber E, Zach D, Gleispach H, Windischhofer W. 1997. Phenotypic heterogeneity of osteoblast-like MC3T3-E1 cells: changes of bradykinin-induced prostaglandin E2 production during osteoblast maturation. J Bone Miner Res 12:541-51.

Leis HJ, Zach D, Huber E, Windischhofer W. 1998. Prostaglandin endoperoxide synthase-2 contributes to the endothelin/sarafotoxin-induced prostaglandin E2 synthesis in mouse osteoblastic cells (MC3T3-E1): evidence for a protein tyrosine kinase-signaling pathway and involvement of protein kinase C. Endocrinology 139:1268-77.

Lennon AM, Ramauge M, Dessouroux A, Pierre M. 2002. MAP kinase cascades are activated in astrocytes and preadipocytes by 15-deoxy-Delta(12-14)-prostaglandin J(2) and the thiazolidinedione ciglitazone through peroxisome proliferator activator receptor gamma-independent mechanisms involving reactive oxygenated species. J Biol Chem 277:29681-5.

Levonen AL, Dickinson DA, Moellering DR, Mulcahy RT, Forman HJ, Darley-Usmar VM. 2001. Biphasic effects of 15-deoxy-delta(12,14)-prostaglandin J(2) on glutathione induction and apoptosis in human endothelial cells. Arterioscler Thromb Vasc Biol 21:1846-51.

Levonen AL, Landar A, Ramachandran A, Ceaser EK, Dickinson DA, Zanoni G, Morrow JD, Darley-Usmar VM. 2004. Cellular mechanisms of redox cell signalling: role of cysteine modification in controlling antioxidant defences in response to electrophilic lipid oxidation products. Biochem J 378:373-82.

Li L, Julien B, Grenard P, Teixeira-Clerc F, Mallat A, Lotersztajn S. 2004. Molecular mechanisms regulating the antifibrogenic protein heme-oxygenase-1 in human hepatic myofibroblasts. J Hepatol 41:407-13.

Li L, Tao J, Davaille J, Feral C, Mallat A, Rieusset J, Vidal H, Lotersztajn S. 2001a. 15-deoxy-Delta 12,14-prostaglandin J2 induces apoptosis of human hepatic myofibroblasts. A pathway involving oxidative stress independently of peroxisome-proliferator-activated receptors. J Biol Chem 276:38152-8.

Li LY, Luo X, Wang X. 2001b. Endonuclease G is an apoptotic DNase when released from mitochondria. Nature 412:95-9.

Li P, Nijhawan D, Budihardjo I, Srinivasula SM, Ahmad M, Alnemri ES, Wang X. 1997. Cytochrome c and dATP-dependent formation of Apaf-1/caspase-9 complex initiates an apoptotic protease cascade. Cell 91:479-89.

Liao Z, Mason KA, Milas L. 2007. Cyclo-oxygenase-2 and its inhibition in cancer: is there a role? Drugs 67:821-45.

Lim HJ, Lee KS, Lee S, Park JH, Choi HE, Go SH, Kwak HJ, Park HY. 2007. 15d-PGJ2 stimulates HO-1 expression through p38 MAP kinase and Nrf-2 pathway in rat vascular smooth muscle cells. Toxicol Appl Pharmacol 223:20-7.

Lin TH, Tang CH, Hung SY, Liu SH, Lin YM, Fu WM, Yang RS. 2010. Upregulation of heme oxygenase-1 inhibits the maturation and mineralization of osteoblasts. J Cell Physiol 222:757-68.

Lin TN, Cheung WM, Wu JS, Chen JJ, Lin H, Liou JY, Shyue SK, Wu KK. 2006. 15d-prostaglandin J2 protects brain from ischemia-reperfusion injury. Arterioscler Thromb Vasc Biol 26:481-7.

Liu B, Shi ZL, Feng J, Tao HM. 2008. Celecoxib, a cyclooxygenase-2 inhibitor, induces apoptosis in human osteosarcoma cell line MG-63 via down-regulation of PI3K/Akt. Cell Biol Int 32:494-501.

Liu CH, Chang SH, Narko K, Trifan OC, Wu MT, Smith E, Haudenschild C, Lane TF, Hla T. 2001. Overexpression of cyclooxygenase-2 is sufficient to induce tumorigenesis in transgenic mice. J Biol Chem 276:18563-9.

Liu JD, Tsai SH, Lin SY, Ho YS, Hung LF, Pan S, Ho FM, Lin CM, Liang YC. 2004. Thiol antioxidant and thiol-reducing agents attenuate 15-deoxy-delta 12,14-prostaglandin J2-induced heme oxygenase-1 expression. Life Sci 74:2451-63.

Liu JJ, Liu PQ, Lin DJ, Xiao RZ, Huang M, Li XD, He Y, Huang RW. 2007. Downregulation of cyclooxygenase-2 expression and activation of caspase-3 are involved in peroxisome proliferator-activated receptor-gamma agonists induced apoptosis in human monocyte leukemia cells in vitro. Ann Hematol 86:173-83.

Livak KJ, Schmittgen TD. 2001. Analysis of relative gene expression data using real-time quantitative PCR and the 2(-Delta Delta C(T)) Method. Methods 25:402-8.

Lu Y, Wahl LM. 2005. Oxidative stress augments the production of matrix metalloproteinase-1, cyclooxygenase-2, and prostaglandin E2 through enhancement of NF-kappa B activity in lipopolysaccharide-activated human primary monocytes. J Immunol 175:5423-9.

Lucarelli E, Sangiorgi L, Maini V, Lattanzi G, Marmiroli S, Reggiani M, Mordenti M, Alessandra Gobbi G, Scrimieri F, Zambon Bertoja A, Picci P. 2002. Troglitazione affects survival of human osteosarcoma cells. Int J Cancer 98:344-51.

Luo X, Budihardjo I, Zou H, Slaughter C, Wang X. 1998. Bid, a Bcl2 interacting protein, mediates cytochrome c release from mitochondria in response to activation of cell surface death receptors. Cell 94:481-90.

Ma K, Vattem KM, Wek RC. 2002. Dimerization and release of molecular chaperone inhibition facilitate activation of eukaryotic initiation factor-2 kinase in response to endoplasmic reticulum stress. J Biol Chem 277:18728-35.

Mallat Z, Tedgui A. 2000. Apoptosis in the vasculature: mechanisms and functional importance. Br J Pharmacol 130:947-62.

Malle E, Gleispach H, Kostner GM, Leis HJ. 1989. Isotope dilution gas chromatography-mass spectrometry for the study of eicosanoid metabolism in human blood platelets. J Chromatogr 488:283-93.

Martinez B, Perez-Castillo A, Santos A. 2005. The mitochondrial respiratory complex I is a target for 15-deoxy-delta12,14-prostaglandin J2 action. J Lipid Res 46:736-43.

Masi L, Recenti R, Silvestri S, Pinzani P, Pepi M, Paglierani M, Brandi ML, Franchi A. 2007. Expression of cyclooxygenase-2 in osteosarcoma of bone. Appl Immunohistochem Mol Morphol 15:70-6.

McIntyre TM, Pontsler AV, Silva AR, St Hilaire A, Xu Y, Hinshaw JC, Zimmerman GA, Hama K, Aoki J, Arai H, Prestwich GD. 2003. Identification of an intracellular receptor for lysophosphatidic acid (LPA): LPA is a transcellular PPARgamma agonist. Proc Natl Acad Sci U S A 100:131-6.

Meade EA, McIntyre TM, Zimmerman GA, Prescott SM. 1999. Peroxisome proliferators enhance cyclooxygenase-2 expression in epithelial cells. J Biol Chem 274:8328-34.

Mestre JR, Subbaramaiah K, Sacks PG, Schantz SP, Tanabe T, Inoue H, Dannenberg AJ. 1997a. Retinoids suppress epidermal growth factor-induced transcription of cyclooxygenase-2 in human oral squamous carcinoma cells. Cancer Res 57:2890-5.

Mestre JR, Subbaramaiah K, Sacks PG, Schantz SP, Tanabe T, Inoue H, Dannenberg AJ. 1997b. Retinoids suppress phorbol ester-mediated induction of cyclooxygenase-2. Cancer Res 57:1081-5.

Mochizuki M, Ishii Y, Itoh K, Iizuka T, Morishima Y, Kimura T, Kiwamoto T, Matsuno Y, Hegab AE, Nomura A, Sakamoto T, Uchida K, Yamamoto M, Sekizawa K. 2005. Role of 15-deoxy delta(12,14) prostaglandin J2 and Nrf2 pathways in protection against acute lung injury. Am J Respir Crit Care Med 171:1260-6.

Monick MM, Robeff PK, Butler NS, Flaherty DM, Carter AB, Peterson MW, Hunninghake GW. 2002. Phosphatidylinositol 3-kinase activity negatively regulates stability of cyclooxygenase 2 mRNA. J Biol Chem 277:32992-3000.

Monneret G, Li H, Vasilescu J, Rokach J, Powell WS. 2002. 15-Deoxy-delta 12,14-prostaglandins D2 and J2 are potent activators of human eosinophils. J Immunol 168:3563-9.

Moos PJ, Edes K, Cassidy P, Massuda E, Fitzpatrick FA. 2003. Electrophilic prostaglandins and lipid aldehydes repress redox-sensitive transcription factors p53 and hypoxia-inducible factor by impairing the selenoprotein thioredoxin reductase. J Biol Chem 278:745-50.

Morishima N, Nakanishi K, Takenouchi H, Shibata T, Yasuhiko Y. 2002. An endoplasmic reticulum stress-specific caspase cascade in apoptosis. Cytochrome c-independent activation of caspase-9 by caspase-12. J Biol Chem 277:34287-94.

Morita I. 2002. Distinct functions of COX-1 and COX-2. Prostaglandins Other Lipid Mediat 68-69:165-75.

Movassagh M, Foo RS. 2008. Simplified apoptotic cascades. Heart Fail Rev 13:111-9.

Mueller F, Fuchs B, Kaser-Hotz B. 2007. Comparative biology of human and canine osteosarcoma. Anticancer Res 27:155-64.

Muller-Decker K, Neufang G, Berger I, Neumann M, Marks F, Furstenberger G. 2002. Transgenic cyclooxygenase-2 overexpression sensitizes mouse skin for carcinogenesis. Proc Natl Acad Sci U S A 99:12483-8.

Mutoh M, Watanabe K, Kitamura T, Shoji Y, Takahashi M, Kawamori T, Tani K, Kobayashi M, Maruyama T, Kobayashi K, Ohuchida S, Sugimoto Y, Narumiya S, Sugimura T, Wakabayashi K. 2002. Involvement of prostaglandin E receptor subtype EP(4) in colon carcinogenesis. Cancer Res 62:28-32.

Muzio M, Chinnaiyan AM, Kischkel FC, O'Rourke K, Shevchenko A, Ni J, Scaffidi C, Bretz JD, Zhang M, Gentz R, Mann M, Krammer PH, Peter ME, Dixit VM. 1996. FLICE, a novel FADD-homologous ICE/CED-3-like protease, is recruited to the CD95 (Fas/APO-1) death--inducing signaling complex. Cell 85:817-27.

Na HK, Surh YJ. 2003. Peroxisome proliferator-activated receptor gamma (PPARgamma) ligands as bifunctional regulators of cell proliferation. Biochem Pharmacol 66:1381-91.

Nakagawa T, Zhu H, Morishima N, Li E, Xu J, Yankner BA, Yuan J. 2000. Caspase-12 mediates endoplasmic-reticulum-specific apoptosis and cytotoxicity by amyloid-beta. Nature 403:98-103.

Nakano K, Vousden KH. 2001. PUMA, a novel proapoptotic gene, is induced by p53. Mol Cell 7:683-94.

Nakata S, Yoshida T, Shiraishi T, Horinaka M, Kouhara J, Wakada M, Sakai T. 2006. 15-Deoxy-Delta12,14-prostaglandin J(2) induces death receptor 5 expression through mRNA stabilization independently of PPARgamma and potentiates TRAIL-induced apoptosis. Mol Cancer Ther 5:1827-35.

Narita M, Shimizu S, Ito T, Chittenden T, Lutz RJ, Matsuda H, Tsujimoto Y. 1998. Bax interacts with the permeability transition pore to induce permeability transition and cytochrome c release in isolated mitochondria. Proc Natl Acad Sci U S A 95:14681-6.

Narko K, Zweifel B, Trifan O, Ristimaki A, Lane TF, Hla T. 2005. COX-2 inhibitors and genetic background reduce mammary tumorigenesis in cyclooxygenase-2 transgenic mice. Prostaglandins Other Lipid Mediat 76:86-94.

Naruse T, Nishida Y, Hosono K, Ishiguro N. 2006. Meloxicam inhibits osteosarcoma growth, invasiveness and metastasis by COX-2-dependent and independent routes. Carcinogenesis 27:584-92.

Nencioni A, Lauber K, Grunebach F, Van Parijs L, Denzlinger C, Wesselborg S, Brossart P. 2003. Cyclopentenone prostaglandins induce lymphocyte apoptosis by activating the mitochondrial apoptosis pathway independent of external death receptor signaling. J Immunol 171:5148-56.

Newton R, Kuitert LM, Bergmann M, Adcock IM, Barnes PJ. 1997. Evidence for involvement of NF-kappaB in the transcriptional control of COX-2 gene expression by IL-1beta. Biochem Biophys Res Commun 237:28-32.

Nishitoh H, Matsuzawa A, Tobiume K, Saegusa K, Takeda K, Inoue K, Hori S, Kakizuka A, Ichijo H. 2002. ASK1 is essential for endoplasmic reticulum stress-induced neuronal cell death triggered by expanded polyglutamine repeats. Genes Dev 16:1345-55.

O'Brien JJ, Baglole CJ, Garcia-Bates TM, Blumberg N, Francis CW, Phipps RP. 2009. 15-deoxy-Delta12,14 prostaglandin J2-induced heme oxygenase-1 in megakaryocytes regulates thrombopoiesis. J Thromb Haemost 7:182-9.

Oakes SA, Scorrano L, Opferman JT, Bassik MC, Nishino M, Pozzan T, Korsmeyer SJ. 2005. Proapoptotic BAX and BAK regulate the type 1 inositol trisphosphate receptor and calcium leak from the endoplasmic reticulum. Proc Natl Acad Sci U S A 102:105-10.

Obrig TG, Culp WJ, McKeehan WL, Hardesty B. 1971. The mechanism by which cycloheximide and related glutarimide antibiotics inhibit peptide synthesis on reticulocyte ribosomes. J Biol Chem 246:174-81.

Oda E, Ohki R, Murasawa H, Nemoto J, Shibue T, Yamashita T, Tokino T, Taniguchi T, Tanaka N. 2000. Noxa, a BH3-only member of the Bcl-2 family and candidate mediator of p53-induced apoptosis. Science 288:1053-8.

Oh JY, Giles N, Landar A, Darley-Usmar V. 2008. Accumulation of 15-deoxy-delta(12,14)-prostaglandin J2 adduct formation with Keap1 over time: effects on potency for intracellular antioxidant defence induction. Biochem J 411:297-306.

Ohshiba T, Miyaura C, Ito A. 2003. Role of prostaglandin E produced by osteoblasts in osteolysis due to bone metastasis. Biochem Biophys Res Commun 300:957-64.

Okada M, Yan SF, Pinsky DJ. 2002. Peroxisome proliferator-activated receptor-gamma (PPAR-gamma) activation suppresses ischemic induction of Egr-1 and its inflammatory gene targets. FASEB J 16:1861-8.

Okano H, Shiraki K, Inoue H, Yamanaka Y, Kawakita T, Saitou Y, Yamaguchi Y, Enokimura N, Yamamoto N, Sugimoto K, Murata K, Nakano T. 2003. 15-deoxy-delta-12-14-PGJ2 regulates apoptosis induction and nuclear factor-kappaB activation via a peroxisome proliferator-activated receptor-gamma-independent mechanism in hepatocellular carcinoma. Lab Invest 83:1529-39.

Oliva JL, Perez-Sala D, Castrillo A, Martinez N, Canada FJ, Bosca L, Rojas JM. 2003. The cyclopentenone 15-deoxy-delta 12,14-prostaglandin J2 binds to and activates H-Ras. Proc Natl Acad Sci U S A 100:4772-7.

Oshima M, Murai N, Kargman S, Arguello M, Luk P, Kwong E, Taketo MM, Evans JF. 2001. Chemoprevention of intestinal polyposis in the Apcdelta716 mouse by rofecoxib, a specific cyclooxygenase-2 inhibitor. Cancer Res 61:1733-40.

Pan Y, Haines DS. 1999. The pathway regulating MDM2 protein degradation can be altered in human leukemic cells. Cancer Res 59:2064-7.

Park JM, Kanaoka Y, Eguchi N, Aritake K, Grujic S, Materi AM, Buslon VS, Tippin BL, Kwong AM, Salido E, French SW, Urade Y, Lin HJ. 2007. Hematopoietic prostaglandin D synthase suppresses intestinal adenomas in ApcMin/+ mice. Cancer Res 67:881-9.

Paumi CM, Smitherman PK, Townsend AJ, Morrow CS. 2004. Glutathione S-transferases (GSTs) inhibit transcriptional activation by the peroxisomal proliferator-activated receptor gamma (PPAR gamma) ligand, 15-deoxy-delta 12,14prostaglandin J2 (15-d-PGJ2). Biochemistry 43:2345-52.

Paumi CM, Wright M, Townsend AJ, Morrow CS. 2003. Multidrug resistance protein (MRP) 1 and MRP3 attenuate cytotoxic and transactivating effects of the cyclopentenone prostaglandin, 15-deoxy-Delta(12,14)prostaglandin J2 in MCF7 breast cancer cells. Biochemistry 42:5429-37.

Perez-Sala D, Cernuda-Morollon E, Canada FJ. 2003. Molecular basis for the direct inhibition of AP-1 DNA binding by 15-deoxy-Delta 12,14-prostaglandin J2. J Biol Chem 278:51251-60.

Person EC, Waite LL, Taylor RN, Scanlan TS. 2001. Albumin regulates induction of peroxisome proliferator-activated receptor-gamma (PPARgamma) by 15-deoxy-delta(12-14)-prostaglandin J(2) in vitro and may be an important regulator of PPARgamma function in vivo. Endocrinology 142:551-6.

Piecyk M, Wax S, Beck AR, Kedersha N, Gupta M, Maritim B, Chen S, Gueydan C, Kruys V, Streuli M, Anderson P. 2000. TIA-1 is a translational silencer that selectively regulates the expression of TNF-alpha. EMBO J 19:4154-63.

Pignatelli M, Sanchez-Rodriguez J, Santos A, Perez-Castillo A. 2005. 15-deoxy-Delta-12,14-prostaglandin J2 induces programmed cell death of breast cancer cells by a pleiotropic mechanism. Carcinogenesis 26:81-92.

Pilbeam CC, Raisz LG, Voznesensky O, Alander CB, Delman BN, Kawaguchi H. 1995. Autoregulation of inducible prostaglandin G/H synthase in osteoblastic cells by prostaglandins. J Bone Miner Res 10:406-14.

Pontsler AV, St Hilaire A, Marathe GK, Zimmerman GA, McIntyre TM. 2002. Cyclooxygenase-2 is induced in monocytes by peroxisome proliferator activated receptor gamma and oxidized alkyl phospholipids from oxidized low density lipoprotein. J Biol Chem 277:13029-36.

Pradelli LA, Beneteau M, Ricci JE. 2010. Mitochondrial control of caspase-dependent and -independent cell death. Cell Mol Life Sci 67:1589-97.

Ptasinska A, Wang S, Zhang J, Wesley RA, Danner RL. 2007. Nitric oxide activation of peroxisome proliferator-activated receptor gamma through a p38 MAPK signaling pathway. FASEB J 21:950-61.

Qiao L, Dai Y, Gu Q, Chan KW, Ma J, Lan HY, Zou B, Rocken C, Ebert MP, Wong BC. 2008. Loss of XIAP sensitizes colon cancer cells to PPARgamma independent antitumor effects of troglitazone and 15-PGJ2. Cancer Lett 268:260-71.

Qin S, McLaughlin AP, De Vries GW. 2006. Protection of RPE cells from oxidative injury by 15-deoxy-delta12,14-prostaglandin J2 by augmenting GSH and activating MAPK. Invest Ophthalmol Vis Sci 47:5098-105.

Ragazzini P, Gamberi G, Benassi MS, Orlando C, Sestini R, Ferrari C, Molendini L, Sollazzo MR, Merli M, Magagnoli G, Bertoni F, Bohling T, Pazzagli M, Picci P. 1999. Analysis of SAS gene and CDK4 and MDM2 proteins in low-grade osteosarcoma. Cancer Detect Prev 23:129-36.

Rajakariar R, Hilliard M, Lawrence T, Trivedi S, Colville-Nash P, Bellingan G, Fitzgerald D, Yaqoob MM, Gilroy DW. 2007. Hematopoietic prostaglandin D2 synthase controls the onset and resolution of acute inflammation through PGD2 and 15-deoxyDelta12 14 PGJ2. Proc Natl Acad Sci U S A 104:20979-84.

Reyes-Martin P, Ramirez-Rubio S, Parra-Cid T, Bienes-Martinez R, Lucio-Cazana J. 2008. 15-Deoxy-delta12,14-prostaglandin-J(2) up-regulates cyclooxygenase-2 but inhibits prostaglandin-E(2) production through a thiol antioxidant-sensitive mechanism. Pharmacol Res 57:344-50.

Ricart KC, Bolisetty S, Johnson MS, Perez J, Agarwal A, Murphy MP, Landar A. 2009. The permissive role of mitochondria in the induction of haem oxygenase-1 in endothelial cells. Biochem J 419:427-36.

Riedl SJ, Salvesen GS. 2007. The apoptosome: signalling platform of cell death. Nat Rev Mol Cell Biol 8:405-13.

Rockwell P, Martinez J, Papa L, Gomes E. 2004. Redox regulates COX-2 upregulation and cell death in the neuronal response to cadmium. Cell Signal 16:343-53.

Rossi A, Kapahi P, Natoli G, Takahashi T, Chen Y, Karin M, Santoro MG. 2000. Anti-inflammatory cyclopentenone prostaglandins are direct inhibitors of IkappaB kinase. Nature 403:103-8.

Rouzer CA, Marnett LJ. 2009. Cyclooxygenases: structural and functional insights. J Lipid Res 50 Suppl:S29-34.

Ryter SW, Alam J, Choi AM. 2006. Heme oxygenase-1/carbon monoxide: from basic science to therapeutic applications. Physiol Rev 86:583-650.

Saito Y, Nishio K, Numakawa Y, Ogawa Y, Yoshida Y, Noguchi N, Niki E. 2007. Protective effects of 15-deoxy-Delta12,14-prostaglandin J2 against glutamate-induced cell death in primary cortical neuron cultures: induction of adaptive response and enhancement of cell tolerance primarily through up-regulation of cellular glutathione. J Neurochem 102:1625-34.

Saitoh M, Nishitoh H, Fujii M, Takeda K, Tobiume K, Sawada Y, Kawabata M, Miyazono K, Ichijo H. 1998. Mammalian thioredoxin is a direct inhibitor of apoptosis signal-regulating kinase (ASK) 1. EMBO J 17:2596-606.

Sakahira H, Enari M, Nagata S. 1998. Cleavage of CAD inhibitor in CAD activation and DNA degradation during apoptosis. Nature 391:96-9.

Sandberg AA, Bridge JA. 2003. Updates on the cytogenetics and molecular genetics of bone and soft tissue tumors: osteosarcoma and related tumors. Cancer Genet Cytogenet 145:1-30.

Sawano H, Haneda M, Sugimoto T, Inoki K, Koya D, Kikkawa R. 2002. 15-Deoxy-Delta12,14-prostaglandin J2 inhibits IL-1beta-induced cyclooxygenase-2 expression in mesangial cells. Kidney Int 61:1957-67.

Sawyer N, Cauchon E, Chateauneuf A, Cruz RP, Nicholson DW, Metters KM, O'Neill GP, Gervais FG. 2002. Molecular pharmacology of the human prostaglandin D2 receptor, CRTH2. Br J Pharmacol 137:1163-72.

Scher JU, Pillinger MH. 2005. 15d-PGJ2: the anti-inflammatory prostaglandin? Clin Immunol 114:100-9.

Sengupta S, Jang BC, Wu MT, Paik JH, Furneaux H, Hla T. 2003. The RNA-binding protein HuR regulates the expression of cyclooxygenase-2. J Biol Chem 278:25227-33.

Shanmugam N, Reddy MA, Natarajan R. 2008. Distinct roles of heterogeneous nuclear ribonuclear protein K and microRNA-16 in cyclooxygenase-2 RNA stability induced by S100b, a ligand of the receptor for advanced glycation end products. J Biol Chem 283:36221-33.

Shen YM, Hung GY, Yen HJ, Hsieh MY, Hsieh TK. 2009. Early development of acute myeloid leukemia following treatment of osteosarcoma: a case report and review of the literature. Pediatr Neonatol 50:239-44.

Sheng H, Shao J, Dubois RN. 2001. K-Ras-mediated increase in cyclooxygenase 2 mRNA stability involves activation of the protein kinase B1. Cancer Res 61:2670-5.

Shibata T, Kondo M, Osawa T, Shibata N, Kobayashi M, Uchida K. 2002. 15-deoxy-delta 12,14-prostaglandin J2. A prostaglandin D2 metabolite generated during inflammatory processes. J Biol Chem 277:10459-66.

Shibata T, Yamada T, Ishii T, Kumazawa S, Nakamura H, Masutani H, Yodoi J, Uchida K. 2003. Thioredoxin as a molecular target of cyclopentenone prostaglandins. J Biol Chem 278:26046-54.

Smith WL, Song I. 2002. The enzymology of prostaglandin endoperoxide H synthases-1 and -2. Prostaglandins Other Lipid Mediat 68-69:115-28.

Soares MP, Usheva A, Brouard S, Berberat PO, Gunther L, Tobiasch E, Bach FH. 2002. Modulation of endothelial cell apoptosis by heme oxygenase-1-derived carbon monoxide. Antioxid Redox Signal 4:321-9.

Song S, Guha S, Liu K, Buttar NS, Bresalier RS. 2007. COX-2 induction by unconjugated bile acids involves reactive oxygen species-mediated signalling pathways in Barrett's oesophagus and oesophageal adenocarcinoma. Gut 56:1512-21.

Strander H. 2007. Interferons and osteosarcoma. Cytokine Growth Factor Rev 18:373-80.

Straus DS, Glass CK. 2001. Cyclopentenone prostaglandins: new insights on biological activities and cellular targets. Med Res Rev 21:185-210.

Straus DS, Glass CK. 2007. Anti-inflammatory actions of PPAR ligands: new insights on cellular and molecular mechanisms. Trends Immunol 28:551-8.

Straus DS, Pascual G, Li M, Welch JS, Ricote M, Hsiang CH, Sengchanthalangsy LL, Ghosh G, Glass CK. 2000. 15-deoxy-delta 12,14-prostaglandin J2 inhibits multiple steps in the NF-kappa B signaling pathway. Proc Natl Acad Sci U S A 97:4844-9.

Subbaramaiah K, Altorki N, Chung WJ, Mestre JR, Sampat A, Dannenberg AJ. 1999. Inhibition of cyclooxygenase-2 gene expression by p53. J Biol Chem 274:10911-5.

Subbaramaiah K, Lin DT, Hart JC, Dannenberg AJ. 2001. Peroxisome proliferator-activated receptor gamma ligands suppress the transcriptional activation of cyclooxygenase-2. Evidence for involvement of activator protein-1 and CREB-binding protein/p300. J Biol Chem 276:12440-8.

Subbaramaiah K, Marmo TP, Dixon DA, Dannenberg AJ. 2003. Regulation of cyclooxgenase-2 mRNA stability by taxanes: evidence for involvement of p38, MAPKAPK-2, and HuR. J Biol Chem 278:37637-47.

Surh YJ, Kundu JK. 2005. Signal transduction network leading to COX-2 induction: a road map in search of cancer chemopreventives. Arch Pharm Res 28:1-15.

Suzuki Y, Imai Y, Nakayama H, Takahashi K, Takio K, Takahashi R. 2001. A serine protease, HtrA2, is released from the mitochondria and interacts with XIAP, inducing cell death. Mol Cell 8:613-21.

Syeda F, Tullis E, Slutsky AS, Zhang H. 2008. Human neutrophil peptides upregulate expression of COX-2 and endothelin-1 by inducing oxidative stress. Am J Physiol Heart Circ Physiol 294:H2769-74.

Ta HT, Dass CR, Choong PF, Dunstan DE. 2009. Osteosarcoma treatment: state of the art. Cancer Metastasis Rev 28:247-63.

Tan ML, Choong PF, Dass CR. 2009. Osteosarcoma: Conventional treatment vs. gene therapy. Cancer Biol Ther 8:106-17.

Tang N, Song WX, Luo J, Haydon RC, He TC. 2008. Osteosarcoma development and stem cell differentiation. Clin Orthop Relat Res 466:2114-30.

Tang XQ, Yu HM, Zhi JL, Cui Y, Tang EH, Feng JQ, Chen PX. 2006. Inducible nitric oxide synthase and cyclooxgenase-2 mediate protection of hydrogen peroxide preconditioning against apoptosis induced by oxidative stress in PC12 cells. Life Sci 79:870-6.

Telliez A, Furman C, Pommery N, Henichart JP. 2006. Mechanisms leading to COX-2 expression and COX-2 induced tumorigenesis: topical therapeutic strategies targeting COX-2 expression and activity. Anticancer Agents Med Chem 6:187-208.

Tewari M, Quan LT, O'Rourke K, Desnoyers S, Zeng Z, Beidler DR, Poirier GG, Salvesen GS, Dixit VM. 1995. Yama/CPP32 beta, a mammalian homolog of CED-3, is a CrmA-inhibitable protease that cleaves the death substrate poly(ADP-ribose) polymerase. Cell 81:801-9.

Tiano HF, Loftin CD, Akunda J, Lee CA, Spalding J, Sessoms A, Dunson DB, Rogan EG, Morham SG, Smart RC, Langenbach R. 2002. Deficiency of either cyclooxygenase (COX)-1 or COX-2 alters epidermal differentiation and reduces mouse skin tumorigenesis. Cancer Res 62:3395-401.

Tsatsanis C, Androulidaki A, Venihaki M, Margioris AN. 2006. Signalling networks regulating cyclooxygenase-2. Int J Biochem Cell Biol 38:1654-61.

Uchida K, Shibata T. 2008. 15-Deoxy-Delta(12,14)-prostaglandin J2: an electrophilic trigger of cellular responses. Chem Res Toxicol 21:138-44.

Urakawa H, Nishida Y, Naruse T, Nakashima H, Ishiguro N. 2009. Cyclooxygenase-2 overexpression predicts poor survival in patients with high-grade extremity osteosarcoma: a pilot study. Clin Orthop Relat Res 467:2932-8.

Vanel D, Henry-Amar M, Lumbroso J, Lemalet E, Couanet D, Piekarski JD, Masselot J, Boddaert A, Kalifa C, Le Chevalier T, et al. 1984. Pulmonary evaluation of patients with osteosarcoma: roles of standard radiography, tomography, CT, scintigraphy, and tomoscintigraphy. AJR Am J Roentgenol 143:519-23.

Wachtel M, Schafer BW. 2010. Targets for cancer therapy in childhood sarcomas. Cancer Treat Rev 36:318-27.

Wang D, Dubois RN. 2006. Prostaglandins and cancer. Gut 55:115-22.

Wang D, Dubois RN. 2010. Eicosanoids and cancer. Nat Rev Cancer 10:181-93.

Wang HG, Pathan N, Ethell IM, Krajewski S, Yamaguchi Y, Shibasaki F, McKeon F, Bobo T, Franke TF, Reed JC. 1999. Ca2+-induced apoptosis through calcineurin dephosphorylation of BAD. Science 284:339-43.

Wang X, Wang Y, Kim HP, Nakahira K, Ryter SW, Choi AM. 2007. Carbon monoxide protects against hyperoxia-induced endothelial cell apoptosis by inhibiting reactive oxygen species formation. J Biol Chem 282:1718-26.

Wei G, Lonardo F, Ueda T, Kim T, Huvos AG, Healey JH, Ladanyi M. 1999. CDK4 gene amplification in osteosarcoma: reciprocal relationship with INK4A gene alterations and mapping of 12q13 amplicons. Int J Cancer 80:199-204.

Winterbourn CC, Hampton MB. 2008. Thiol chemistry and specificity in redox signaling. Free Radic Biol Med 45:549-61.

Wolf G. 2006. Is 9-cis-retinoic acid the endogenous ligand for the retinoic acid-X receptor? Nutr Rev 64:532-8.

Wu WS, Wu JR, Hu CT. 2008. Signal cross talks for sustained MAPK activation and cell migration: the potential role of reactive oxygen species. Cancer Metastasis Rev 27:303-14.

Xie C, Ming X, Wang Q, Schwarz EM, Guldberg RE, O'Keefe RJ, Zhang X. 2008. COX-2 from the injury milieu is critical for the initiation of periosteal progenitor cell mediated bone healing. Bone 43:1075-83.

Xu K, Kitchen CM, Shu HK, Murphy TJ. 2007. Platelet-derived growth factor-induced stabilization of cyclooxygenase 2 mRNA in rat smooth muscle cells requires the c-Src family of protein-tyrosine kinases. J Biol Chem 282:32699-709.

Xu Z, Choudhary S, Voznesensky O, Mehrotra M, Woodard M, Hansen M, Herschman H, Pilbeam C. 2006. Overexpression of COX-2 in human osteosarcoma cells decreases proliferation and increases apoptosis. Cancer Res 66:6657-64.

Yamamoto K, Arakawa T, Ueda N, Yamamoto S. 1995. Transcriptional roles of nuclear factor kappa B and nuclear factor-interleukin-6 in the tumor necrosis factor alpha-dependent induction of cyclooxygenase-2 in MC3T3-E1 cells. J Biol Chem 270:31315-20.

Yamazaki K, Shimizu M, Okuno M, Matsushima-Nishiwaki R, Kanemura N, Araki H, Tsurumi H, Kojima S, Weinstein IB, Moriwaki H. 2007. Synergistic effects of RXR alpha and PPAR gamma ligands to inhibit growth in human colon cancer cells--phosphorylated RXR alpha is a critical target for colon cancer management. Gut 56:1557-63.

Yanase T, Yashiro T, Takitani K, Kato S, Taniguchi S, Takayanagi R, Nawata H. 1997. Differential expression of PPAR gamma1 and gamma2 isoforms in human adipose tissue. Biochem Biophys Res Commun 233:320-4.

Yang E, Zha J, Jockel J, Boise LH, Thompson CB, Korsmeyer SJ. 1995. Bad, a heterodimeric partner for Bcl-XL and Bcl-2, displaces Bax and promotes cell death. Cell 80:285-91.

Yang G, Nguyen X, Ou J, Rekulapelli P, Stevenson DK, Dennery PA. 2001. Unique effects of zinc protoporphyrin on HO-1 induction and apoptosis. Blood 97:1306-13.

Yeh WC, Pompa JL, McCurrach ME, Shu HB, Elia AJ, Shahinian A, Ng M, Wakeham A, Khoo W, Mitchell K, El-Deiry WS, Lowe SW, Goeddel DV, Mak TW. 1998. FADD: essential for embryo development and signaling from some, but not all, inducers of apoptosis. Science 279:1954-8.

Yoneda T, Imaizumi K, Oono K, Yui D, Gomi F, Katayama T, Tohyama M. 2001. Activation of caspase-12, an endoplastic reticulum (ER) resident caspase, through tumor necrosis factor

receptor-associated factor 2-dependent mechanism in response to the ER stress. J Biol Chem 276:13935-40.

Yu X, Egner PA, Wakabayashi J, Wakabayashi N, Yamamoto M, Kensler TW. 2006. Nrf2-mediated induction of cytoprotective enzymes by 15-deoxy-Delta12,14-prostaglandin J2 is attenuated by alkenal/one oxidoreductase. J Biol Chem 281:26245-52.

Zamzami N, Marchetti P, Castedo M, Decaudin D, Macho A, Hirsch T, Susin SA, Petit PX, Mignotte B, Kroemer G. 1995. Sequential reduction of mitochondrial transmembrane potential and generation of reactive oxygen species in early programmed cell death. J Exp Med 182:367-77.

Zhang X, Lu L, Dixon C, Wilmer W, Song H, Chen X, Rovin BH. 2004. Stress protein activation by the cyclopentenone prostaglandin 15-deoxy-delta12,14-prostaglandin J2 in human mesangial cells. Kidney Int 65:798-810.

Zhang X, Schwarz EM, Young DA, Puzas JE, Rosier RN, O'Keefe RJ. 2002. Cyclooxygenase-2 regulates mesenchymal cell differentiation into the osteoblast lineage and is critically involved in bone repair. J Clin Invest 109:1405-15.

Zimmermann KC, Bonzon C, Green DR. 2001. The machinery of programmed cell death. Pharmacol Ther 92:57-70.

Zong WX, Lindsten T, Ross AJ, MacGregor GR, Thompson CB. 2001. BH3-only proteins that bind pro-survival Bcl-2 family members fail to induce apoptosis in the absence of Bax and Bak. Genes Dev 15:1481-6.

CURRICULUM VITAE

PERSONAL DATA

Name: Kerstin Kitz
Date of Birth: September 7th, 1982
Nationality: Austria

Affiliation: University Clinic of Pediatrics and Adolescent Medicine
Research Unit of Osteological Research and Mass Spectrometry
Medical University of Graz
Auenbruggerplatz 34
8036 Graz

Phone: 0316 385 14036
Email: kerstin.kitz@medunigraz.at

EDUCATION

2007 – 2011: PhD studies in the PhD program "Molecular Medicine" at the Medical University of Graz, Austria (www.medunigraz/phd)

2007: Master thesis "Tools for the expression of genes from higher eukaryotics in yeasts". Supervisor: Prof. Dr. Anton Glieder, Research Center Applied Biocatalysis, Graz, Austria

2005 – 2007: Master studies "Molecular Microbiology" at the Karl Franzens-University in Graz, Austria

2002 – 2005: Bachelor studies in "Molecular Biology" at the Karl Franzens-University in Graz, Austria

2002: School leaving examination (university entrance qualification) at a Higher Secondary School for Occupations in the Economy in Klagenfurt, Austria

INTERNSHIPS AND ADVANCED LAB COURSES

2010: FEBS practical course "Techniques in Free Radical Biology", Debrecen, Hungary

2009: Radiation protection course: basics and unsealed radionuclides, Graz, Austria

2005: Internship at AGES (Austrian Agency for Health and Food Safety); laboratory occupation, Klagenfurt, Austria

2004: Internship at the Major Hospital in Klagenfurt, Austria, Department of Medical and Chemical Laboratory Diagnostics; administrative occupation

PUBLICATIONS

Peer-reviewed articles

Kitz K, Windischhofer W, Leis HJ, Huber E, Kollroser M, Malle E.
15d-PGJ_2 induces Cox-2 expression in human osteosarcoma cells through MAPK and EGFR activation involving reactive oxygen species.
Free Radical Biol Med (2011), in press.

Abad S*, **Kitz K***, Hörmann A, Schreiner U, Hartner FS and Glieder A.
Real-time PCR-based determination of gene copy numbers in *Pichia pastoris.*
Biotechnol J (2010), 5, 413–420. (* equally contributed)

Poster presentations at international conferences

Kitz K, Malle E, Leis HJ, Windischhofer W.
Cox-2 expression is modulated by intracellular glutathione status in human osteosarcoma cells.
Gordon Research Conference "Thiol-based Redox Regulation & Signaling" (9-14 May 2010), Lucca, Italy [Poster]

Kitz K, Malle E, Leis HJ, Windischhofer W.
15-Deoxy-$\Delta^{12,14}$-prostaglandin J_2 induces Cox-2 expression and ROS-dependent apoptosis in human osteosarcoma cells.
Bone. 2009; 45: S103-S104. - 5th International Conference on Children's Bone Health (23-26 June 2009), Cambridge, UK [Poster]

Kitz K, Malle E, Leis HJ, Windischhofer W.
Peroxisome proliferator-activated receptor gamma agonists induce cyclooxygenase 2 expression and apoptosis in human osteosarcoma cells.
Bone. 2009; 44(2):S285-S285. - 36th Symposium of Calcified Tissues (23-27 May 2009), Vienna, Austria [Poster]

Kitz K, Malle E, Leis HJ, Windischhofer W.
PPARγ-agonists induce expression of COX-2 in human osteosarcoma cells.
ÖGMBT (Austrian Association of Molecular Life Sciences and Biotechnology) Meeting (22-24 Sept 2008), Graz, Austria; [Poster]

Declaration

I hereby declare that this thesis is my own original work and that I have fully acknowledged by name all of those individuals and organisations that have contributed to the research for this thesis. Due acknowledgement has been made in the text to all other material used. Throughout this thesis and in all related publications I followed the guidelines of “Good Scientific Practice”.

Date *Signature*